INTRODUCTION TO ENGINEERING DESIGN

Air to Air

A Wind Turbine Powered Air Compressor

Spring 2012

Submitted to Dr.Gadhamshetty & Linda Teitelman McCloskey

Executive Summary

Air-to-Air is an innovative wind turbine powered air compressor that utilizes wind energy to compress air. The wind energy is initially harnessed by a two-tiered Savonius type turbine. The rotation of the turbine blades causes the drive shaft to rotate. The revolutions of the drive shaft are matched to the compressor through a gearing system, consisting of multiple gears and pulleys. The rotation of the gear on the compressor causes the piston to oscillate and compress air. This compressed air is then stored in an external tank.

The team began work on the project by researching existing products. This information was then integrated into selection of the team's design project. An overall design of the prototype was determined, and each team member was designated a subsystem to develop. Through individual work on the subsystems, as well as work done as a team, the prototype was built with very few complications. The collection of data and testing of the prototype allowed the team to conclude that it was a functioning model of the intended design.

Overall, the wind turbine powered air compressor was a functional model. Underperforming subsystems would need slight revisions in order for the system to perform at the desired level defined at the onset of the project. Through further testing and a slight design modification, this prototype could be developed into a form ready for manufacturing. This product could then provide businesses and households with compressed air at a reduced cost.

Version History

Version	Date	Content
1.0	5/4/2012	Initial Individual Sections
2.0	5/5/2012	Compilation of Individual Sections
2.1	5/5/2012	First Edit of Compiled Document
2.2	5/6/2012	Second Edit, Added Content
3.0	5/6/2012	Compiled and Formatted Document in MS Word
3.1	5/6/2012	Third Edit
3.2	5/7/2012	Fourth Edit, References and Appendices Added
3.3	5/7/2012	Fifth and Final Edit

Table of Contents

1 Introduction

In modern society, many useful forms of energy are wasted or harnessed unproductively. The dual conversion process of wind energy into electrical energy then electrical energy into another form of energy is less efficient than a direct conversion. Thus, the design team is addressing the problem of finding more efficient ways to harness wind energy, specifically in the area of direct mechanical energy storage.

The team's solution targets a customer seeking energy in the final form of compressed air. The product will harness the wind's kinetic energy via a turbine in order to compress surrounding air and store it, thus transferring wind energy directly to compressed air energy.

This system will be used by small businesses or fabrication sites that consistently use pneumatic tools. Because of this, the prototype must provide a stable, high quality, and safe source of sustainable energy. In order to provide a benefit to the company, the system will also have to be low maintenance and have an appropriate payoff period.

Through this wind-powered turbine system, the team plans to supplement an existing source of air while reducing the overall cost of compressing air through electricity or gasoline. This method will be both environmentally friendly and cost-effective.

This document will discuss team objectives and scope of the project, research on pre-existing technologies, and concept selection and development. Next, each subsystem and its testing will be discussed, followed by a section on the testing of the entire prototype and data gathered. The results and conclusion section will then close the report with a discussion of the feasibility and usefulness of the overall project.

2 Project Objectives and Scope

The team developed a multitude of objectives to meet throughout the semester. These objectives ranged from plans for the prototype to the improvement of team members' skills and teamwork. Following is a list of these objectives:

- Design a wind powered air compressor in order to convert kinetic wind energy into stored pressure energy.
- The designed wind powered air compressor must fully meet customer requirements in terms of produced power and pressure.
- Design the wind-powered air compressor to be both scalable and modular.
- Create a design which augments or offsets unsustainable air compression methods used by companies.
- Overcome the expense and difficulty associated with acquiring materials and the lack of fabrication skills of team members.
- To improve on the weaknesses of existing designs.
- Obtain an 'A' grade on the final project.

- Have the final design reflect the entirety of the engineering design process.
- Utilize the individual strengths of members of the group to create a product reflecting the sum of those strengths.
- To improve the weaknesses of team members.

The scope of the team's project is to create one working prototype that satisfies the customer requirements. Creating a plan for mass-marketing of the prototype and streamlining the product for manufacturing is out of the project's scope. These restrictions were placed on the team due to both limited budget and time.

2.1 Mission Statement

***Table 2.1**: Mission Statement*

Benefits:	A sustainable energy source which directly translates wind energy into the mechanical energy of compressed air, thus skipping the conversion into electrical energy.
Goals:	To produce a wind turbine powered air compressor utilizing a low cost, quality design in a safe and reliable manner. Also, it must satisfy the requirements of the primary and secondary customers.
Primary Market:	Small businesses that use pneumatic tools.
Secondary Market:	Homeowners who commonly do carpentry or craftsmanship.
Assumptions:	Consumer has previous training with high pressure vessels. Customer will use this device to supplement another source of compressed air. Device will meet all customer requirements.
Stakeholders:	Development team, IED instructors, Potential investors

2.2 Customer Requirements and Technical Specifications

The primary customers of this project are owners and operators of small businesses, specifically those who use hand-held pneumatic tools or pneumatic devices in general. Examples of this type of small business include lobster trap producers, automotive service centers, and construction firms.

Secondary customers include homeowners who do a large amount of craftsmanship or carpentry with compressed air based powered tools, or in general homeowners who have or use pneumatic devices.

The following table is a list of the most important customer requirements and their interpreted technical specifications. The customer requirements were ranked in level of

importance, with 5 being the most important and 3 being the least important. The list was expanded during the development process as more customer requirements were obtained. A full list of all customer requirements, along with their technical specifications can be found in Section 11.2.

These customer requirements were developed based on three sources. The product's primary customers were interviewed directly. Specifically, the team contacted Pike Bartlett of Friendship Trap Company, George's Auto Repair, Fitzgerald's Garage, and Rensselaer Honda. Their verbal responses to questioning were translated to specific customer needs. Also, the team, as stakeholders in the project, brainstormed a variety of needs they had for the project. Cost, for instance, was of particular importance to the team. Finally, the needs of the instructors were pulled from the team project description and incorporated into the table below. Some of the needs and requirements were subject to change and expansion as the project progressed.

***Table 2.2**: Customer Requirements and Technical Specifications*

Customer Requirement	Importance	Technical Specification	Target Value / Range of Values
Return on Investment	5	Payoff period	5 years
Stability-It shouldn't fall over.	5	Wind speed required for tip condition	70 mph
Sustainable energy	5	Wind energy	-
Safe to the surrounding environment	5	Gives off no toxins or harmful substances	-
Pressure needed	5	Minimum air pressure	100 psi
Safe	5	Factor of Safety of Pressure Vessel	3

3 Assessment of Relevant Existing Technologies

Competing products and solutions were investigated with external research into existing products. Creation of a wind turbine for supplementing energy costs has been performed by individuals and companies in the past, and their work has been made available to the public via online publication. Researching wind turbine publications introduced a variety of possibilities and highlighted beneficial and detrimental qualities to be taken into consideration during the wind turbine powered air compressor development process. Listed in Table 3.1 below are the types of wind turbines studied.

***Table 3.1**: Competitive Benchmarking and Patents*

Competitive Product	Patent Number	Title / Description	Relation to This Project
BroadStar AeroCam Type III	United States Patent No. 7,365.448 B2. Date of issuance: April 28, 2008	- Horizontal Axis Wind Turbine - Darrieus Type Turbine	- Concept for Wind Turbine Type
CorrectEnergySolutions XDOBS	Patent Pending	- Vertical Axis Wind Turbine - Savonius Type Turbine - Air Compressor Option	- Concept for Wind Turbine Type - Could Compress Air

3.1 BroadStar AeroCam Type III

***Figure 3.1:** BroadStar AeroCam Type III © (BroadStar Wind Corporation, 2011)*

The BroadStar AeroCam Type III (Figure 3.1), developed by BroadStar Wind Corporation, is a large scale, self-starting, horizontal axis wind turbine (HAWT) with dimensions 32 feet by 52 feet. It features lift-generating blades, a blade pitch control system, self-regulating speed control, direct drive, and a three-phase AC generator. This design uses the same principles as a Darrieus type wind turbine in order to create a usable torque. Due to rotation and incoming wind, the relative flow is at a non-zero angle of attack with respect to the chord line of the symmetric airfoils. Because of this angle of attack, the lift force is directed such that it does not intersect the angle of rotation and a net torque is generated. In addition, a blade pitch control system is implemented to optimize each blade's angle of attack independently for maximum lift generation. The self-regulating speed controller applies braking if the system begins rotating at unsafe speeds, such as in severe storms, preventing the system from experiencing catastrophic failure. Direct drive of the generator is utilized as the turbine produces enough torque to drive the AC generator. The AC generator outputs three-phase power to be further regulated to 60 Hz. The

rated output of the turbine is 250 KW at 30 mph winds (80 mph max). Table 3.2 describes the advantages and disadvantages of this model (BroadStar Wind Corporation, 2011).

Table 3.2: *BroadStar AeroCam Type III © Qualities*

Advantages	Disadvantages
• 3328 ft^2 cross section • 250KW output • $1 / Watt • Blade pitch control system • Speed control system • 80mph max wind speed • Self-starting	• Too large to be used by a single consumer • Two stage energy conversion resulting in less efficiency • Complex mechanism for pitch control system • Complex installation process

3.2 CorrectEnergySolutions XDOBS

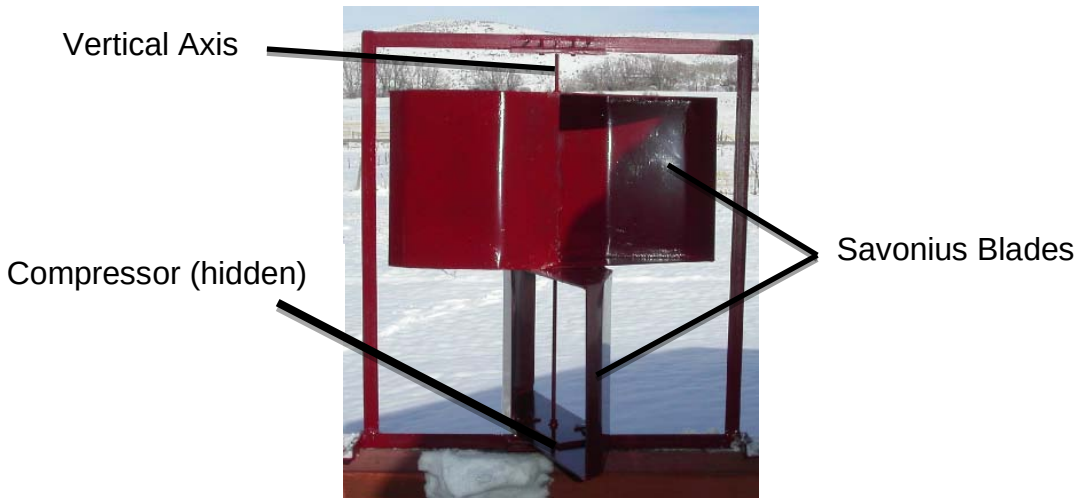

Figure 3.2: *CorrectEnergySolutions© XDOBS (CorrectEnergySolutions, 2005)*

The XDOBS (Figure 3.2), created by CorrectEnergySolutions, is a small scale, self-starting, vertical axis wind turbine (VAWT) with dimensions of 50 inches by 48 inches. It features two pairs of Savonius blades, low friction bearings, direct drive, reinforcing support structure, and compressor. The Savonius blades of the turbine are designed to "cup" the incoming wind and do not directly produce lift, relying instead on a difference in drag forces between the two blades. The blade pairs are offset by 90 degrees to enable self-starting of the wind turbine, which occurs at approximately 1 mph. The turbine features low friction bearings

on rotating components to facilitate self-starting and to reduce frictional losses. The turbine drive shaft is connected directly to the turbine's compression system without the use of torque conversion. A reinforcing support structure extends above the top of the Savonius blades to provide support to the vertical axis of the drive shaft. A compressor is driven by the turbine for use in an external air system. The CorrectEnergySolutions XDOBS's advantages and disadvantages are shown in Table 3.3 (CorrectEnergySolutions, 2005).

Table 3.3: *CorrectEnergySolutions© XDOBS Qualities*

Advantages	**Disadvantages**
• Direct conversion to compressed air • Single person installation • Useable in urban areas • 1.5 KW output • Low-friction bearings • 100mph max wind speed • Self-starting	• Blade design is geometrically simple and not aerodynamically founded • Ground level system reducing air speeds

4 Professional and Societal Considerations

The Air-to-Air compression system will work to help reduce the carbon footprint of small businesses who utilize pneumatic devices in their operation as well as homeowners. Reduction of an organization's or an individual's carbon footprint is one small step towards the betterment of the environment as a whole. The team's design is one part of a transition to cleaner and more environmentally responsible technology.

Another significant concern is the safety of the system's usage. The team's system is designed to remove the greatest possible source of error—human intervention. The design of the system is such that, upon installation, limited human intervention or action is necessary for the system's use. Components are designed in such a way so as not to require maintenance nor require the customer to come near it. The device is also intended for rooftop installation, further extending the safety of the system by limiting physical access to the device.

The only subsystem which would require human intervention after the device's installation is the braking system. This system, however, is implemented in such a way as to allow the user to operate it from a small distance from the turbine, minimizing safety risk.

The largest safety issue in the system is the spinning turbine, which when rotating at full speed, moves fast enough that objects in their path would be at a safety risk. The team's solution to this issue is to blunt the edges of the blades with a PVC rubber coating, significantly

increasing the surface area of the edges. Also, to enhance safety, the turbine's design is a mix of yellow and red, which are cautionary colors, to alert users to the possible dangers presented by the turbine.

5 System Concept Development and Selection

5.1 Mind Mapping

With information gathered through benchmarking competitors, a session of brainstorming was performed in which a variety of wind turbine qualities were examined. Ideas generated were categorized into a hierarchal mind map shown below in Figure 5.1. This organization allowed the development team to realize connections between concepts for further development consideration.

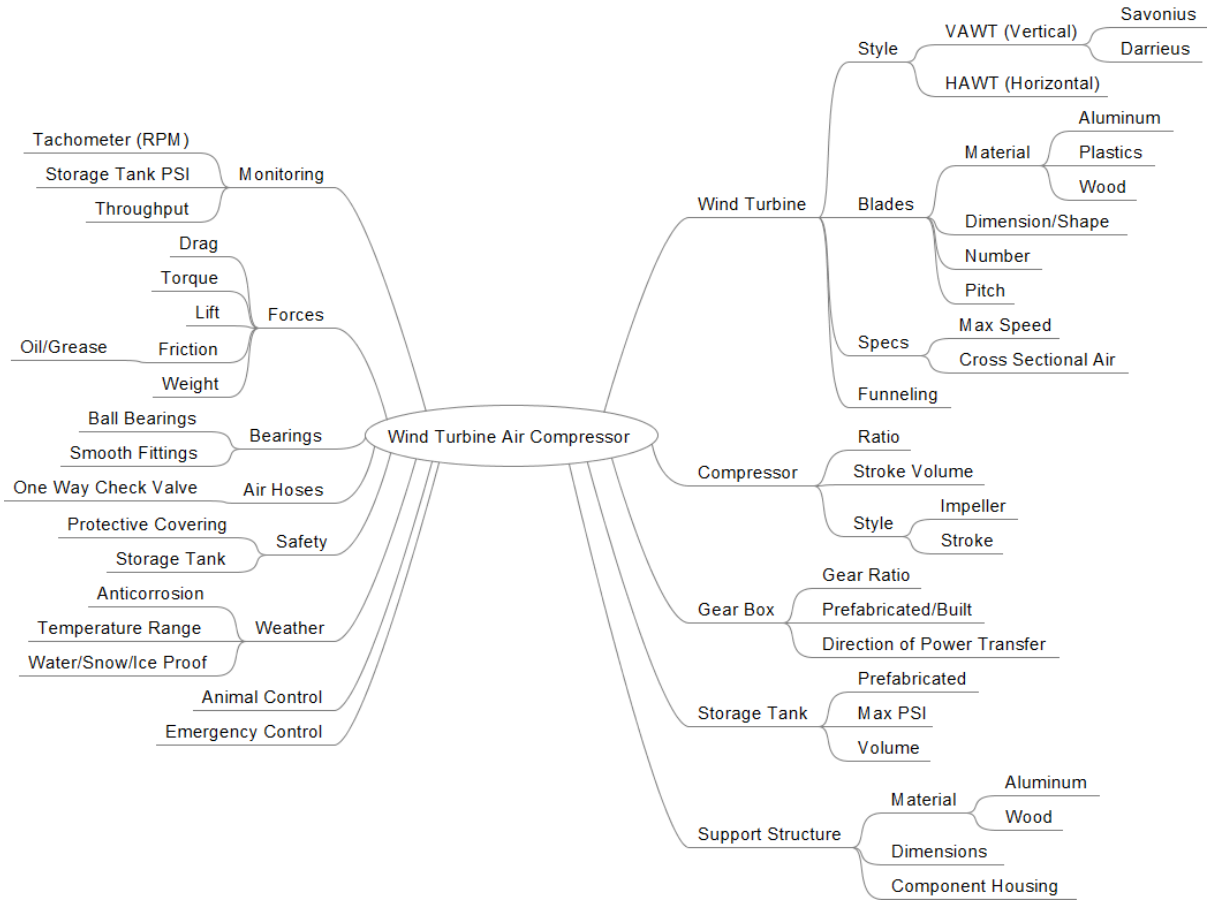

Figure 5.1: *Wind Turbine Air Compressor Mind Map*

5.2 Concept Combinations

By investigating the different children of the mind map, multiple sub-problems were recognized and respective solutions proposed. Table 5.1 organizes these sub-problems with their corresponding candidate solutions.

Table 5.1: *Sub-problem Concept Combinations*

Turbine Orientation	**Blade Material**	**Blade Shape**	**Torque Transfer**
VAWT (Vertical)	Metal	Foil	Drive Shaft
HAWT (Horizontal)	Plastic	Savonius	Hydraulic
	Wood	Darrieus	
Torque Conversion	**Lubrication**	**Rotational Bearings**	**Electronic Monitor**
Gear Box	Oil	Ball	Analog
V-Belts	Grease	Taper	Microcontroller
	Powder	Magnetic	
Base/Housing	**Compressor**	**Air Storage Tank**	
Metal	Reciprocating	Prefabricated	
Wood	Impeller		
	Screw		

5.3 Concept Sketches

With information collected during the benchmarking and concept combination phase, sketches were created to investigate the physical positioning of components in possible solution designs. Two sketches of possible designs are shown below in Figure 5.2 and Figure 5.3.

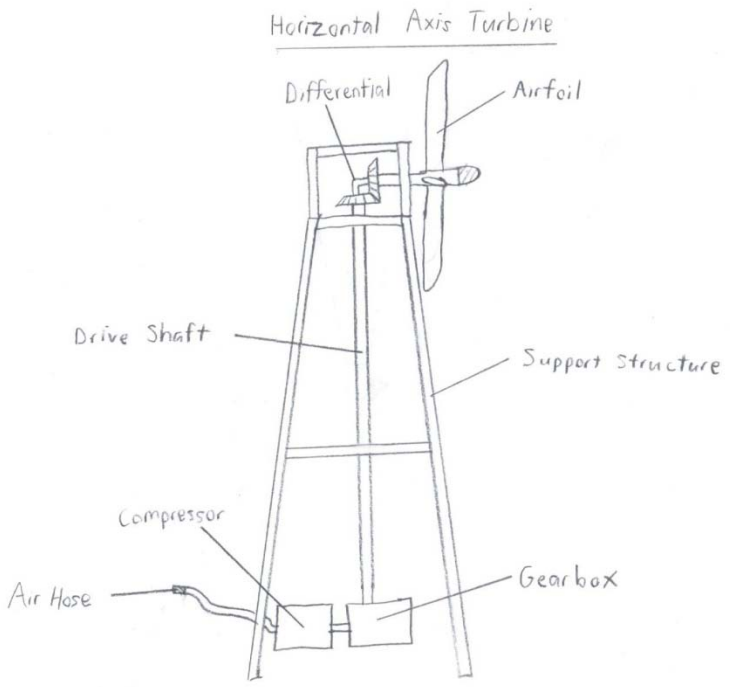

Figure 5.2: *Horizontal Axis Wind Turbine*

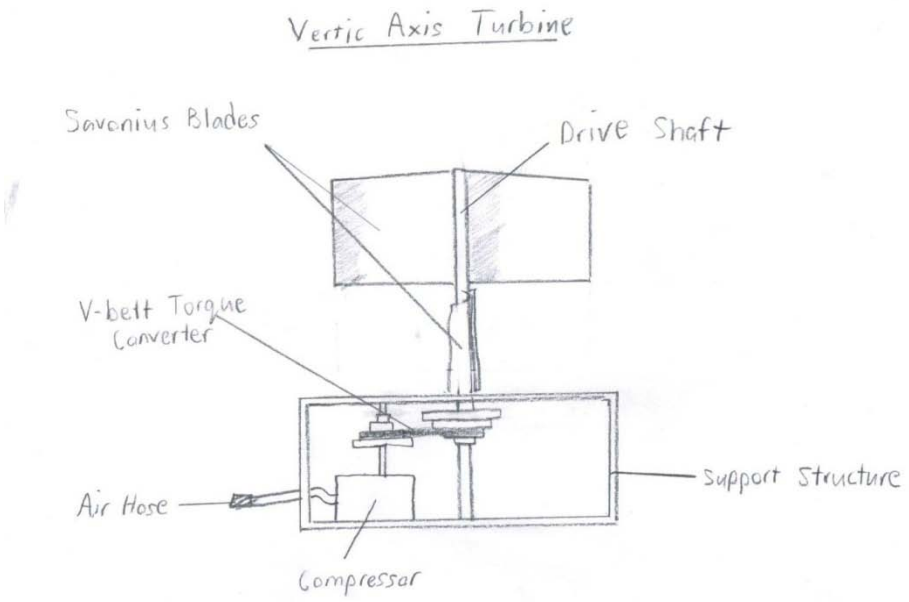

Figure 5.3: *Vertical Axis Wind Turbine*

5.4 Selection Matrix

A selection matrix was created to analyze the five most viable combinations of basic components. Combinations A to E are shown in Table 5.2. Each combination varies among properties listed vertically in the top left; such as turbine orientation, blade type, blade material, drive shaft segments, etc. A possibility for the listed property appears in the same row as that property and below the combination letter.

Table 5.2: *Concept Selection Matrix (Note: "Mic.Con." stands for Microcontroller)*

		A		B		C		D		E	
Orientation		**Horizontal**		**Horizontal**		**Vertical**		**Vertical**		**Vertical**	
Blade Type		**Airfoil**		**Airfoil**		**Darrieus**		**Savonius**		**Savonius**	
Blade Material		**Metal**		**Plastic**		**Metal**		**Metal**		**Plastic**	
Drive Shaft		**Segmented**		**Segmented**		**Direct**		**Direct**		**Direct**	
Torque Converter		**Gear Box**		**V-Belt**		**Gear Box**		**Gear Box**		**V-Belt**	
Bearings		**Ball**		**Taper**		**Magnetic**		**Taper**		**Ball**	
Compressor		**Line**		**Line**		**Screw**		**Reciprocating**		**Reciprocating**	
Monitoring		**Mic.Con.**		**Analog**		**Analog**		**Mic.Con.**		**Mic.Con.**	
Selection Criteria	Weight	Rating	Wtd	Rating	Wtd	Rating	Wtd	Rating	Wtd	Rating	Wtd
Cost	15%	-1	-0.15	0	0.00	0	0.00	1	0.15	1	0.15
Feasability	20%	-1	-0.20	0	0.00	-1	-0.20	0	0.00	1	0.20
Creativity	5%	0	0.00	0	0.00	0	0.00	0	0.00	1	0.05
Practicality	15%	0	0.00	0	0.00	-1	-0.15	1	0.15	1	0.15
Reliability	15%	-1	-0.15	-1	-0.15	-1	-0.15	1	0.15	1	0.15
Performance	10%	1	0.10	1	0.10	1	0.10	0	0.00	0	0.00
Efficiency	5%	1	0.05	1	0.05	1	0.05	0	0.00	0	0.00
Durability	15%	0	0.00	-1	-0.15	0	0.00	1	0.15	1	0.15
Total Score		-0.35		-0.15		-0.35		0.60		0.85	
Rank											
Continue?		No		No		No		No		Yes	

Selection criteria were chosen and assigned weight values determined with respect to project requirements and customer needs. Feasibility, performance, and reliability are of highest priority as they are directly observed by the customer. A product that does not perform to the extent that the customer expects is not a desirable product. Cost is an important characteristic of the design to both the design team as well as the final customer to ensure competitiveness in the

turbine market. Reliability and durability add value to the final product through its longevity, making them viable criteria. Creativity and efficiency of the design are of lower priority than other criteria because it is more important to have a final design that meets project requirements than to have an innovative design. Each combination was then rated on a scale of negative one to one, with negative one indicating below average performance and one indicating above average performance. Ratings were assigned based on evidence collected during the benchmarking phase of the design process.

Once all ratings had been assigned, the total score was calculated with weight taken into consideration. Combination E had the highest score and was chosen as the basis for further project development.

5.5 Proposed Solution

The development team proposes to design a wind turbine powered air compressor to transfer kinetic wind energy into compressed air energy for use in pneumatic tools. The design developed by the design team will be of a smaller scale than required by the final customer but will illustrate the feasibility of a larger scale design through its functionality and scalability. An illustration of the projected design is shown in Figure 5.4.

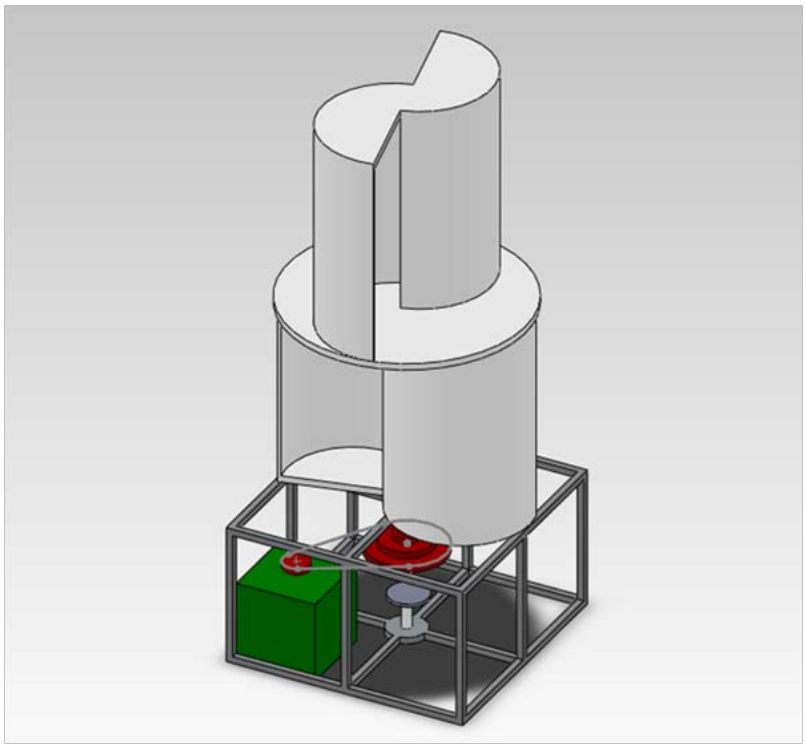

Figure 5.4: *CAD Sketch of the Proposed Solution*

5.6 Subsystems

The design features seven subsystems with each subsystem depending on other subsystems and each contributing to the overall success of the design. The subsystems (Figure 5.5) include: turbine blades, turbine drive shaft, compressor, gearing, braking, electronic monitoring, and base housing. Subsystems are assigned to team members who are responsible for the design and fabrication of their respective subsystem. Figure 5.6 shows the interdependence of each subsystem on the other subsystems.

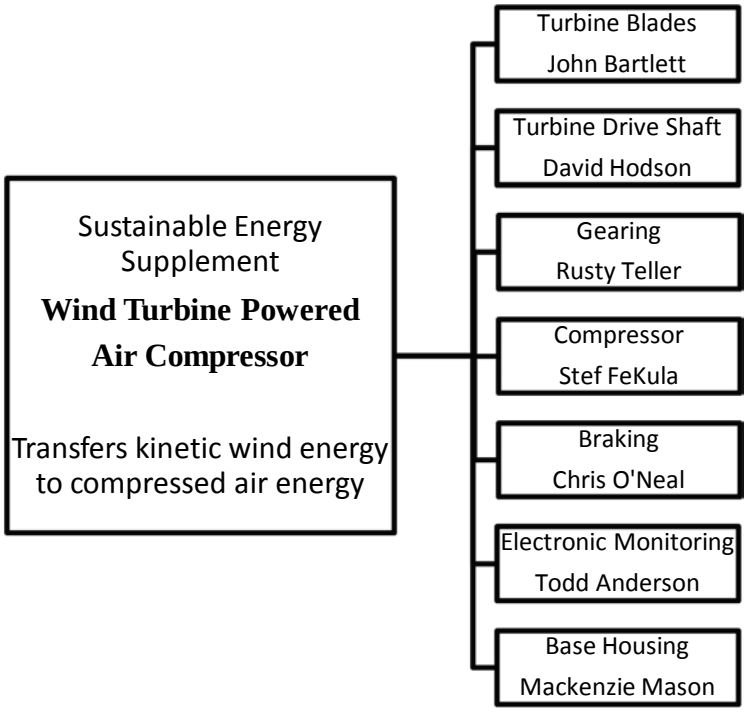

Figure 5.5: *Proposed Solution Subsystems*

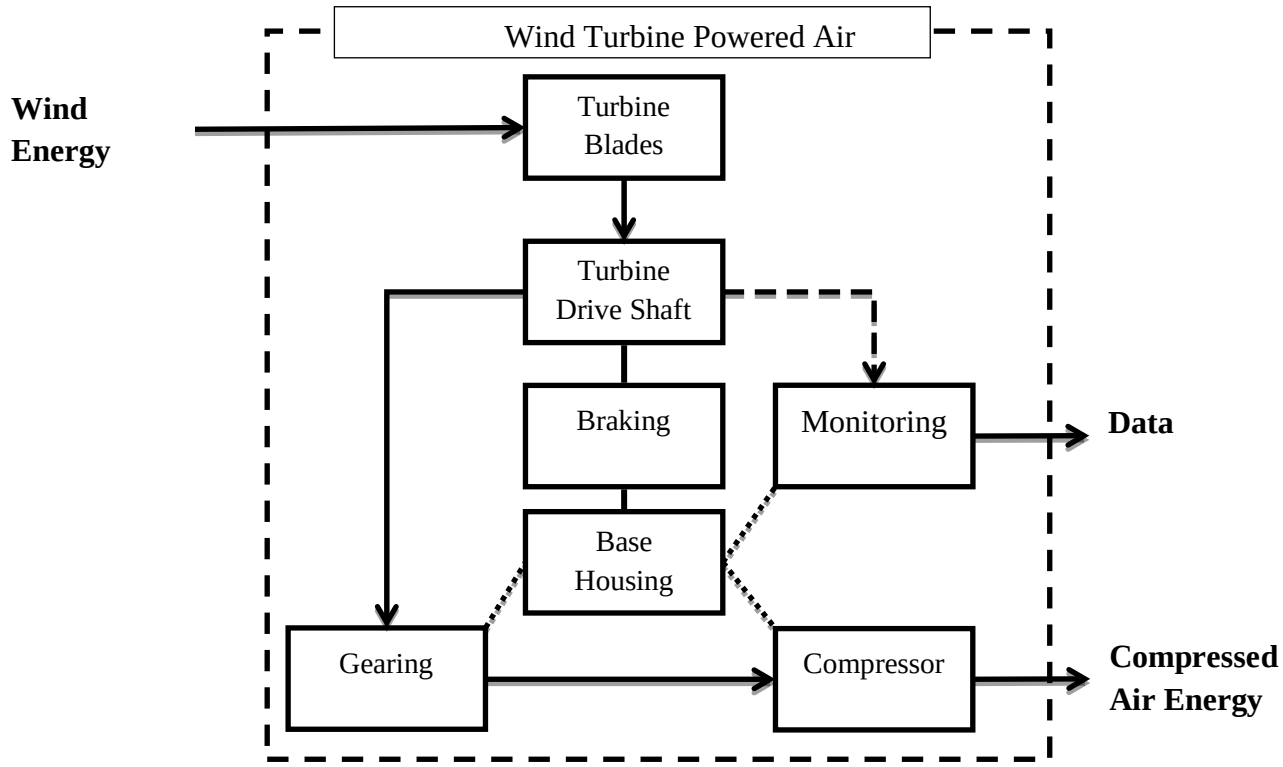

Figure 5.6: *Subsystem Dependencies and System Inputs/Outputs*

5.7 Feasibility

5.7.1 **Modularity/Simplicity**

The proposed solution features discrete subsystems with each subsystem having defined objectives and requirements. Because each subsystem will accomplish its minor objectives without dependence on another subsystem, issues arising in the development of one subsystem will not affect the other subsystems. This allows team members to work independently with minimal problem resolution among neighboring subsystems. The proposed solution also incorporates components that are physically simple and can be manufactured using facilities available to the development team. Components requiring more sophisticated machinery for manufacture, such as electronics and bearings, are readily available for purchase from manufacturing companies.

5.7.2 **Scalability**

The wind turbine powered air compressor proposed has the ability to be scaled without the removal or introduction of completely new subsystems. Scaling of the design would be done with the purpose of altering the rate of energy collection at a certain wind speed. To increase the

rate of energy collection, larger turbine blades could be implemented along with a higher torque conversion gearing subsystem and a suitable compressor. Adjustments in the measurements of supporting structural pieces would also need to be made to accommodate the changes in component properties.

The proposed design has the ability to be connected to a compressed air system in parallel with other air compressors, regardless of the source of power utilized by the other compressors. Therefore, the design proposed can supplement any compressed air system operating at or below its maximum output pressure. For example, a customer seeking to increase the output of their compression system can do so by installing the team's solution and connecting it to the existing air system.

5.7.3 Member Capabilities

The wind turbine powered air compressor proposed by the team requires expertise in a variety of fields including aerodynamics, static and dynamic mechanics, electric circuits, materials, and fabrication. The group is composed of members with the necessary expertise to design and construct the proposed solution. Three team members major in the field of Aeronautical Engineering and will provide input into the design of the turbine blades. Three team members major in the field of Mechanical Engineering and, with this expertise, can provide design input for the turbine drive shaft, gearing subsystem, compressor, and base housing. One team member is majoring in Electrical Engineering and will design the electronic monitoring system. One team member is majoring in Materials Science and will provide input into the materials selection process. Several members have experience in general fabrication, which will be sufficient for the team's design.

6 Subsystems

6.1 Turbine

The turbine subsystem is responsible for capturing the kinetic energy of the incoming wind flow in order to create a torque about the drive shaft. It must be able to do this at low wind speeds from any direction and be constructed with a structure capable of withstanding 70 mph wind speeds. Since this product is intended to offset the cost of compressed air for business owners, an efficient design with a high coefficient of power may not in fact be the best turbine to select. If a larger, less efficient turbine can output the same power at a lower cost, this design would more effectively fulfill the customer needs.

The results of the overall concept selection process yielded a two-step Savonius turbine design. In order to optimize the shape and dimensions of this turbine, a combination of research and experimentation with prototypes was used. Three different possible configurations were discovered during research, and selected for prototyping. These include the standard Savonius turbine consisting of two overlapping half cylinders, the standard turbine with the addition of

one-way flaps, and a modified design with a shallow blade shape. Prototypes were constructed out of corrugated cardboard and polyethylene terephthalate and tested in a rudimentary wind tunnel. Due to limited resources available for testing, the metric used to assess the performance of the three configurations was maximum RPM.

***Figure 6.1**: Prototypes; Top View (Left) and Side View (Right)*

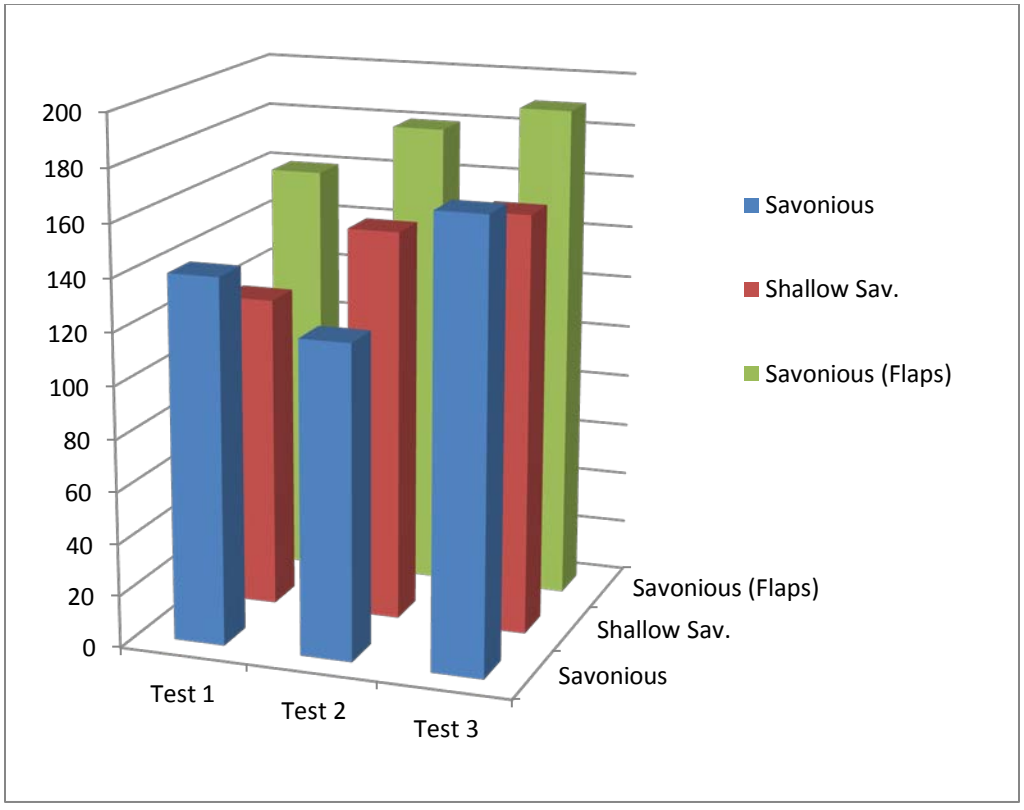

***Figure 6.2**: Small Scale Turbine Data*

Although the data is imperfect, it shows that all three configurations are likely to be similar in terms of power output. The standard design with the addition of one way flaps was selected since the experimental data suggested it would outperform the other two designs. Also, theoretical analysis and consultation with senior undergraduates who have experience in aerodynamics confirmed that a flapped design would yield more torque and power than a standard Savonius wind turbine. Figures 6.3 and 6.4 illustrate this. The torque about the drive shaft is created due to the greater drag force on the right blade than the left. Decreasing the drag force on the left blade would increase the torque and power output of the turbine. Assuming the drag force is mostly due to pressure drag, the resultant force is simply the integral of pressure over the surface area of the blade. Therefore, to reduce the drag force, the design needs to be modified to either reduce the pressure differential across the blade or reduce the frontal area of the blade. One-way flaps incorporate both of these effects by allowing air to flow from the high pressure outside of the blade to the low pressure interior. In addition, the flaps act as windows, reducing frontal area of the blade. These flaps are hinged such that they only open and reduce drag when the turbine blade is oriented with the convex side facing the incoming flow. The flaps are also hinged on the side closest to the drive shaft. This is important since it aligns the flaps with the streamlines as shown in Figure 6.4 and does not interfere with the flow in the overlap region.

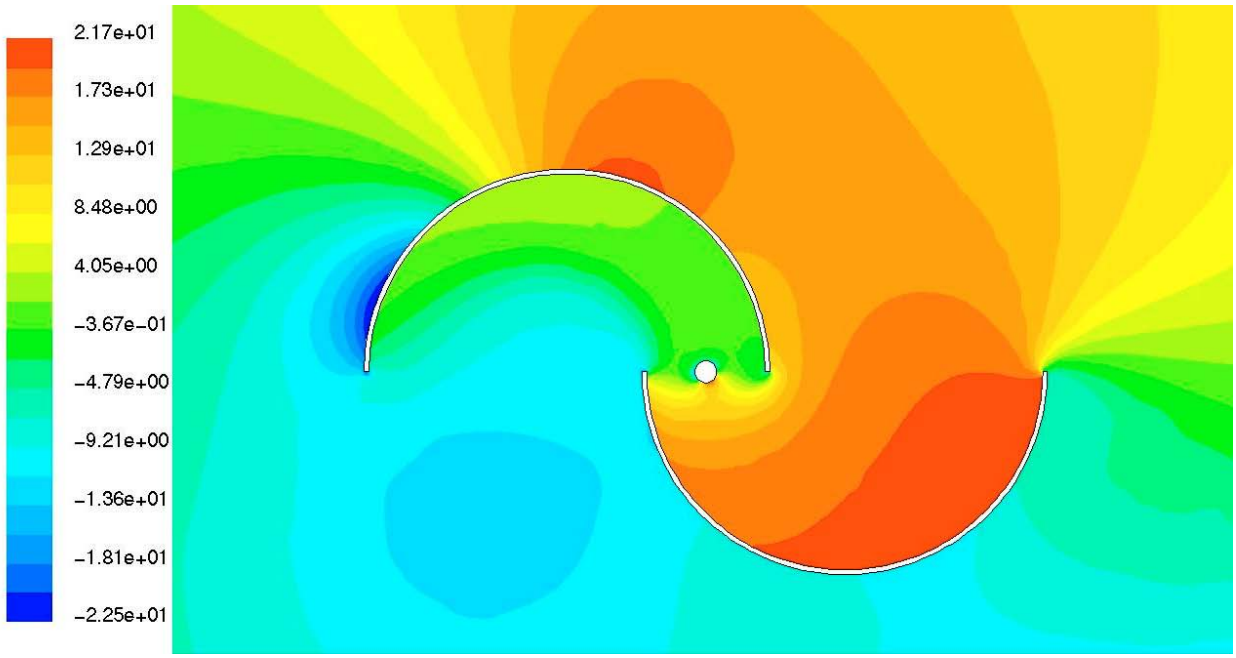

***Figure 6.3**: Pressure Distribution at Re=1.56*10^6*

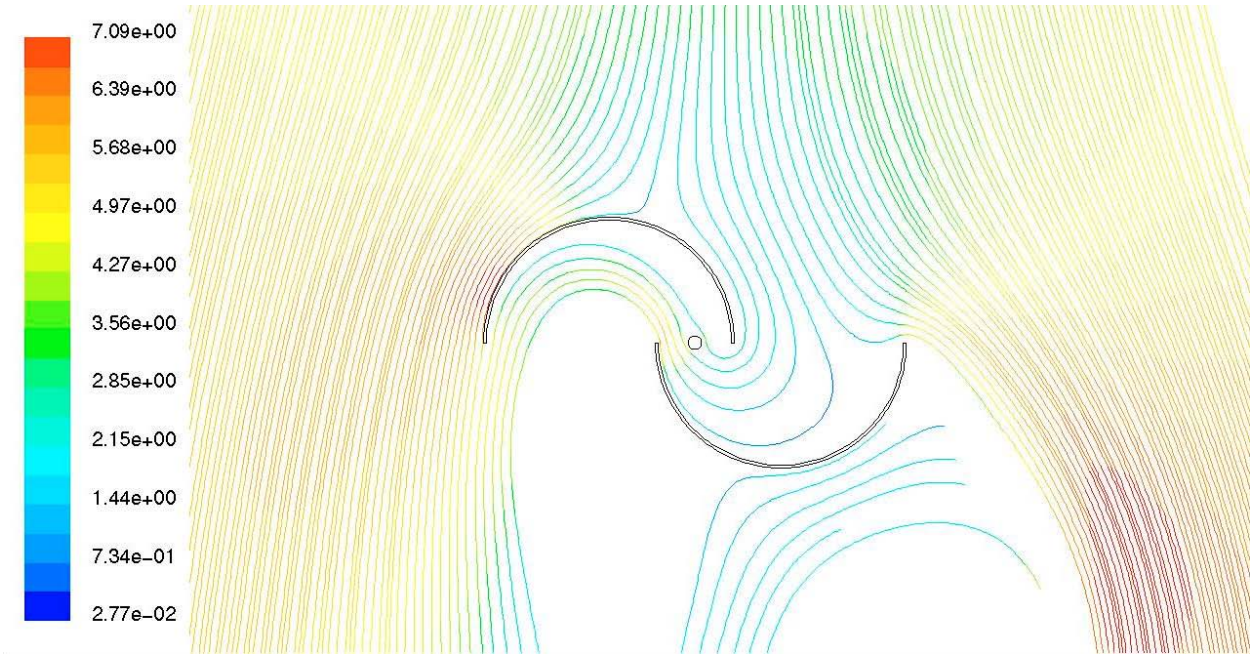

***Figure 6.4**: Streamlines at R_e = 1.56*10⁶ and v = 5 m/s*

The dimensions of the turbine were based directly off the product's technical specifications. For purpose of demonstrating the feasibility of the product, the turbine was designed to be as large as possible while still meeting the technical specification of being able to fit through an 80 inch by 30 inch door frame. Thus, the diameter of the turbine assembly was set at 29 inches. According to preliminary research, the optimum overlap ratio, the result of dividing the blade overlap "e" in Figure 6.5 by the diameter of the blades is approximately 0.242. Using this information the optimum turbine blade diameter is 15 inches. In addition the blade height needs to be similar to the blade diameter for the optimum turbine design. As such, the blade height (also the height of each step of the turbine) is 18 inches. This was also based on structural concerns for the drive shaft since the bending moment, maximum stresses, and deflection will increase exponentially with the height of the turbine.

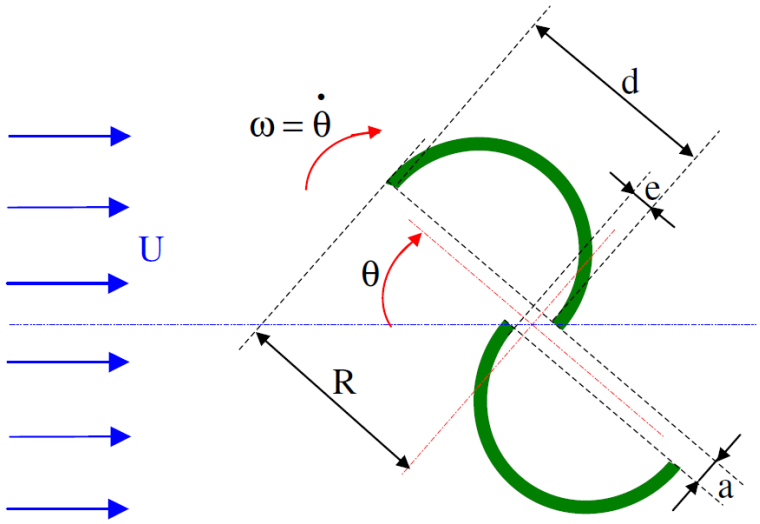

***Figure 6.5**: Savonius Turbine Defining Dimensions*

A selection matrix was created for the various turbine material choices. The options were rated on a scale from 1-5. Cost is the most important category since the critical technical specification is payoff period, a metric directly related to the cost of production. In explanation of some of the selection scores, Aluminum's low score was the result of its high cost and difficulty in welding. Wood was effectively ruled out by the difficulty in creating curved surfaces such as the blades and the possibility of deterioration with time. The top two material choices were selected for further cost analysis as seen in Table 6.1.

***Table 6.1**: Materials Selection Matrix*

Criteria	Cost	Feasibility	Durability	Weather Resistance	Total
Weight	30%	20%	25%	25%	**100%**
Aluminum	1	3	3	5	**2.9**
PVC	3	4	2	4	**3.2**
Steel	3	4	4	3	**3.45**
Wood	4	3	2	2	**2.8**

By comparison, the sheet of mild carbon sheet steel purchased for constructing the turbine costs $45 compared to more than $200 for the comparable PVC. Steel is also more rigid, durable, and easier to assemble through welding. Thus sheet steel was selected as the material for the turbine.

It should be noted that the team initially considered using a material which was already cylindrical in shape for the turbine. However, PVC piping was the only material available in compatible dimensions and was prohibitively expensive; 16 inch diameter PVC pipe costs $58.31 per foot length and at least three feet would be necessary for the complete turbine. This would represent almost half the budgeted cost of the turbine, and was deemed unacceptable.

Finite element analysis (FEA) was also performed on the turbine assembly to optimize the thickness of the sheet steel. Figure 6.6 shows the results of this stress analysis under a few simplifying assumptions. First the wind loading was calculated for all four individual blades. For the blades oriented concave side, convex side, and parallel to the flow, coefficients of drag of 2, 1, and 0.8 were assumed respectively. The density of the flow was assumed to be 1.225 kg/m^3 and the free stream velocity was 70 mph, approximately 32 m/s. The connection to the drive shaft was assumed to be fixed and the effects of gravity were included. In addition, the wind loading force was evenly distributed over the face of the blades.

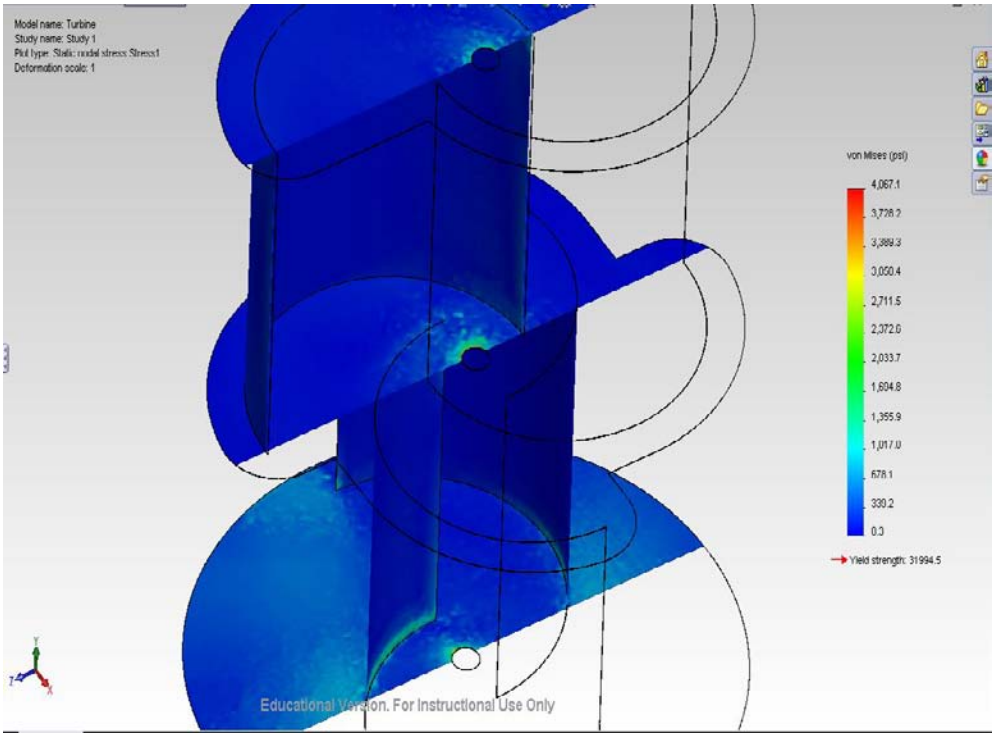

***Figure 6.6**: Finite Element Analysis of the Turbine Assembly*

The results in Figure 6.6 are for blades and mounting plates of 0.03 inch thickness, which corresponds to 22 gauge sheet steel. This is the thinnest and most inexpensive sheet steel still considered weld-able. As the FEA shows, the factor of safety for this thickness is 8 at 70 mph. This is more than sufficient and thus 22 gauge steel was selected as a material.

Finally, the abrasive water jet was the only option available for cutting the sheet steel and used to create the blades directly from the CAD files created by the team. A Hobart 140 amp flux core welder was used for assembly of the blades and mounting plates and flanged shaft collars were used to mount the assembly to the drive shaft.

The flaps needed to be constructed from a flexible, inexpensive, and weatherproof material. 1/16 inch thick vinyl rubber fulfilled all of these criteria and was thus selected for use on the turbine.

6.1.1 Challenges

The major challenge encountered for the turbine subsystem was the manufacturing of the mounting plates and blades. The CNC plasma cutter would have been ideal for cutting the contours out of sheet steel since it is free to use, has a one day turnaround, and the team had previous experience in its use. Unfortunately, the plasma cutter was non-functioning due to a broken part and it was uncertain when it would be operational again. The abrasive water jet (AWJ) was used instead as the next best choice for cutting sheet material. The downsides of this process compared to the plasma cutter included the cutting fee of $24 and the exposure of the sheet steel to moisture, causing premature corrosion. However, the AWJ did yield a cleaner cut and ultimately resulted in a higher quality product with lower tolerances.

In addition, the method of mounting the turbine to the drive shaft was an issue that required the team to seek out the advice of more experienced engineers. Initially, the team planned to weld the turbine to the drive shaft. However, Tony Peto, a Senior Mechanical Engineer and member of Formula Hybrid, pointed out that this would be very difficult to align and weld due to the difference in thickness of the materials. It would also make modification and disassembly of the product difficult. He suggested the use of flanged shaft collars, which would allow the turbine to be bolted to the drive shaft instead. This simple alternative was selected for the final design.

Another challenge was encountered in the assembly of the turbine. Welding thin sheet metal often results in thermally induced stress, which can and did warp the material. While this did not diminish the structural integrity of the turbine, it reduced its aesthetic quality. In an industrial environment, a large copper or aluminum heat absorbing fixture would be used to absorb the heat created during welding and prevent warping.

6.1.2 Results

The turbine subsystem met or exceeded all of its requirements. It was self-starting at low wind speeds from any wind direction, namely 3-4 mph when unloaded and 8 mph when connected to the air compressor. It also did not deform under wind loading.

***Table 6.2**: Cost of the Turbine Subsystem*

Item	*Unit Price*	*Quantity*	*Item Total*	*Actual Cost to Team*
32 sq ft of 22 Gauge Steel	$45.00	1	$45.00	$45.00
Threaded Shaft Collar	$7.98	3	$23.94	$23.94
3 sq ft of PVC Rubber	$15.90	1	$15.90	$15.90
Water Jet Cutting	$24.00	1	$24.00	$24.00
Shipping	$19.48	1	$19.48	$19.48
Total				**$128.32**

6.2 Drive Shaft

6.2.1 **Objective**

The purpose of the drive shaft system is two-fold. First, the system must bring the kinetic energy captured from the wind by the turbine subsystem to the gearing and compression subsystems without deformation. Second, the drive shaft system must support the weight of the turbine without deformation at the highest speed specification of 70 mph.

6.2.2 **Dimensions**

The drive shaft itself is a 1 inch diameter general low carbon steel tube that is 4 feet long. The shaft is supported primarily by a steel plate at the top of the base and by a flange bearing at the bottom of the shaft. The rotation of the shaft is allowed by a covered steel thrust bearing secured by aluminum blocks at the top of the base and by the flange bearing at the bottom. Figure 6.7 below shows the entirety of the system as it was assembled.

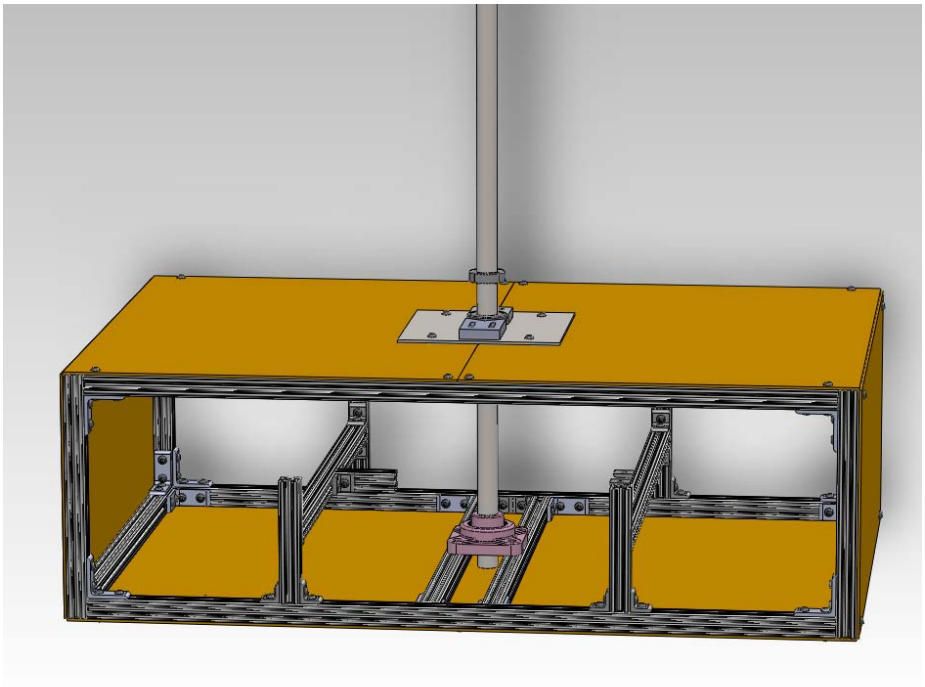

***Figure 6.7**: CAD Model of the Drive Shaft Subsystem,*

6.2.3 **Challenges**

Two issues arose in the construction of this subsystem. The first was how well the chosen material would endure the highest technically specified wind speed, and the second was how to effectively constrain the ball bearing that allows rotation of the shaft at the top support.

The material chosen for the drive shaft is based on a mechanical evaluation of the forces incident on the proposed designed. Prospective customers stated that the final product must be

able to withstand winds of up to 70 mph. With the proposed design's shape, the component with the greatest strain placed upon it by the force of a 70 mph wind is the drive shaft of the turbine. Of all of the pieces of the design, it must have the greatest rigidity and must yield the least to incoming forces. The force of the wind incident on the design can be calculated with the use of Equation 6.1:

$$F_D = \frac{1}{2}\rho v^2 C_d A,$$

Equation 6.1: *Force from Incident Wind*

In Equation 6.1, F_d is the total incident force, ρ is the density of incoming air, v is the velocity of incoming air, C_d is the coefficient of drag of the object, and A is the area being acted on by the wind. For the purposes of this calculation, the drag coefficient of the design is approximated to the worst-case scenario of 2, which is the drag coefficient of an entirely flat surface. The turbine is also approximated as a 2 x 2 x 3 foot rectangular prism to estimate the worst case scenario possibly encountered.

$$F_d = \frac{1}{2} \times 1.2041 \times 31.2928^2 \times 2 \times (.6069 \times .9144)$$

Equation 6.2: *Force from Incident Wind (evaluated)*

This result of Equation 6.2 is an incoming force of 667.253 N. From this force, the required Young's modulus of the drive shaft is calculated through approximating the drive shaft as a cantilever beam with a uniformly distributed load (Figure 6.8). Delta is the max deflection, omega is the distributed force on the member, *l* is the length of the beam, E is the Young's modulus, and *I* is the second moment of area.

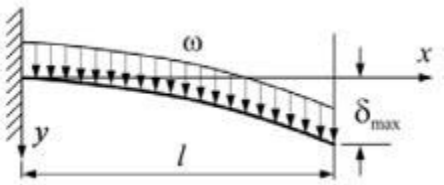

Figure 6.8: *Diagram of Cantilever Beam with Distributed Load*

For a Cantilever beam of this type, the Equation 6.3 is used to find the maximum deflection of the beam.

$$\delta_{max} = \frac{\omega l^4}{8EI}$$

Equation 6.3: *Maximum Deflection for a Cantilever Beam with Distributed Load*

Solving Equation 6.3 for E yields Equation 6.4, which can be used to find the Young's modulus required for the turbine drive shaft when a 70 mph wind is incident on it.

$$E = \frac{\omega \times l^4}{8 \times \delta_{max} \times I}$$

Equation 6.4: *Young's Modulus for a Cantilever Beam with Distributed Load*

All variables of Equation 6.4 are known with the exception of the second moment of area, which for a tube is defined in Equation 6.5. J_{zz} is the second moment of area, D_o is the outside diameter, D_i is the inside diameter, r_o is the outside radius, and r_i is the inside radius:

$$J_{zz} = \frac{\pi}{64}(D_O{}^4 - D_I{}^4) = \frac{\pi}{4}(r_O{}^4 - r_I{}^4)$$

Equation 6.5: *Second Moment of Area for a Hollow Cylinder*

By substituting known values into Equation 6.4 and assumptions of a 2 inch diameter drive shaft with ¼ inch thick wall, allowing 5 mm in deflection, and 3 feet in length, Equation 6.6 is found.

$$E = \frac{718.781 \times 0.9144^4}{8 \times 0.005 \times \frac{\pi}{64}(0.0508^4 - 0.0381^4)}$$

Equation 6.6: *Maximum Deflection of Theoretical Drive Shaft (evaluated)*

The result of Equation 6.6 is a Young's modulus of 56.21 GPa. This information can be applied to the diagram of Young's Modulus vs. Density from Ashby's Materials Selection in Mechanical Design (Figure 6.9), from which it is clear that a steel alloy would be appropriate for this subsystem.

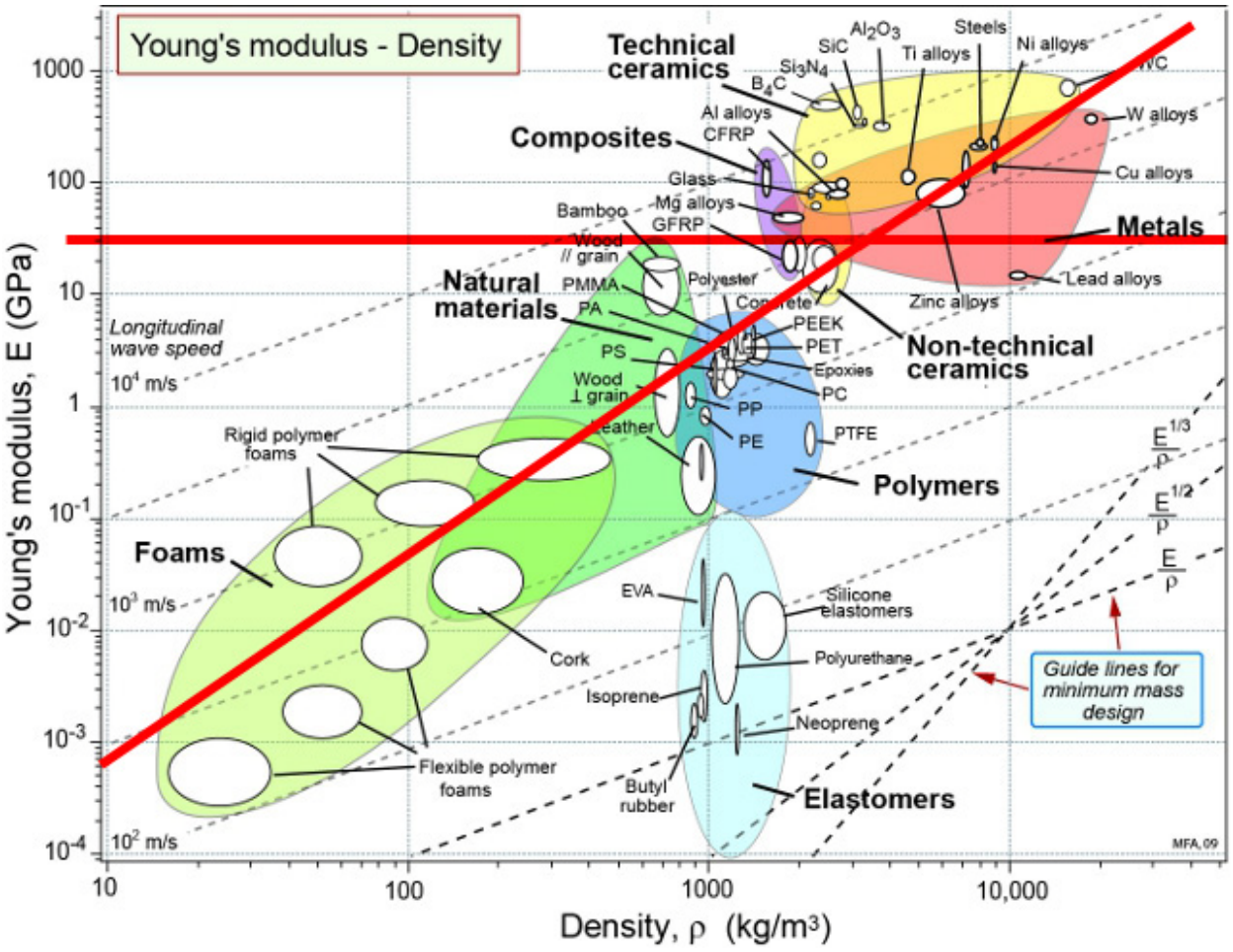

***Figure 6.9**: Modulus vs. Density table - Modified to show requirements*

CAD program simulations of the drive shaft system at the most strenuous conditions allowed in the technical specifications showed that the general low carbon steel used to construct the shaft is not sufficient to withstand the applied forces. Seen in figure 6.10 below, the maximum applied force on the shaft at its most vulnerable point in its design has a stress of just below 50,000 psi incident upon it. The maximum stress that general low carbon steel is capable of withstanding is roughly 30,000 psi. This information indicated to the design team that a different material choice had to be made to meet the technical specifications.

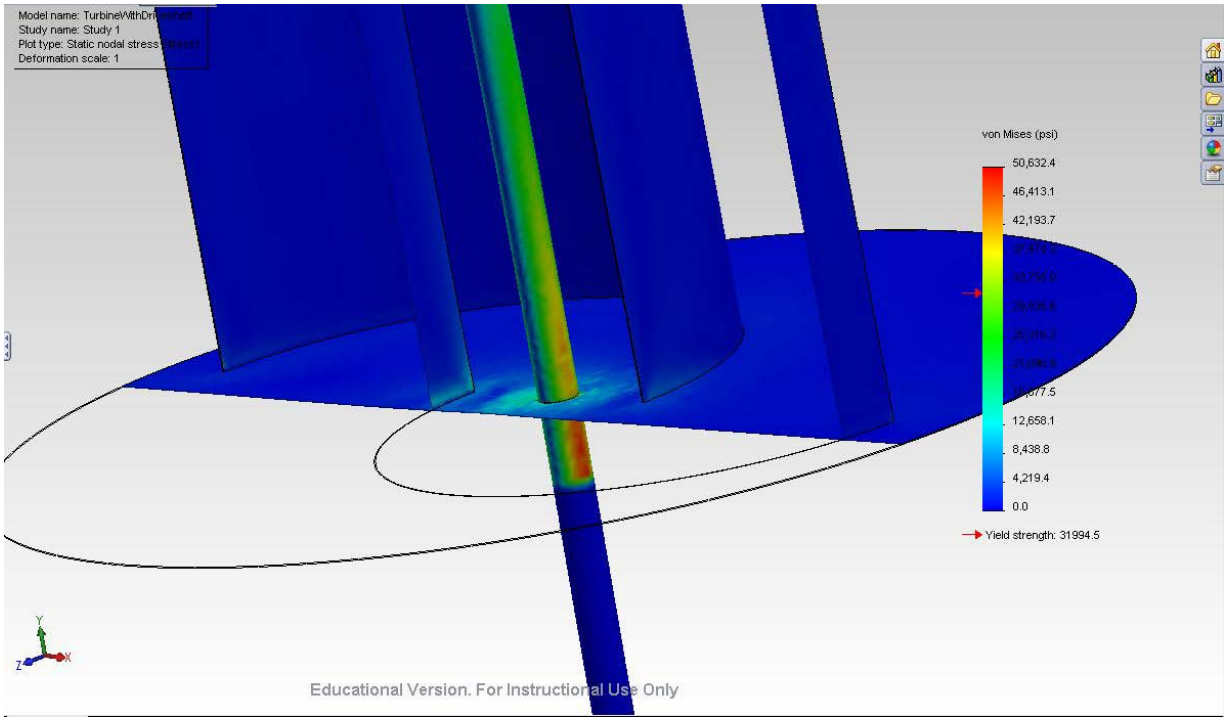

***Figure 6.10**: CAD simulation of force on the drive shaft at top support*

From research, steel alloy 4130 is an ideal choice for the drive shaft. It meets the young's modulus qualifications in addition to meeting the strength requirement evident from above. The strength rating of steel alloy 4130 is 50,000 psi, which puts it above the maximum observable stress in Figure 6.10 above. Steel alloy 4130 wasn't used in the prototype, however, because of its cost, which is nearly triple that of the low carbon steel used, at $32.60.

The second issue from above that needed to be addressed was constraining the ball bearing associated with the top support. To find a solution to this problem, Professor William Foley was consulted to find an ideal mechanical arrangement that would be both easy to machine as well as able to fully support the ball bearing. In Figure 6.11 below is a CAD rendering of the assembly suggested by Professor Foley.

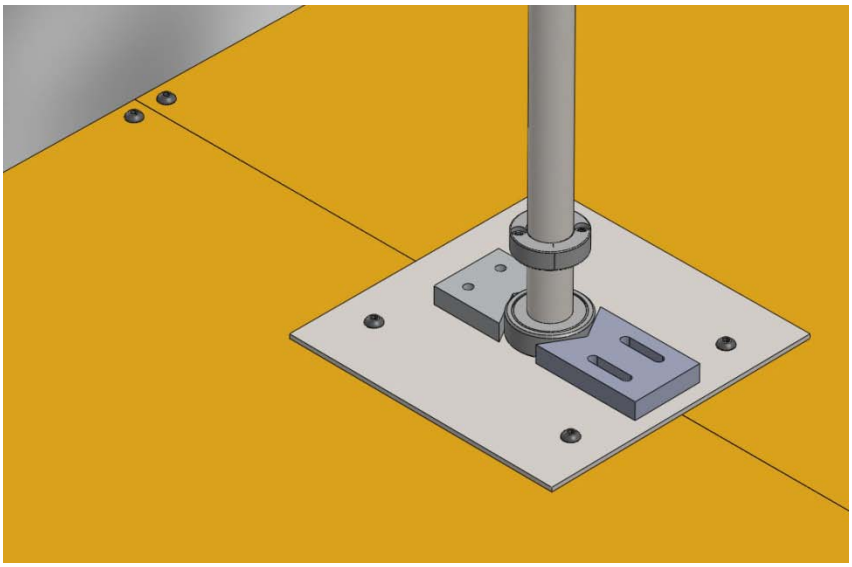

***Figure 6.11**: CAD model of ball bearing assembly*

In this assembly, non-axial forces are constrained by aluminum blocks holding the ball bearing centered on the supporting steel plate. Aluminum was selected in constraining the blocks for its high strength as well as relative softness in comparison to the steel of the ball bearing. The aluminum blocks will also deform to the surface of the steel bearing, allowing the strength of the connection holding the bearing in place to increase over time.

In answering these design issues, the drive shaft meets the first of its objectives, which is to withstand the force of a 70 mph wind. It further meets its second objective through the use of precision-machined shaft collars fully supporting the weight of the turbine on the ball bearing, as shown in Fig. 6.11 above. With this, it is clear that the drive shaft meets all of its objectives and assigned specifications in its functioning.

6.2.4 **Expenses**

Below in table 6.3 is a list of each part ordered and used in the construction of the drive shaft subsystem.

***Table 6.3**: Expenses for the Drive Shaft Subsystem*

Item	*Unit Price*	*Quantity*	*Item Total*	*Paid For It?*	*Actual Cost to Team*
Low-Carbon Steel 6' long 1" OD tube	$11.78	1	$11.78	Yes	$11.78
1" ID Shielded Thrust Bearing	$20.26	1	$20.26	Yes	$20.26
Black Oxide steel 1" ID Shaft Collar	$3.27	2	$6.54	Yes	$6.54
Aluminum Sliding Holder Pieces	$10.82	1	$10.82	No	$0.00
Steel Plate (McMaster Price)	$27.54	1	$27.54	No	$0.00
Steel Plate (Scrap Price)	$6.00	1	$6.00	Yes	$6.00
Assorted Fasteners (Whole Project)	$20.00	1	$20.00	Yes	$20.00
Flange Bearing	$9.30	1	$9.30	Yes	$9.30
Total					**$73.88**

Each subsystem was given a $50 budget, and the drive shaft subsystem went over this budget by $23.88.

6.3 Monitoring Subsystem

6.3.1 **Overview**

The monitoring system collects real-time revolutions per minute (RPM) readings of the turbine drive shaft and displays this reading on a liquid crystal display (LCD). The main components of the monitoring subsystem are the detector, the base microcontroller, the display microcontroller, the display, serial communication, header connection, housing, and power connection. The general connection of each of these components can be seen below in Figure 6.12.

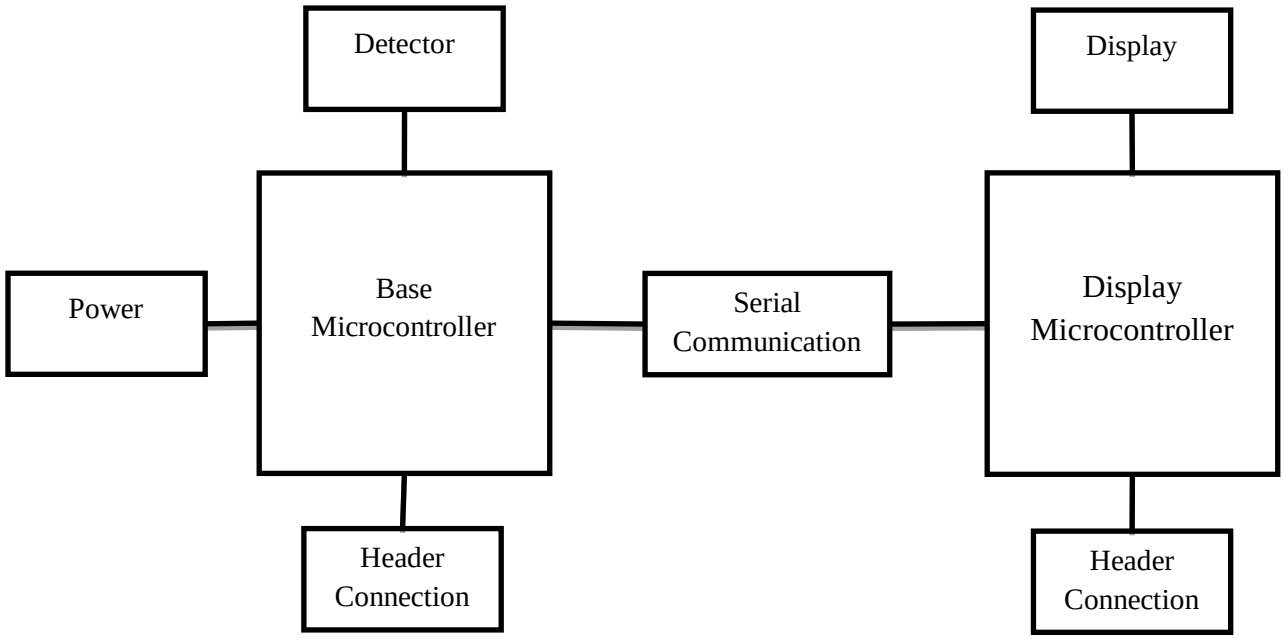

Figure 6.12: *Monitoring Subsystem Component Layout*

6.3.2 **Detector**

The detector of the subsystem is responsible for detecting the rotation of the drive shaft by generating an oscillating voltage for the base microcontroller to analyze. Frequency of the oscillating voltage generated is dependent on angular velocity or RPM of the brake disk, which is connected directly to the drive shaft. A contactless optical method is utilized featuring an infrared (IR) LED and an infrared (IR) transistor pointed at each other in a mount with a 0.75 inch gap. Infrared components are utilized so that light of the visible spectrum cannot interfere with the monitoring system's operation. Figure 6.13 shows the mount holding the IR LED and IR transistor. Figure 6.14 shows the circuit diagram of the detector.

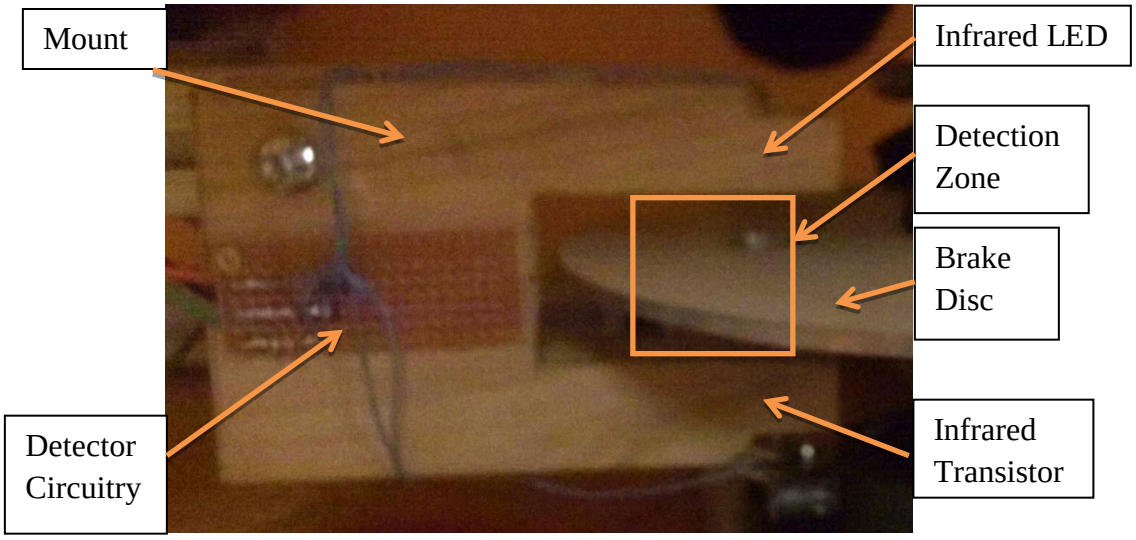

***Figure 6.13**: Picture of Wooden Mount*

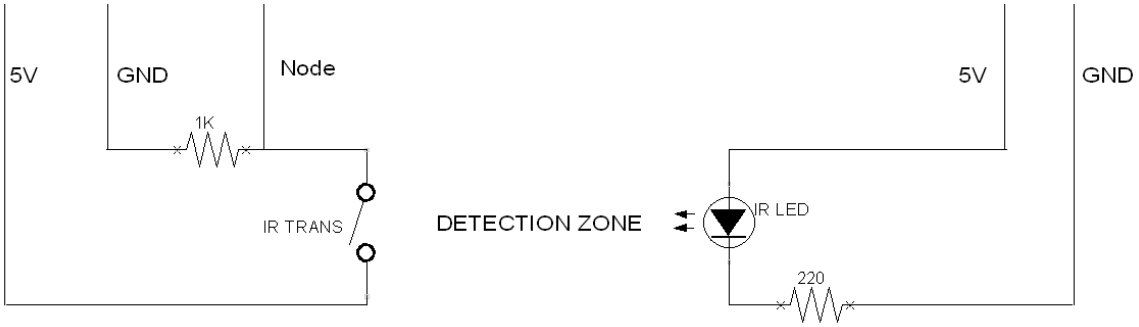

***Figure 6.14**: Detector Circuit Diagram*

The IR LED is rated to operate at a current of 0.022 A. Utilizing Ohm's law (Equation 6.7) a series resistance of 220 ohms was determined to provide the required amperage.

$$\frac{V}{I} = R \qquad \frac{5}{0.022} \approx 220$$

***Equation 6.7**: Ohm's Law*

When the detection zone between the IR LED and IR transistor is not obstructed, the voltage at the node is high relative to the voltage at the node when the zone is obstructed. This is caused by the IR transistor's resistance dependence on the intensity of IR light incident on it. To provide the base microcontroller with an oscillating voltage of the highest resolution, testing of the node voltage with respect to the series resistance of the IR transistor was performed. It can be seen from test data in Figure 6.15 that the highest resolution, or greatest difference between the unblocked and blocked node voltage, occurs when the series resistance is 1K ohms.

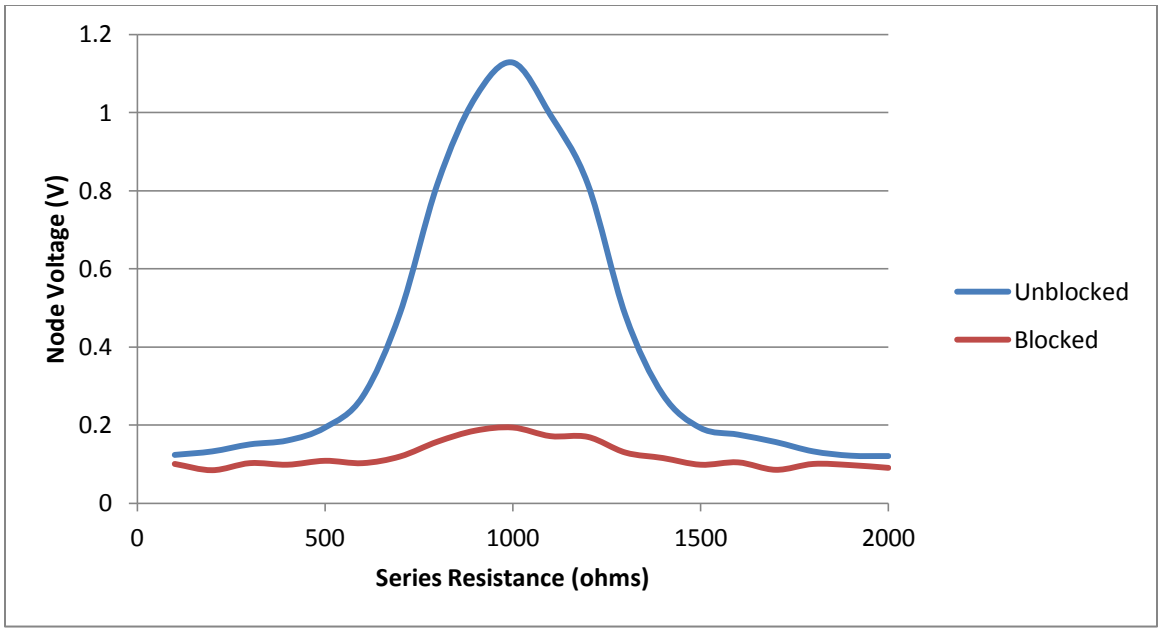

Figure 6.15: *Node Voltage vs. Series Resistance*

Oscillation of the node voltage occurs when the detection zone is repetitively blocked and unblocked. To accomplish this as the drive shaft rotates; the detector is positioned the brake disk, such that the 0.25 inch holes in the brake disk allow the detector to become unobstructed as they pass through it. This transition from a blocked state to an unblocked state and back leads to an oscillating voltage for the base microcontroller to analyze. An example of an oscillation is shown below in Figure 6.16.

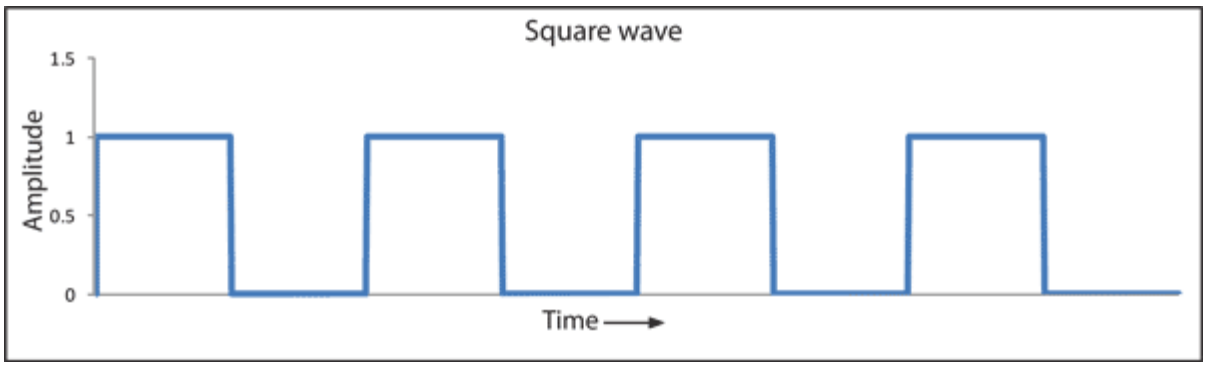

Figure 6.16*: Square Wave Oscillation (Mine Lab, 2006)*

6.3.3 Base Microcontroller

The base microcontroller circuit is responsible for analyzing the oscillating node voltage provided by the detector to determine the RPM of the drive shaft and transmitting this value to the display microcontroller. The specific microcontroller utilized is the ATmega328P-PU which features a clock speed of 16 MHz, 32 KB program memory, 23 input/output pins, and 6 analog-

to digital-conversion (ADC) pins. The ATmega328P-PU can be seen in Figure 6.17 below with its pinout following in Figure 6.18. (Atmel, 2009)

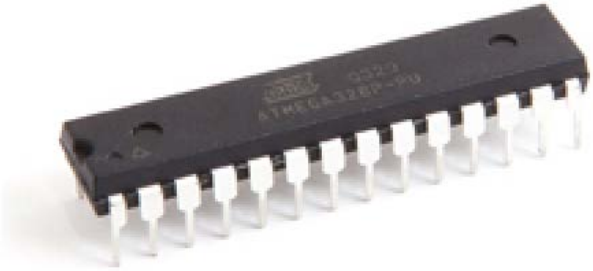

Figure 6.17: *ATMega328P-PU Integrated Circuit Chip (ATMega DIP Chip)*

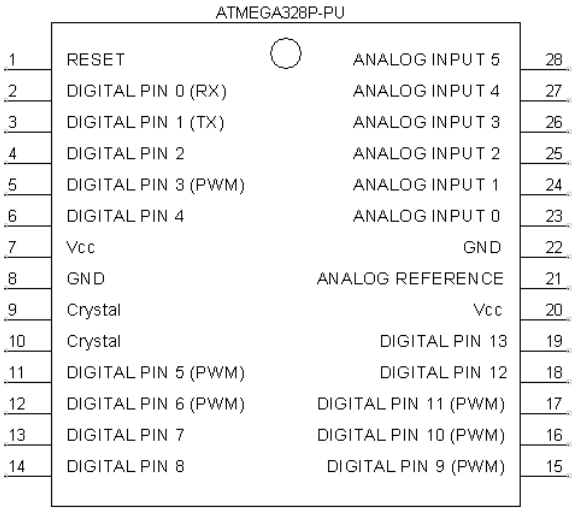

Figure 6.18: *ATMega328P-PU Pinout*

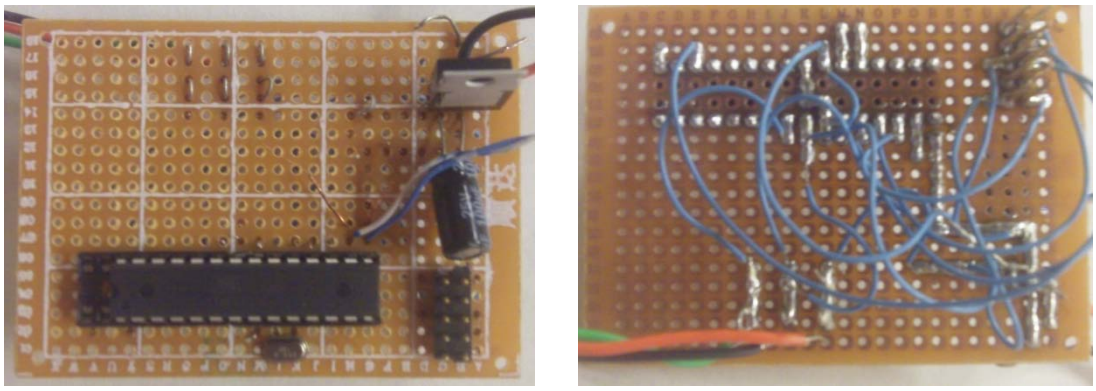

Figure 6.19*: Base Circuit Front and Back*

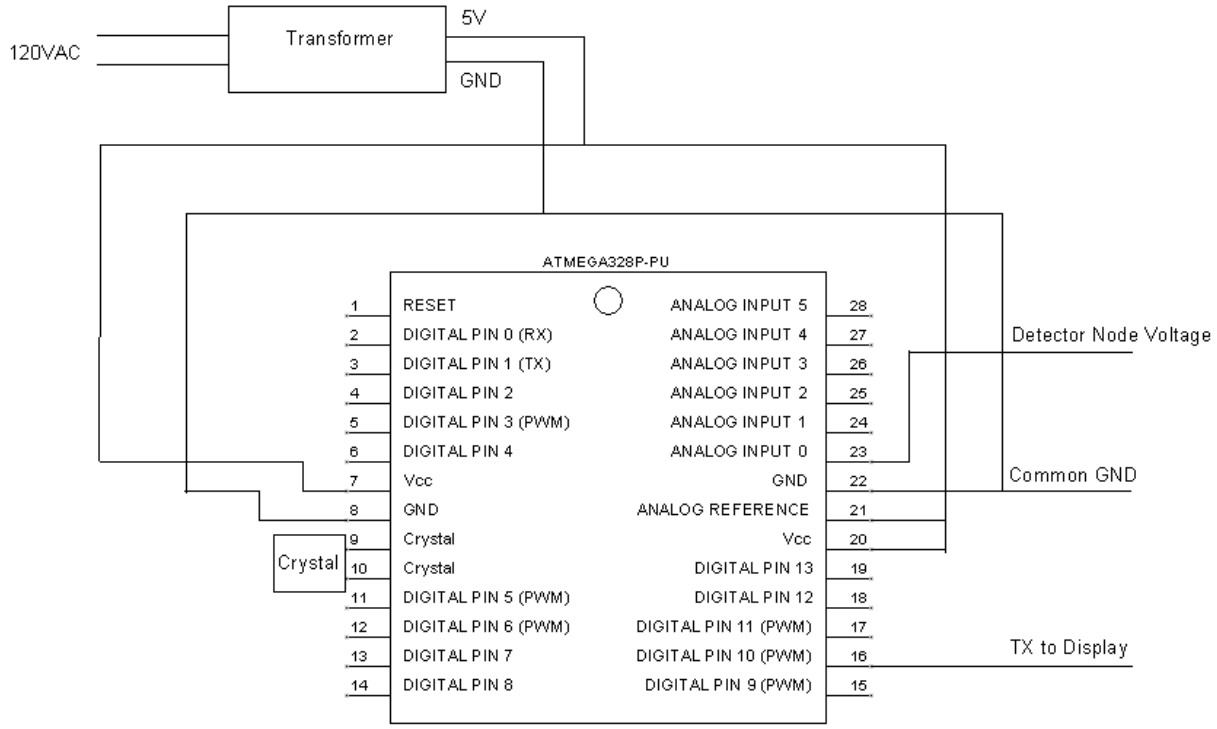

***Figure 6.20**: Base Microcontroller Circuit Diagram*

The circuit board created for the base microcontroller can be seen above in Figure 6.19 with a corresponding circuit diagram in Figure 6.20. The circuit board measures 2 x 3 inches. The microcontroller is placed within a microcontroller socket and connected to power and ground, an oscillating crystal for timing, a set of header pins for programming, serial connection, and the detector's node voltage. The node voltage of the detector is connected to analog-to-digital converter (ADC) pin 23 of the microcontroller so that it can be analyzed by the software of the microcontroller. Through the programming header connections, Arduino C code is uploaded to the microcontroller which drives the analysis of the node voltage.

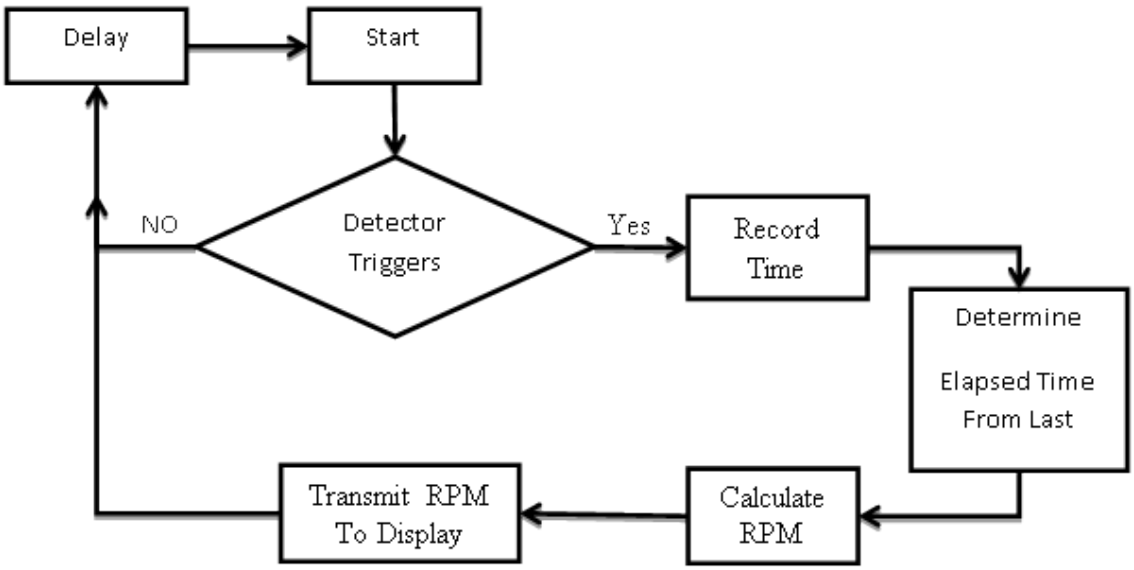

Figure 6.21: *Base Microcontroller Pseudo-code Diagram*

The base microcontroller pseudo-code diagram is shown above in Figure 6.21, while a full set of code can be found in Appendix I. The loop in the code of the base microcontroller is executed five thousand times per second. Within each iteration of the loop, the microcontroller determines if the detector has switched from a blocked state to an unblocked state. If the detector has triggered, the microcontroller compares the current time to the time of the previous trigger to calculate the elapsed time between the two triggers. Because the holes of the brake disk are situated 90 degrees apart, the RPM of the drive shaft can be determined from the elapsed time (in milliseconds) through Equation 6.8 below. The RPM value calculated is then transmitted to the display microcontroller via serial communication.

$$RPM = \frac{60000}{(Elapsed\ Time) * (\frac{360}{90})}$$

Equation 6.8*: RPM Calculation*

6.3.4 **Display Microcontroller**

The display microcontroller circuit is responsible for receiving the RPM reading value from the base microcontroller and displaying this value on the LCD display. An ATMega328P-PU microcontroller is implemented in the display circuitry seen below in Figure 6.22 and the corresponding circuit diagram in Figure 6.23. The circuit board measures 2 x 3 inches.

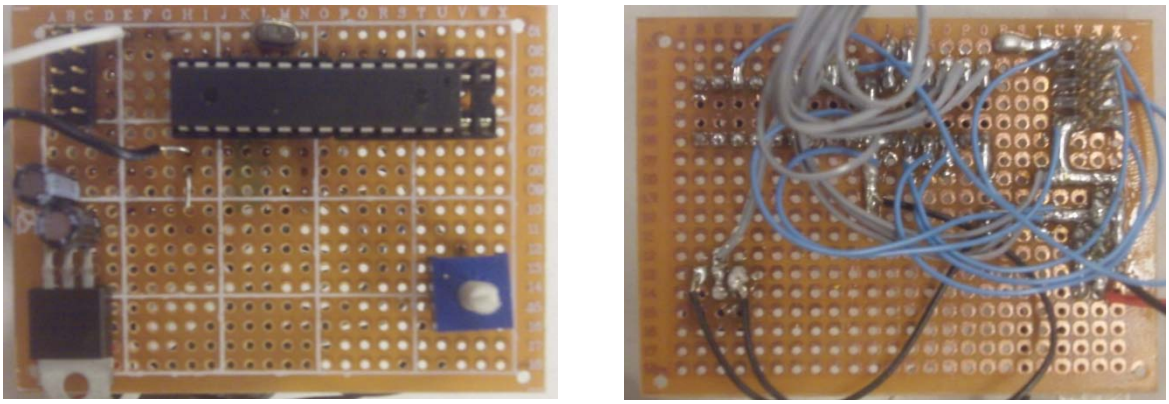

***Figure 6.22**: Display Circuit Front and Back*

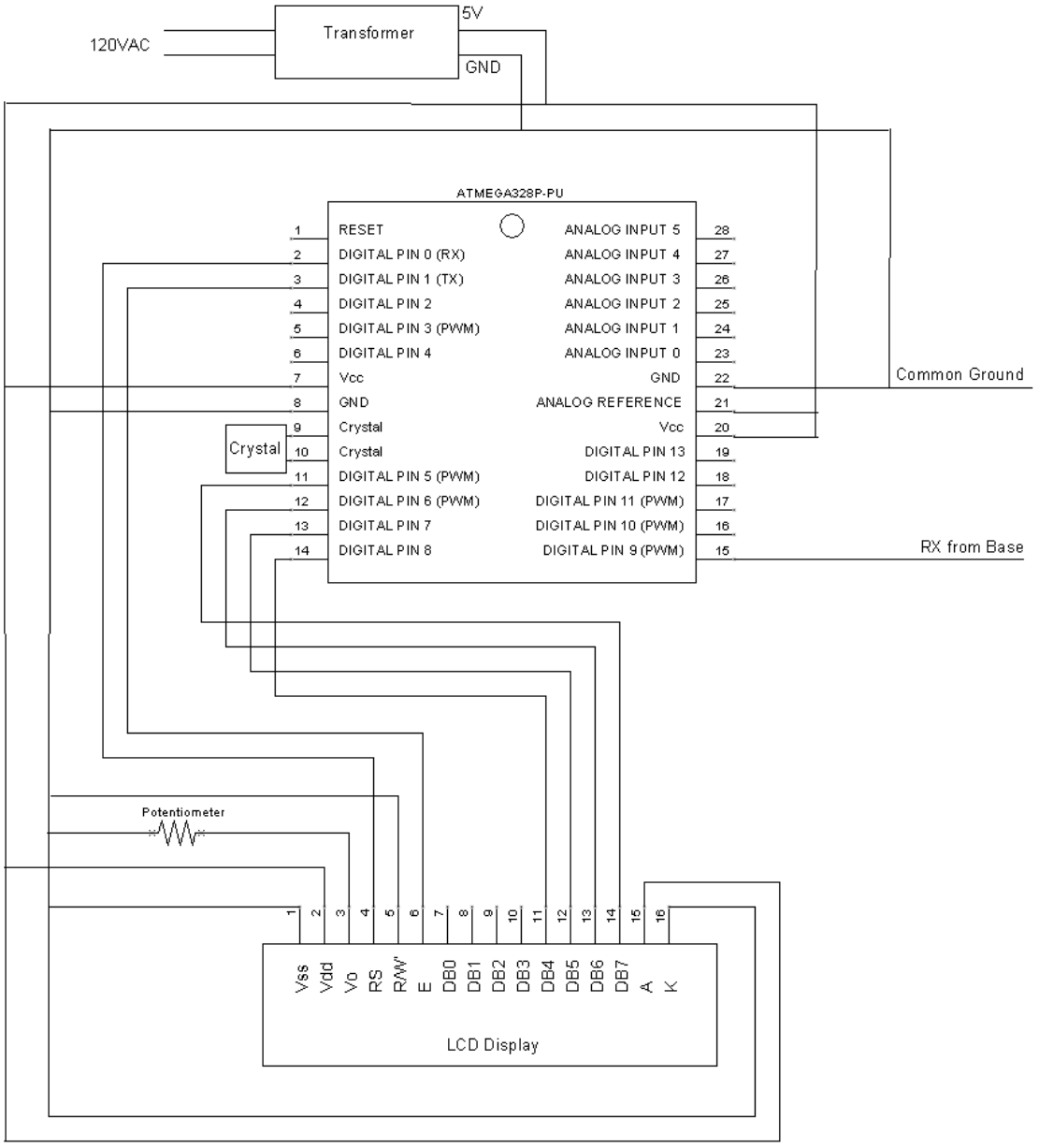

***Figure 6.23**: Circuit Diagram of Display Circuit*

The microcontroller is placed within a microcontroller socket and connected to power and ground, an oscillating crystal for timing, a set of header pins for programming, serial connection, and the LCD display ribbon cable. Through the programming header connections, Arduino C code is uploaded to the microcontroller which drives the LCD display.

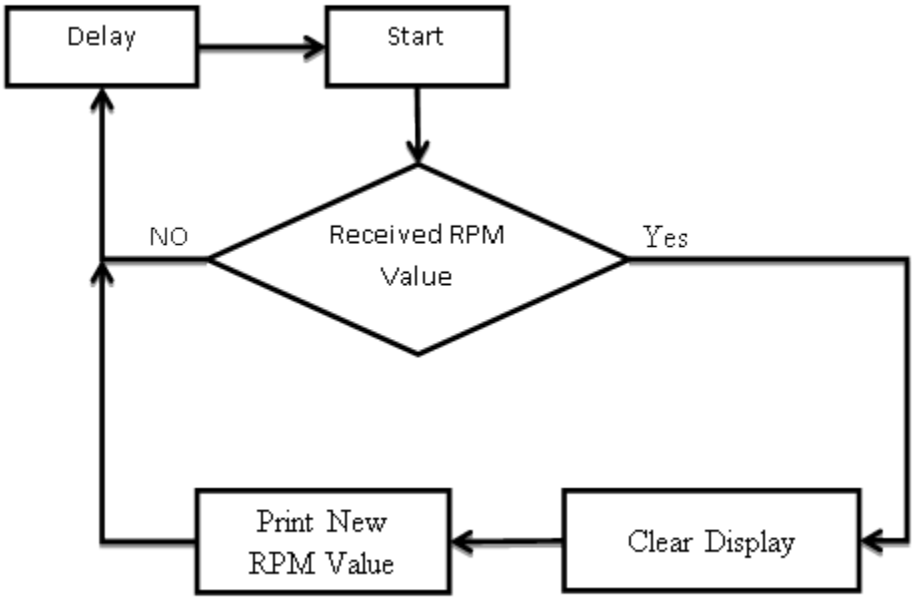

***Figure 6.24**: Display Microcontroller Pseudo-code Diagram*

The base microcontroller pseudo-code diagram is shown above in Figure 6.24, while a full set of code can be found in Appendix I. The above loop is executed ten times per second. With each iteration of the loop, the microcontroller checks if it has received an RPM value from the base microcontroller. If a new value has been received, the microcontroller clears the LCD display and prints out the new RPM value.

6.3.5 Liquid Crystal Display

The liquid crystal display (LCD) is responsible for displaying the current RPM reading of the turbine to the user. The specific LCD display utilized in the monitoring subsystem is the NHD-0216K1Z display by Newhaven Display. The display can display a maximum of 32 characters in a 2 x 16 character array. A picture of the display is shown below in Figure 6.25.

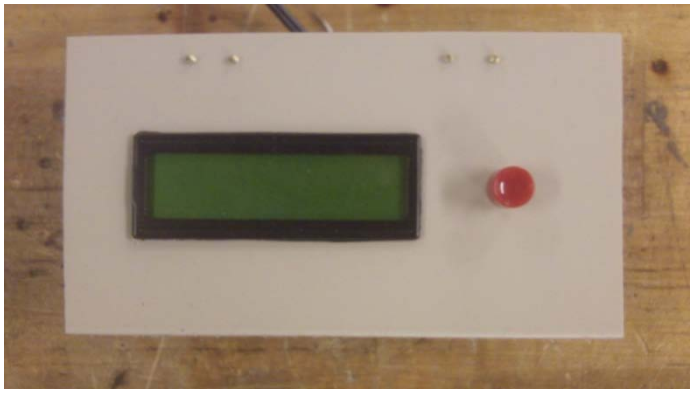

***Figure 6.25:** LCD Display in Housing*

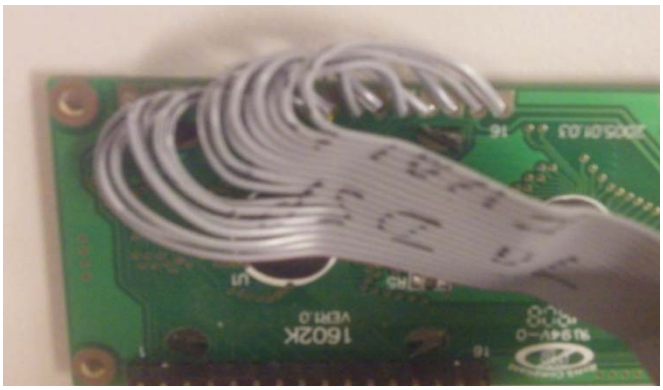

Figure 6.26: *LCD Display Ribbon Cable in Housing*

The LCD display requires twelve connections to function properly. Connections are used for power and ground, contrast control, and data transmission from the display microcontroller. A ribbon cable is connected to the LCD display on the back of the display housing as seen in Figure 6.26 above. For information regarding the ribbon cable connections, refer to the display microcontroller circuit diagram in Figure 6.23.

6.3.6 **Serial Communication**

Serial communication is the process of transmitting data from one device to another in which data bits are sent one after another on a single wire. This is different than parallel communication in which data bits can be sent at the same time on multiple wires. The type of serial communication utilized by the microcontrollers in the monitoring subsystem is one-way asynchronous communication at a data transmission rate, or baud rate, of 9600 bits/second. One-way serial communication is sufficient in this implementation because the base microcontroller's function is static and does not require feedback from the display. Figure 6.27 shows the pin connections between the base microcontroller and the display microcontroller. Two wires, a data transmission wire and a common ground wire, are required for data transmission.

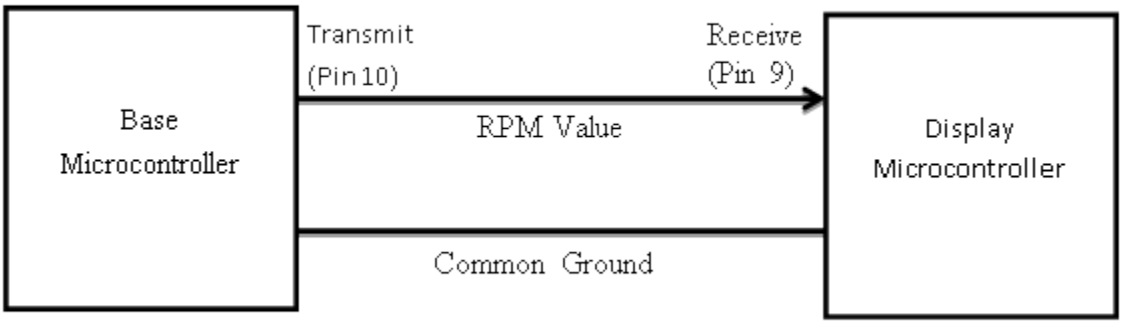

Figure 6.27: *Serial Communication between Microcontrollers*

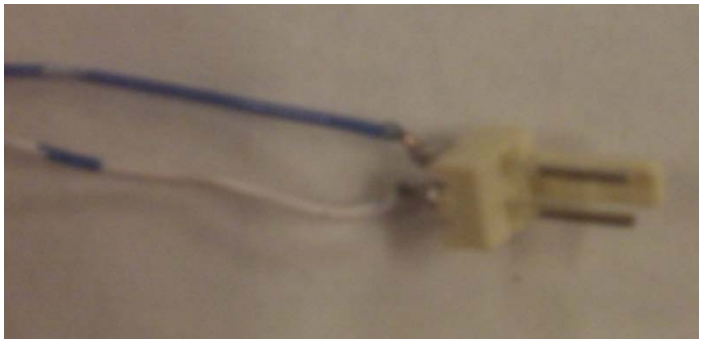

***Figure 6.28**: Serial Connector Wire*

6.3.7 **Header Connection**

The header connection is the set of ten pins located on each of the microcontroller boards of the monitoring system. The ten pins are arranged in a 2 x 5 array and are used for programming the Arduino C code onto the microcontrollers. The header connection is used only when a microcontroller needs to be reprogrammed and is not used by the customer. For this reason, the header connection will not exist in the final product. The header connection circuit diagram is shown below in Figure 6.29.

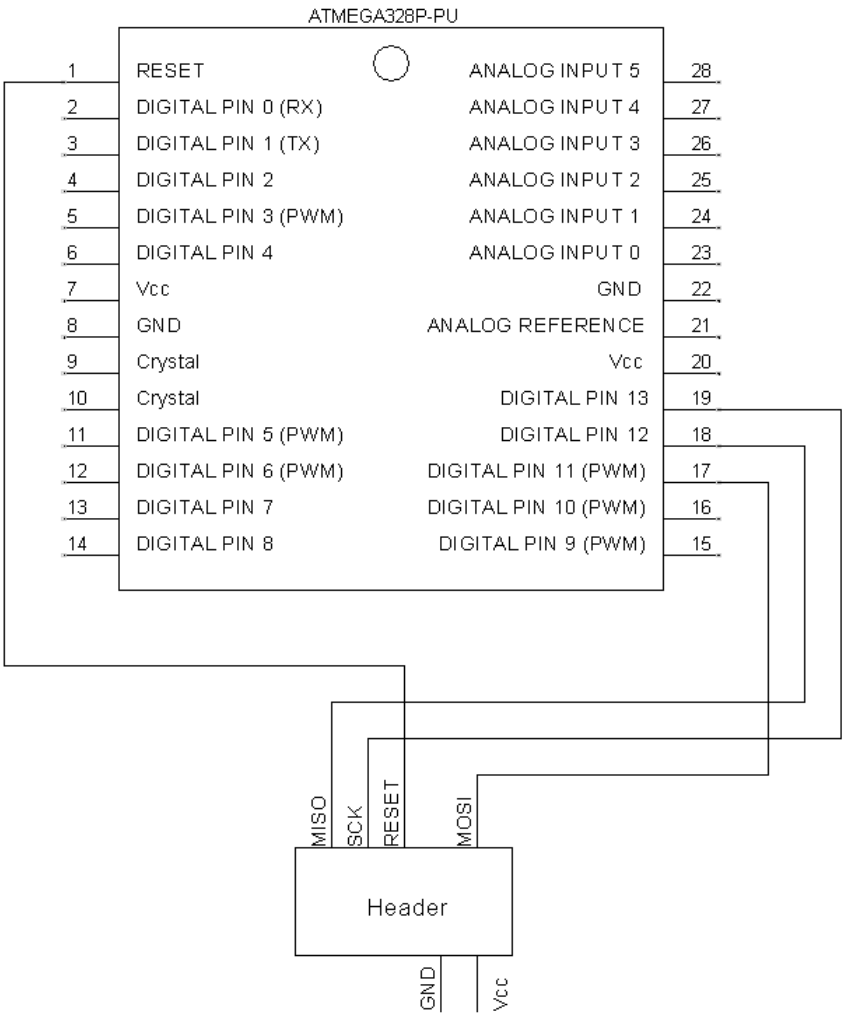

Figure 6.29: *Header Connections to Microcontroller*

6.3.8 **Housings**

The housings of the monitoring system are responsible for holding the subsystems circuit boards and protecting sensitive electronics from external damage. Two housings are utilized in the monitoring subsystem, one to contain the base microcontroller circuit board and the other holds the display microcontroller and LCD display.

***Figure 6.30**: Base Microcontroller Housing*

Figure 6.30 above shows the base microcontroller housing. The housing is 5.5 x 3 x 1.5 inches and is made from PVC sheet plastic. The housing features a hinged cover for access to the circuit board secured inside. Two ¼ inch holes located on the bottom of the housing are used for securing the housing to the inside of the turbine base's frame. A 1 x 0.5 inch opening is located on the side of the housing to facilitate incoming and outgoing wire connections made by the circuit board.

***Figure 6.31**: Display Microcontroller Housing*

Figure 6.31 above shows the display microcontroller and LCD display housing. The housing is 5 x 3 x 1.5 inches and is also made from PVC sheet plastic. The housing features a hinged cover for access to the circuit board inside. The LCD display is press fitted into a rectangular 3 x 1 inch opening on the face of the display housing. Two components installed on the base housing were not utilized due to time restraints of the project. These components are the pushbutton located on the front of the display housing and the serial connector located on the side of the display housing.

6.3.9 **Power Consumption and Cost**

The wind powered air compressor developed does not generate electricity and so it cannot be the source of power for the monitoring subsystem. When the wind powered air compressor is installed, the monitoring subsystem will be connected to the building's 120 Vac 60Hz power. A transformer converts the 120Vac down to 5Vdc, which is useable by the monitoring subsystem. Power consumption of the monitoring subsystem is considered, especially because the project is seeking to offset existing energy costs. The monitoring system consumes 0.032 amps at 5V leading to a total power consumption of 0.16 watts. At an energy cost of $0.18 per kilowatt-hour, the monitoring system will cost the user $0.25 per year, shown below (Administration, 2007).

$$VI = P \qquad (5)(0.032) = 0.16$$

***Equation 6.9**: Power Equation*

$$\frac{(Power)(Time)(Price\ per\ KW - Hr)}{1000} = Cost \qquad \frac{(0.16)(24 * 365)(0.18)}{1000} = 0.25$$

***Equation 6.10**: Cost as a Function of Power*

6.3.10 **Testing**

Before integration of the monitoring subsystem into the final project, testing was performed to verify its operation. The brake disc was spun within the monitoring system's detector and the RPM of the brake disc was measured both manually and by the monitor. Manual measurement was taken by measuring the time the brake disc took to complete a certain number of revolutions. By comparing the actual RPM to the monitor's detected RPM (Figure 6.31 below), it can be seen that the monitoring system functions properly.

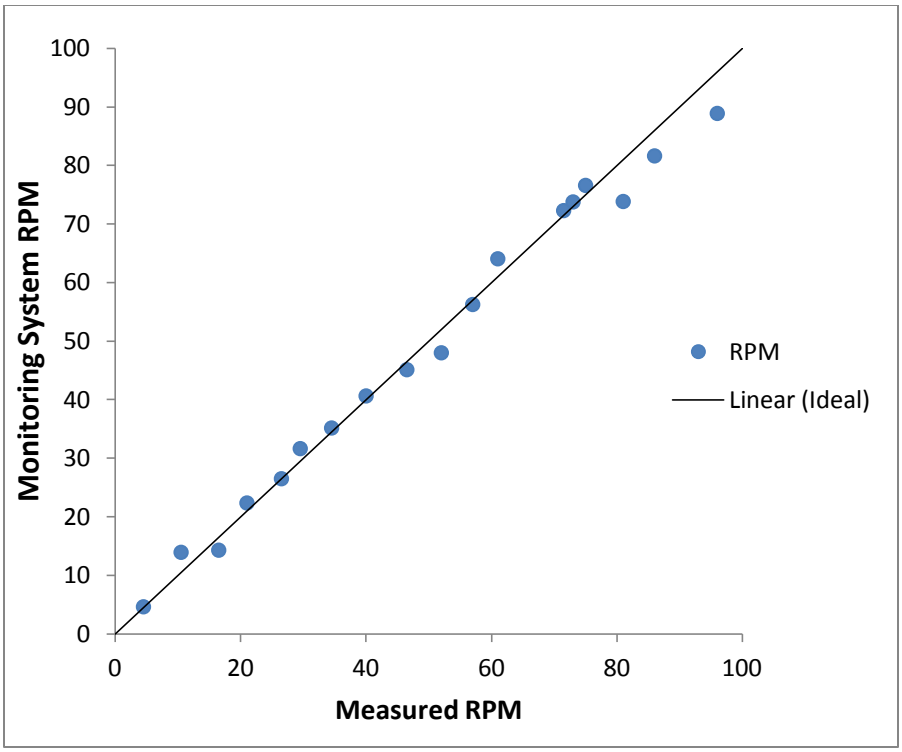

***Figure 6.31**: Testing Accuracy of the Monitoring System*

6.3.11 Expenses

Below is Table 6.4 detailing the component costs of the monitoring subsystem. With each subsystem of the project being allocated $50, the monitoring system is under budget.

***Table 6.4**: Expenses of the Monitoring Subsystem*

Item	*Unit Price*	*Quantity*	*Item Total*	*Paid For It?*	*Actual Cost to Team*
120v to 13v Transformer	$2.90	2	$5.80	No	$0.00
5V Regulator	$0.19	2	$0.38	No	$0.00
Atmel ATMega328	$2.29	2	$4.58	No	$0.00
Capacitor	$0.02	4	$0.08	No	$0.00
Crystal Oscillator	$0.39	2	$0.78	Yes	$0.78
Header Pins	$0.05	1	$0.05	No	$0.00
Hinge Set	$1.19	1	$1.19	Yes	$1.19
Insulated Copper Wire (price / foot)	$0.03	10	$0.30	No	$0.00
LCD Display	$5.90	1	$5.90	No	$0.00
LEDs	$0.04	2	$0.08	No	$0.00
Perf Prototyping Board	$0.20	2	$0.40	Yes	$0.40
Plastic Housing	$0.99	1	$0.99	No	$0.00
Potentiometer	$0.19	1	$0.19	No	$0.00
Resistor	$0.01	5	$0.05	No	$0.00

Ribbon Cable	$0.19	1	$0.19	No	$0.00
Solder (price / gram)	$0.05	10	$0.50	Yes	$0.50
Wire Connector	$0.04	3	$0.12	No	$0.00
Wooden Mount	$0.09	1	$0.09	No	$0.00
Total					**$2.87**

6.4 Braking

6.4.1 **Overview**

The purpose of the braking system is to provide a braking torque that will stop the turbine's rotation in order to perform maintenance on parts of the assembly, or to prevent over rotation of the turbine. The maximum braking torque of at least 21.8 ft-lb that the braking system needs to apply was determined using the equations below based on the torque associated with the turbine rotating at 70 mph and a coefficient of power of 0.1 and a tip speed ratio of 0.6.

$$T = P/\omega$$

***Equation 6.11**: Torque as a Function of Power and Angular Velocity*

$$P = C_p \frac{1}{2} \rho A V^3$$

***Equation 6.12**: Power Equation*

$$\omega = \frac{\lambda V}{R}$$

***Equation 6.13**: Angular Velocity Equation*

In equations 6.11 – 13, ρ is the density of the air, C_p is the coefficient of power, A is the swept area, V is the free stream velocity of the air, λ is the tip speed ratio, and ω is the angular velocity. A single pivot side-pull caliper brake was selected to impart the torque with the equations below in mind. For this style of brake both arms are able to pivot on a single point and one arm is attached to the cable. When there is tension in the cable due to the lever being pulled the brakes close and apply a normal force that creates a frictional torque.

$$\boldsymbol{T = r\ x\ F_k}$$

***Equation 6.14**: Torque Equation*

$$\boldsymbol{F_k = F_n \mu_k}$$

***Equation 6.15**: Frictional Force Equation*

With respect to equations 6.14 and 6.15, F_k is the force due to kinetic friction, F_n is the normal force, r is the braking moment arm, and μ_k is the coefficient of kinetic friction.

6.4.2 **Design**

With the brake selected, a method of mounting the brake and applying the torque to the drive shaft needed to be determined. In order to apply the torque to the shaft, a ¼ inch thick, 5 inch diameter disk was fabricated from a ¼ inch steel plate. Equally spaced holes were then drilled into the plate for the electronic monitoring system. The disk was then attached to the drive shaft using a shaft collar. However, after finishing machining, there was space between the closed brake arms and the disk. In order to fix this, a longer bolt that attaches the brake pad to the brake arm was purchased. Using a 1 foot long hollow steel square bar the brake was mounted to the 80/20 kit below the gearing system. This was done by drilling three holes—two were used to attach the bar to the kit; the third was located between the first two, which was used to attach the brake to the bar. A spacer was fabricated in order to secure the brake to the bar. The brake pads rested 2.25 inches from the drive shaft. The brake line was ran from the brake through a hole in the base's covering so that it could be attached externally to the brake lever and the 1 inch diameter steel round bar that the lever was mounted on. The braking system is pictured in Figure 6.32 below.

***Figure 6.32**: Braking System*

***Figure 6.33**: Brake Caliper*

6.4.3 Analysis

From testing of the braking system, a maximum braking torque due to static friction of 6.1 ft-lb and a maximum braking torque due to kinetic friction of 9.7 ft-lb were determined. In addition, by increasing the temperature of the brake pads, increases in the amount of torque were observed. The static braking torque and increase in the temperature of the brake pad yielded an increase in torque of 36%. These values were still lower than the 21.8 ft-lb that the system is required to produce.

6.4.4 Expenses

The cost of the braking system components are listed in the Table 6.5 below.

***Table 6.5**: Expenses of the Braking Subsystem*

Item	*Unit Price*	*Quantity*	*Item Total*	*Paid For It?*	*Actual Cost to Team*
Brake Disc Steel	$17.81	1	$17.81	No	$0.00
Pad	$0.79	1	$0.79	Yes	$0.79
Lever	$1.69	1	$1.69	Yes	$1.69
Fixture	$2.19	1	$2.19	Yes	$2.19
Cable	$0.49	1	$0.49	Yes	$0.49
Lever Mounting Bar	$7.19	1	$7.19	No	$0.00
Shaft Collar	$7.98	1	$7.98	Yes	$7.98
Shaft Collar Shipping	$4.78	1	$4.78	Yes	$4.78
Total					**$17.92**

6.4.5 **Future Developments**

A number of improvements can be made to the braking system to improve its functionality. In order to reach the specified required torque, the brake's moment arm from the drive shaft can be increased 2.25 times to a distance of 5 inches. An alternative solution is to use brake pads with a higher coefficient of friction or a brake that can apply a larger braking torque. Also for a production model of the turbine, the braking system would be automated, instead of operated by a hand lever, and integrated into the monitoring subsystem.

6.5 Torque Conversion:

6.5.1 **The Compressor Gear**

The compressor selected is powered by a reciprocating piston attached to a gear. As the gear rotates, the piston translates and the air is compressed. The purpose of this subsystem is to transmit the power captured by the wind turbine to this gear. A CAD model of the compressor gear is shown in Figure 6.34.

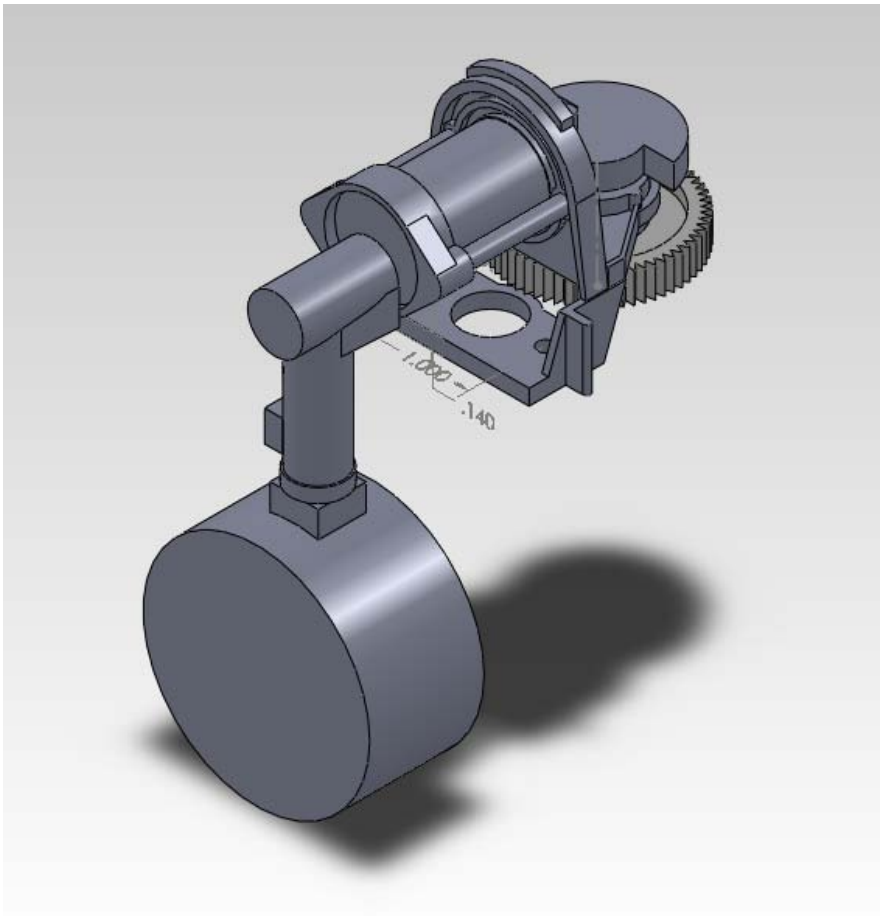

***Figure 6.34**: The Compressor System*

Originally, in the stock model of the compressor, the compressor's gear was paired with another gear, which was connected to a 12V motor. This motor had a 2870 RPM speed at maximum efficiency, which translated to the compressor gear rotating at a speed of 411 RPM (Synchronous Motor, 2012). The motor was removed in the interest of powering the compressor solely with wind energy and no electricity. The drive shaft needed to replace the motor as closely as possible, creating the technical specification of rotating the compressor gear at 411 RPM.

6.5.2 The Second Gear

To achieve 411 RPM, a conversion is needed between the compressor gear and the drive shaft. According to the initial calculations, the wind turbine was projected to rotate at 82 RPM, therefore, a 5:1 ratio was needed to reach the specification. It would seem simple to have a gear five times larger than the compressor gear attached to the drive shaft, orient the two gears, and power the compressor. The problem, however, was that the compressor gear was of an abnormal size with a 1.57 inch diameter and 62 teeth. The cost of ordering a gear five times larger than that with the right pitch was in the thousands of dollars, which exceeded the total product budget of $350. Another solution was required.

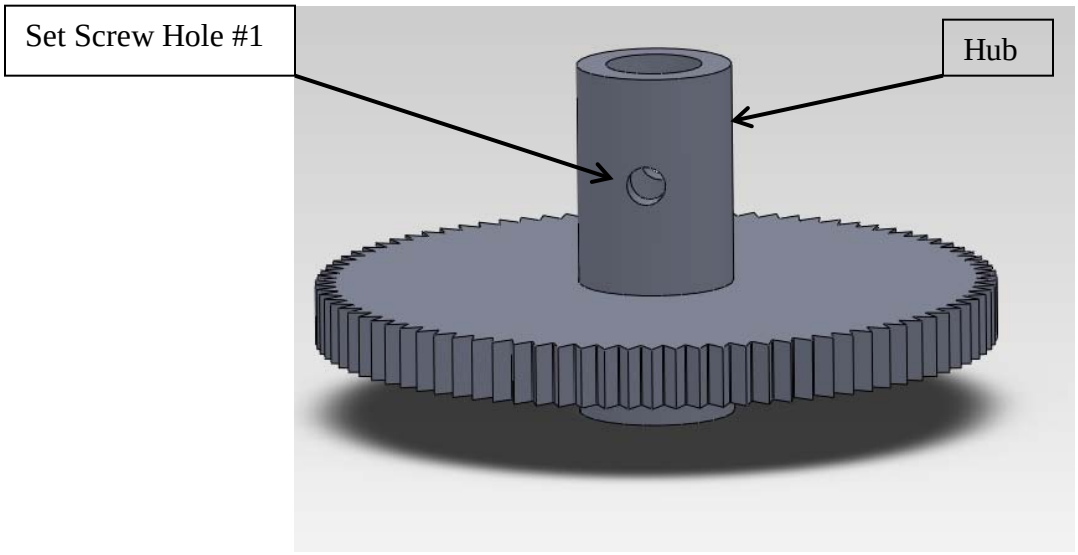

***Figure 6.35**: The Second Gear*

The Engineering Processes shop, on the first floor of the Jonsson Engineering Center, has a stockpile of gears for use. A particular gear, with outer diameter of 2.20 inches, had the right pitch and meshed well with the compressor gear. A set screw hole, ⅛ inch in diameter, was drilled through the hub so the gear could be connected to the bearing rods. The second gear is used in conjunction with a pulley system to provide the correct ratio.

6.5.3 **The Pulley System**

Two pulleys were used to achieve a 5:1 ratio between the drive shaft and the compressor gear's speed. The first pulley was mounted on the same axis as the second gear, so they would have the same angular velocity. The first pulley was then connected by a V-belt to a second, larger pulley centered on the drive shaft. The following equations 6.16 – 6.19 determined the size of the pulleys.

$$w_1 d_1 = w_2 d_2$$

***Equation 6.16**: Angular Velocity and Diameter Ratio*

$$w_2 = w_3$$

***Equation 6.17**: Angular Velocity Translation*

$$w_3 d_3 = w_4 d_4$$

***Equation 6.18**: Angular Velocity and Diameter Ratio*

These three equations simplify to:

$$w_1 d_1 = w_4 d_4 d_2 / d_3$$

***Equation 6.19**: Angular Velocity and Diameter Ratio*

Where w_1 is the angular velocity of the compressor gear, w_2 is that of the second gear, w_3 is that of the small pulley, and w_4 is that of the large pulley; d_1 is the diameter of the compressor gear, d_2 is that of the second gear, and so forth. The optimal combination found through this equation is a 1.5 inch outer diameter of the smaller pulley and a 5.0 inch outer diameter of the larger pulley. Both pulleys were ordered off mcmaster.com, and the V-belt that connects them was found in the IED Shop's recycling containers. The compressor gear reached its goal of rotating at 411 RPM during testing.

6.5.4 **Mounting the Gearing System**

The second gear needed to be aligned with the compressor gear precisely, while still rotating, and with minimal deflection from the applied torque. A gear base provided the support and alignment necessary. A flange bearing bolted into the base allowed the gear to rotate freely. Bearing rods connected the gear to the bearing. Finally, a collar provided stability in the rods to avoid deflection.

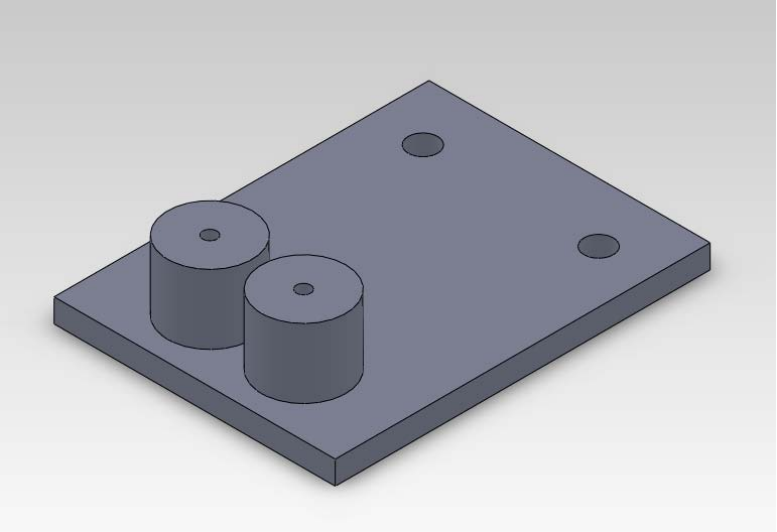

***Figure 6.35**: The Gear Base*

The gear base is shown in the Figure 6.35. It is made out of a ¼ inch thick PVC plastic rectangle 3 inches wide by 4 inches long. Two aluminum cylinders (0.8 inch diameter, 0.76 inch tall) are fastened at one end of the base. Four holes were drilled in the base to accommodate the flange bearing and cylinders. The cylinders account for the height of the compression system and the flange bearing so the two gears are on the same horizontal plane. All materials were found in the Processes Shop, and the only machining required was to cut the plastic down to size and to drill the four holes.

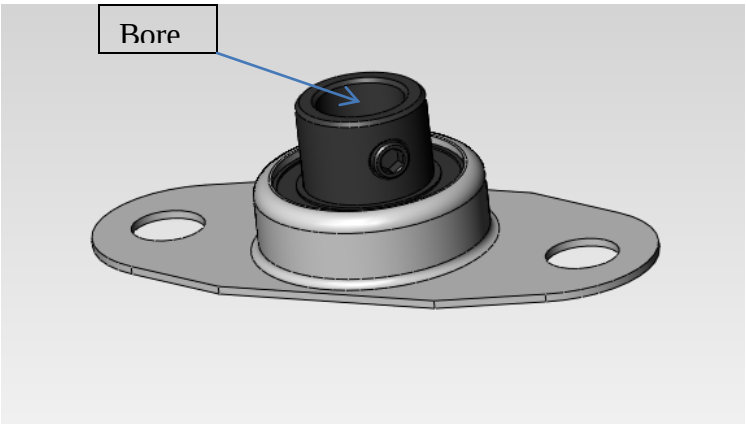

***Figure 6.36**: The Flange Bearing*

The flange bearing was ordered off of mcmaster.com. It connects the second gear to the base while allowing the gear to rotate. It has a 0.375 inch diameter bore that the bottom bearing rod fits into.

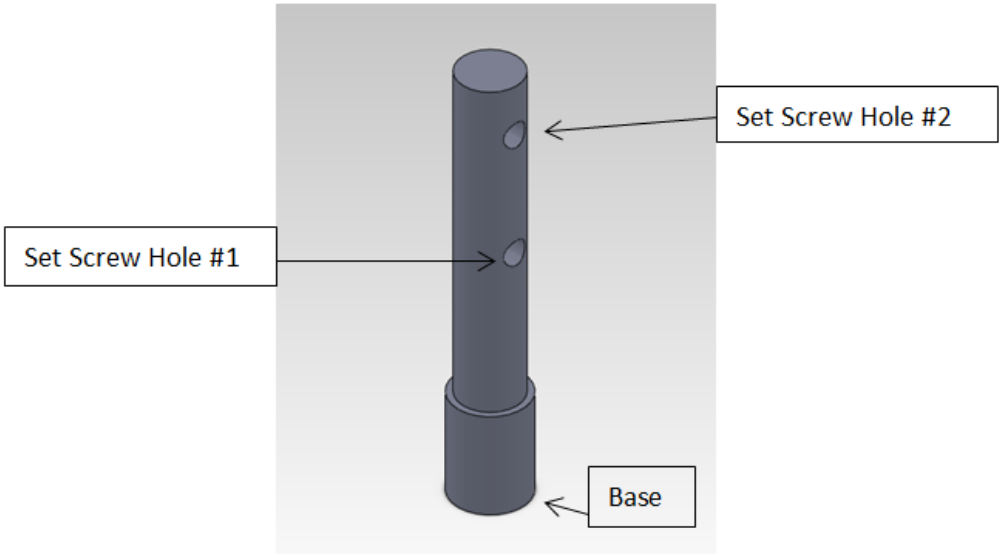

***Figure 6.37**: The Bottom Bearing Rod*

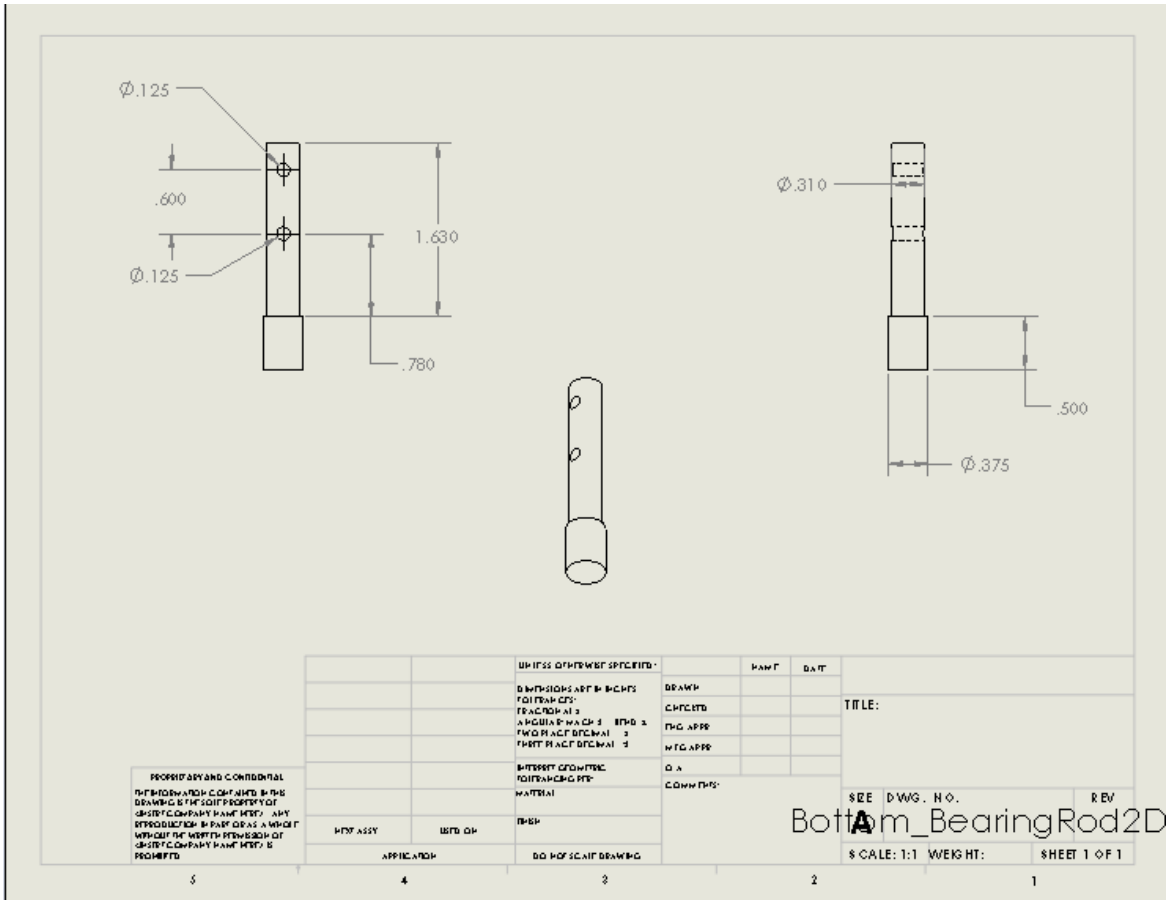

***Figure 6.38**: Bottom Bearing 2D Sketch*

The bottom bearing rod goes through the bore of the second gear, and its base slides into the flange bearing. Set Screw Hole #1 in the bottom bearing rod matches up with Set Screw Hole #1 in the second gear. The bottom bearing rod took quite a bit of machining, so a 2D sketch was drawn up for reference, shown in Figure 6.38. Tolerances were a challenge. The ⅛ inch diameter holes shown in the sketch needed to be precisely centered and the correct distances apart to be able to match up with the holes of the second gear and the top bearing rod. The bottom bearing rod had to be remade because initially this was not the case.

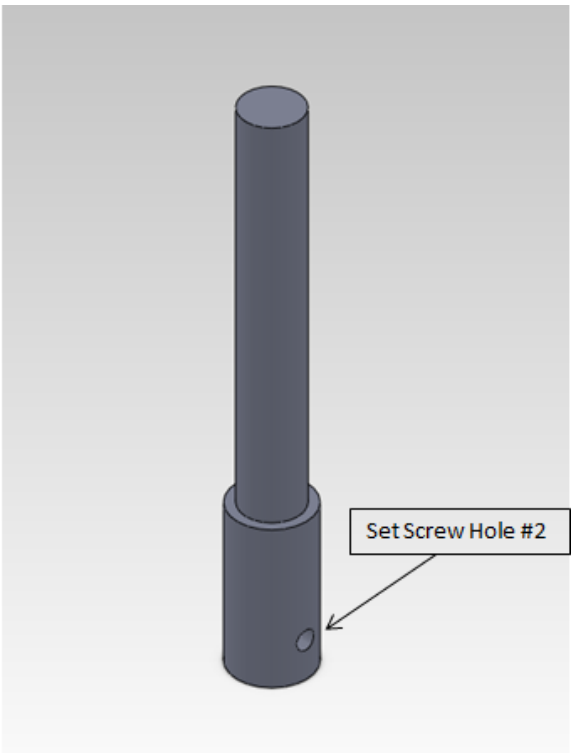

***Figure 6.39**: The Top Bearing Rod*

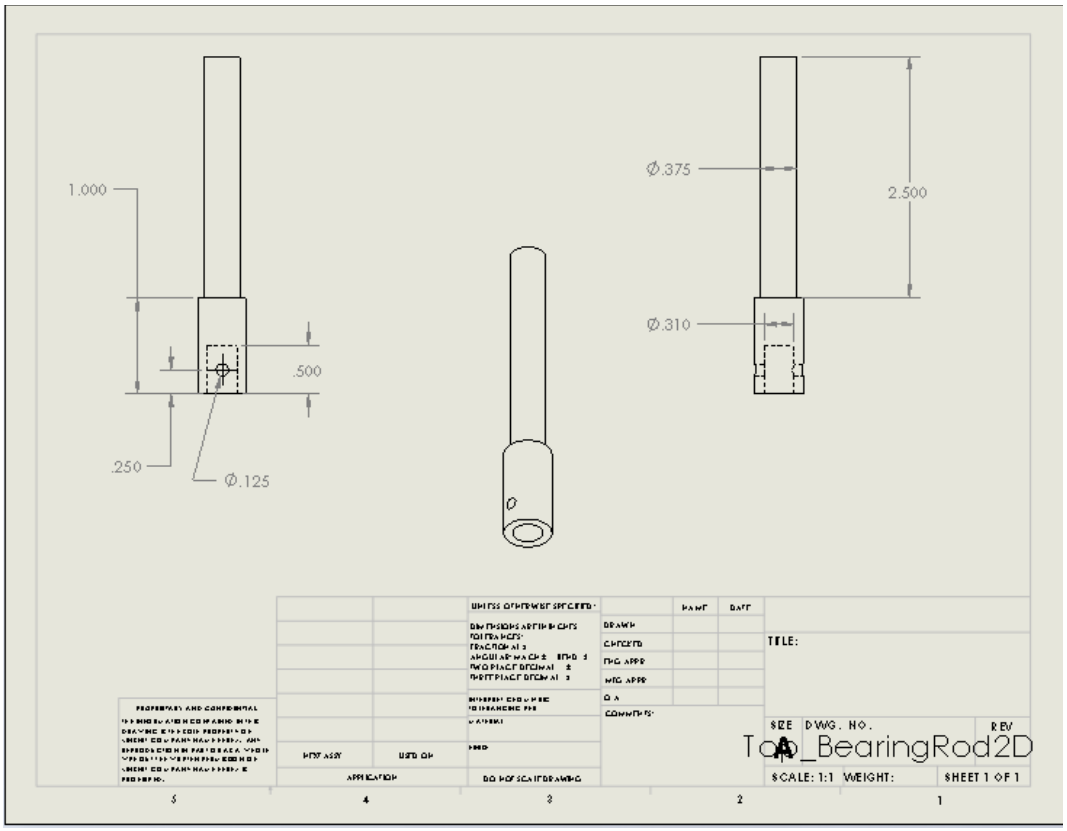

***Figure 6.40**: The Top Bearing Rod 2D Sketch*

The top bearing rod (Figure 6.39) also required machining. The alignment of two holes was critical to properly mounting this piece. On the bottom, a 0.31 inch hole was bored (see Figure 6.40), and houses the top of the bottom bearing rod. Also, a set screw hole is drilled to match up with Set Screw Hole #2 of the bottom bearing rod. Combined, the top and bottom bearing rods hold the second gear while mounted onto the flange bearing. After preliminary testing, the bearing rods suffered too much deflection from the applied torque of the V-belt on the smaller pulley, which was attached to the top of the top bearing rod. So, a collar was fabricated to provide additional support.

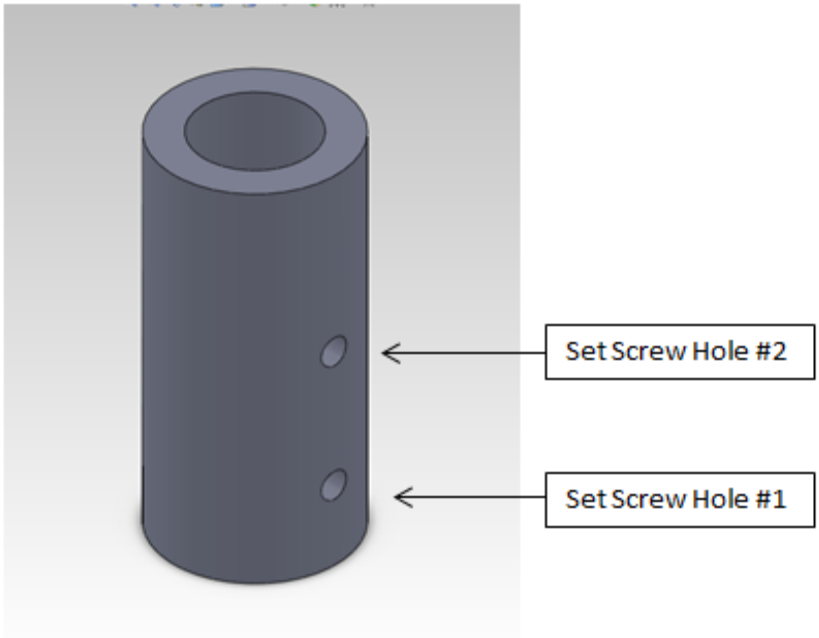

***Figure 6.41**: The Collar*

The collar slides onto the top bearing rod and the hub of the second gear, and its set screw holes match up with Set Screw Holes #1 & #2, discussed earlier. After adding the additional support that the collar provides, the system experienced minimal deflection. The gear assembly is shown in the following figure.

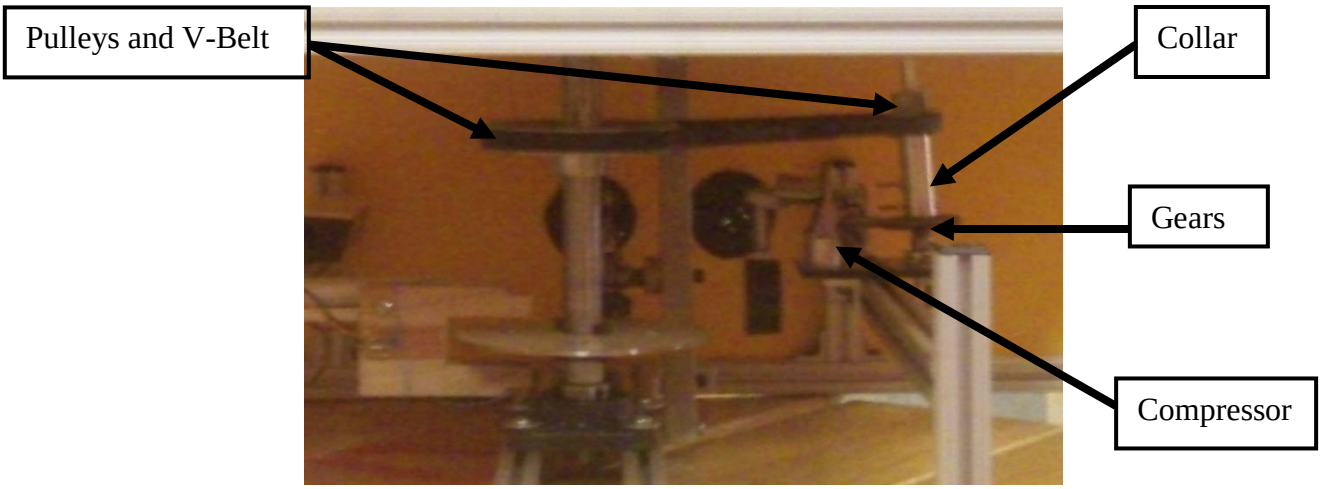

***Figure 6.42**: The Gear Assembly*

6.5.5 Positioning the Torque Conversion Subsystem

Since a pulley and V-belt system was used, alignment between the compressor and the drive shaft was not over constrained. The two constraints were that the compressor's hose could extend outside the base, and that the V-belt could wrap around the two pulleys with enough tension that they turn together. The hose was long enough that the system could be centered in

the width of the base. This allowed for the torque created by the smaller pulley on the bearing rods to be centered axially over the base, creating the least deflection possible. The system was then located 10 inches away from the drive shaft lengthwise so the V-belt was taut, and adjusted so the two pulleys were on the same horizontal plane. The 80/20 kit of the base allowed for adjustment in the length, width, and height of the system.

6.5.6 **Expenses**

Three parts had to be ordered to construct the Torque Conversion Subsystem. A table of the parts and their prices are shown in Table 6.6.

***Table 6.6**: Torque Conversion Expenses*

Item	Unit Price	Quantity	Item Total
Flange Bearing	$22.23	1	$22.23
1.5" Pulley	$3.79	1	$3.79
5" Pulley	$10.52	1	$10.52
Shipping	$4.78	2	$9.56
Total			**$46.10**

Each subsystem allowed for a $50 budget. With a total expense of $46.10, the Torque Conversion subsystem was under budget.

6.5.7 **Conclusion**

The Torque Conversion subsystem transmitted the power from the drive shaft to the compressor. It realized its goal of an optimal speed of 411 RPM in the compressor gear, achieved by creating approximately a 5:1 angular velocity ratio between the compressor gear and the larger pulley attached to the drive shaft. The subsystem fit within the base housing of the overall project. It also was under budget. With respect to the overall project, the Torque Conversion subsystem was a fully functional success.

6.6 Compressor

The objective of the compressor is to translate the rotations of the gearbox into compressed air. For this subsystem, a reciprocating type air compressor was chosen. There is a central crankshaft that drives the piston inside the cylinder. As the pistons draw back gas is pulled into the cylinder of the piston, air is then compressed by the reciprocating action of the piston. The gas is then discharged either to be used immediately by a pneumatic machine, or stored in a compressed air tank. For the purpose of our design, the external motor was removed in order to directly utilize the rotations of the gearing system.

The compressor that was chosen was a 12 Volt, 250 psi Compact Air Compressor. This was chosen in order to meet our target specification of 100 psi. This product was also the only

air compressor the team found that stayed within the subsystem's budget. The compressor was removed from its protective casing and the motor was detached. The large gear on the compressor was utilized in connecting the drive shaft to the compressor via the gearing subsystem. This system was configured in order to match the maximum RPM generated by the original motor, as discussed in the gearing subsystem section.

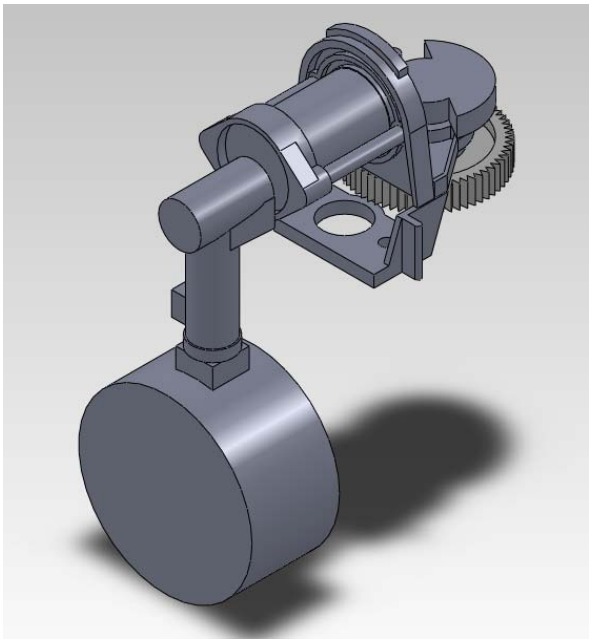

***Figure 6.43**: CAD drawing of the compressor*

The following graph shows the data collected from the compressor. It shows the relationship between wind speed required to produce a specific torque and the maximum air pressure achievable by a specific torque. Therefore, it allows for the relationship between wind speed and pressure to be inferred. For example, a ten mile per hour wind would generate approximately 0.9 ft-lbs of torque, which results in an achievable pressure of 140 psi.

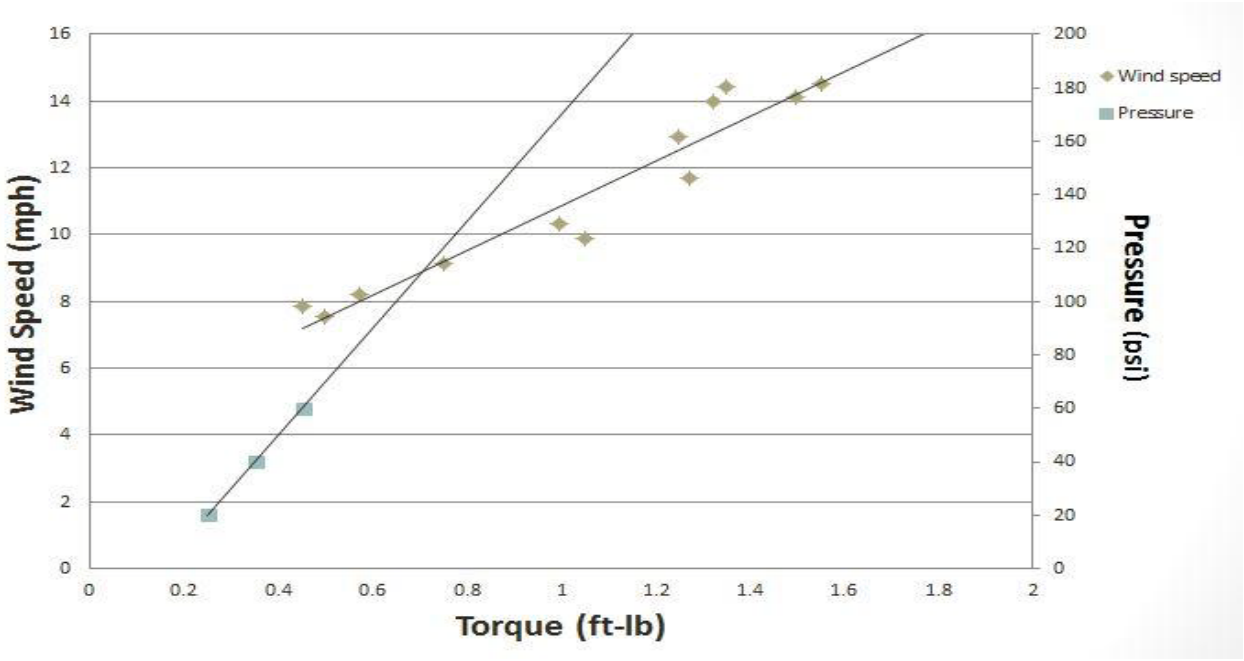

***Figure 6.44**: Graph of Wind Speed and Pressure vs. Torque*

The maximum pressure of the compressor was tested by manually spinning the turbine. The technical specification set forth for the compressor was 100 psi. Unfortunately, the compressor started to leak at 60 psi. The team hypothesized that this occurred because the movement of the piston was slow enough to allow air to leak out after this pressure was reached. This problem may have been resolved if the RPM of the drive shaft were increased. Another solution for this issue would be to purchase a more expensive and higher quality compressor for future developments.

The hose of the air compressor came with a Schrader valve at the end. In order to connect this to a standard air tank, a Schrader valve attachment was purchased for the tank. This was screwed onto the nozzle of tank, after Teflon tape was used to ensure no leakage.

Table 6.7: Expenses of the Compressor Subsystem

Item	***Unit Price***	***Quantity***	***Total Price***
12V, 250 psi compressor	$8.99	1	$8.99
Schrader valves	$3.99	2	$3.99
Teflon tape	$1.99	1	$1.99
Total			**$18.96**

6.7 Base

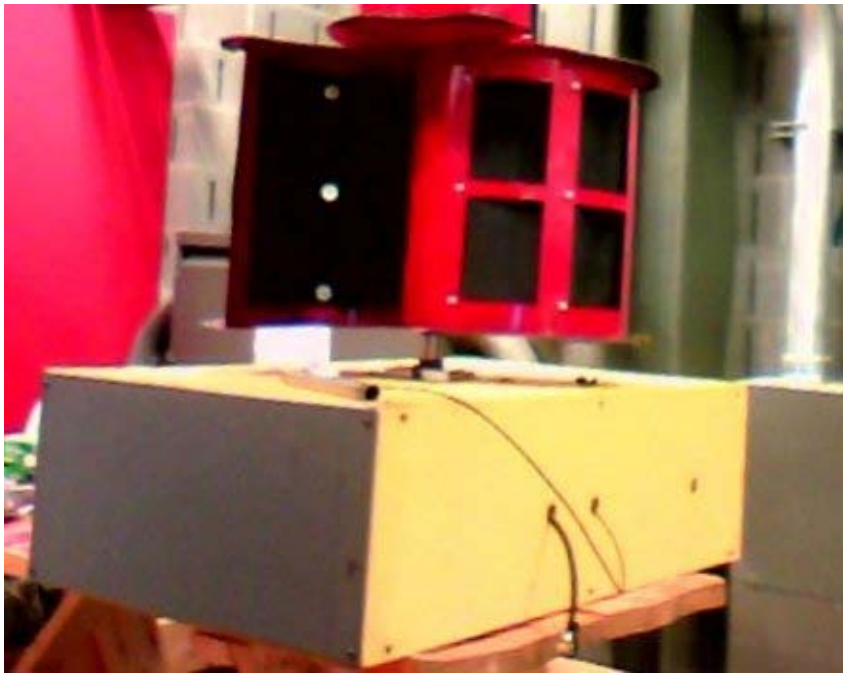

***Figure 6.45**: The Completed Base*

The purpose of the base is to support and contain the other subsystems under varying weather conditions. This means that the base must stand up to different temperatures to account for the seasons as well as wet and dry conditions. Furthermore, the weight-bearing ability must account for the turbine itself as well as outside forces, such as snow, and withstand corrosion for the 25 year period the group specified as the lasting period for this product.

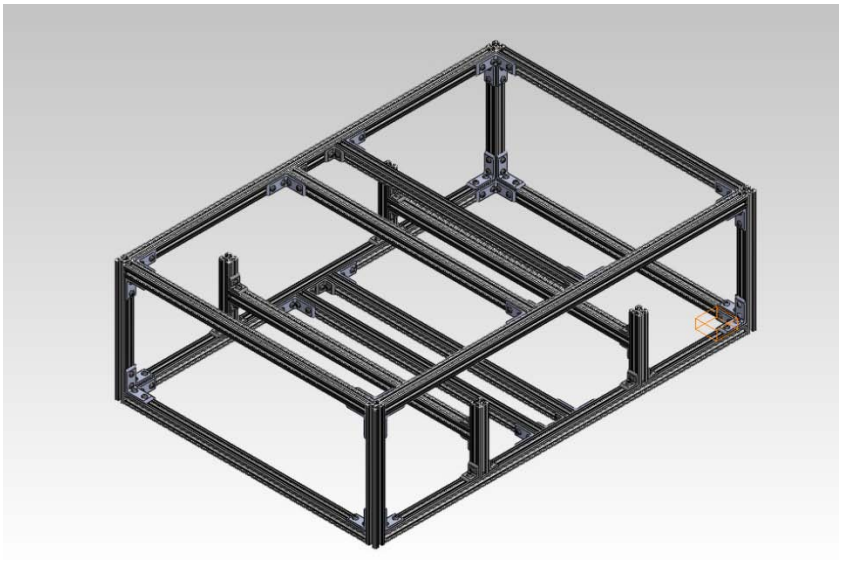

***Figure 6.46**: CAD Model of the Base's 8020 Frame*

6.7.1 **Support System**

The 80/20 T-Slotted Aluminum framing kit provided far greater support than that required for the base. The first worry of support was the weight of the other subsystems; in order for the turbine to work, the base would have to be able to hold up the weight of the entire turbine and all the systems involved.

Using preliminary CAD analysis (excluding the mounting bolts and washers, braking system, or electronic monitoring system), the team found the prototype to weigh 77.4 lbs, which was used as a reference for initial material selection (estimating the excluded weight). Later, after weighing the entire turbine, it was found to be 89 lbs. total. This 89 lb. weight is the standard weight the base must support at all times. Because the outer panels of the base do not affect or provide any of the support for the other subsystems, they were not considered in calculating the base's ability to do so. Each beam was assumed to be held up by two fixed ends to calculate the force that would give several maximum deflections.

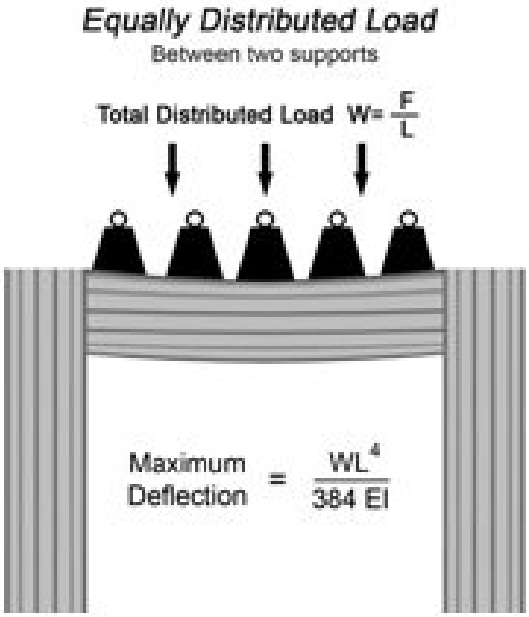

***Figure 6.47**: Equally Distributed Load Between Two Supports*

The equation in Figure 6.47 was used to determine the amount of weight that can be supported by each individual bar, assuming an even distribution of weight. W is the evenly distributed weight imparted on the beam over length L of the beam (F is the total weight); E is the modulus of Elasticity (Young's modulus) for the material of the beam ($E_{80/20}$ = 10,200,000, E_{steel} = 29,500,000); and I is the moment of inertia of the cross-section the force is flowing through ($I_{80/20}$ = .0442 in^4, I_{steel} = .00521 in^4). For a square/rectangular cross section, I is equal to 1/12 of the cross section base (b) times the cross section height (h) cubed, and subscripts denote the values for 80/20 kit and the ½ inch X ½ inch hot-rolled square steel bars that would be used in actual production of the turbine. This would allow the team to calculate how much force the

horizontal beams are able to resist. The results found were recorded in the following tables, which show the maximum bearable load allowing a certain maximum deflection (for both the 36 inch and the 24 inch bars).

***Table 6.8**: Deflections Under Distributed Load (24 inch bars)*

(inches)	80/20 Aluminum (1 inch X 1 inch) Load (lbs.)	A-36 Steel Square Bar (½ inch X ½ inch) Load (lbs.)
.1	1252.3	426.8
.2	2504.7	853.5
.3	3757.0	1280.3
.4	5009.3	1707.1

***Table 6.9**: Deflections Under Distributed Load (36 inch bars)*

(inches)	80/20 Aluminum (1 inch X 1 inch) Load (lbs.)	A-36 Steel Square Bar (½ inch X ½ inch) Load (lbs.)
.1	371.1	126.4
.2	742.1	252.9
.3	1113.2	379.3
.4	1484.3	505.8

These charts show that if allowed a force with a maximum deflection of .1 inches, 371.1 lbs. of weight can be completely supported by the weakest length of beam for the 80/20 kit and 126.4 lbs. for the steel frame. Assuming all the weight at a single central point on each bar, the maximum load will be half of those listed in above tables. Both cases prove that the base is well within its capabilities in supporting the entire turbine.

However, the base must not only account for the system's own weight but also the weight imparted on it by the weather. For this, the panels of the base must also be considered, as they will be the surface supporting most of the load of new snow. As the snow hardens into ice, the base frame will begin resisting most of the weight, since the ice will become its own structured sheet of material lying atop the base and supporting further weight. To account for this snow, only the weakest part of the base, the top surface PVC sheeting, was considered. If the PVC sheeting can completely support the snow, this proves the whole system will be able to. Because

flexible PVC does not have a modulus of elasticity, which are only appointed to rigid materials, testing had to be done to prove the surface's ability to support the weight of snow.

Using hand weights from the Mueller center, the team was able to successfully prove that the base could support 40 lbs. of what would be snow. Because PVC only loses impact strength—it gains both tensile strength and stiffness—in colder temperatures, and snow is low impact, it can be assumed the snow's temperature would have no negative effects on the sheeting's ability to support the weight of it (PWEagle, 1999). Meanwhile, the Vicat softening point is 204°F, which the team neither expects to reach in real-world environmental temperatures nor expects to occur with an added environmental loading (like sand); therefore, the team was most concerned with the issue of snow loading (Toolcraft Plastic). The success of supporting 40 lbs. of weight translated into the following amounts/depths of snow (displaced by the turbine blades) in its different hardening stages supported by the top surface sheeting alone, assuming no help from the 80/20 frame:

***Table 6.10**: Depth of Displaced Snow supported by the PVC Sheeting in Stages*

Snow Type	Density	Depth of Snow (meters) - Static	Depth of Snow (inches) - Static
New	50	.846	33.36
Damp New	100	.423	16.68
Settled	200	.212	8.28
Wind-Packed	350	.121	4.8
Firm	400	.106	4.2
Glacier Ice	830	.510	2.04

This information was found using the different densities of snow it its transition phases (Paterson, 1994) as well as equations 6.20 and 6.21:

$$W_{snow}(kg) * \frac{1}{\rho_{snow}}\left(\frac{m^3}{kg}\right) * \frac{1}{A_{surface}(m^2)} = h_{snow}(m)$$

***Equation 6.20**: Weight of Snow*

$$A_{surface} = A_{top} - A_{turbine}$$

***Equation 6.21**: Effective Area under Snow*

Where W_{snow} is the weight of the snow, $\rho_{snow}$is the density of the snow, $A_{surface}$ is the area of the top PVC surface, excluding the area that the turbine's blade surfaces will be covering, which will give the displaced height of snow that can be supported (h_{snow}) as represented by the 40 lbs. As far as wet snow, the weak PVC sheeting of the base can support 33.36 inches of displaced snow alone. If the strength of the base's frame was included, it could support greater than this amount, especially when considering the weight-bearing abilities of the individual frames of the beam listed earlier.

6.7.2 **Weatherproofing**

To protect the internal subsystems from the weather, the base's PVC walls were installed to contain them. PVC was chosen because it is known to be highly corrosive resistant to many chemicals and water to the point where corrosion would be negligible within the 25 year period. However, because the base is responsible for protecting the internal systems this way, the base itself must be able to withstand weather conditions. Since the 80/20 kit is made out of anodized Aluminum, it is more corrosive resistant than it would be under normal conditions. In a study conducted by the physics department at the University of California, Santa Barbara, researchers found that Aluminum in pure water corrodes at 20 micrometers (μm) per year, making their total corrosion of over the 25 year period .5 millimeters (mm) or approximately .020 inches and should have no effect on the strength of the material (Bayman, 2002). The A-36 steel that would be used in the final production has a corrosion rate of up to 0.7 μm per year at its maximum depth when exposed to the intended urban setting, meaning 1.75 mm or 0.069 inches of corrosion will occur over the 25 year period under the same conditions (LivingSteel, 2010). Therefore, corrosion should be negligible in the final turbine product because the steel will be covered by the PVC sheeting and any corrosion will be because of accidental water leakage due to the removable side panel. However, so that this occurrence will be minimized, the cracks between PVC panels will be sealed with liquid seal or caulking. Because this was not done in the actual prototype (due to possible damages that would cause the 80/20 kit), the team did not test for water exposure—this could be done by pouring certain amounts of water were atop of the turbine and measuring the amount that falls through to central housing, where the internal subsystems rest. However, this was taken into consideration due to the turbine's probable exposure to rain in its real-world application.

6.7.3 **Mounting System**

Mounting the base is necessary to keep the rotational torque generated by the turbine blades at a higher wind speed from tipping the entire system over. The technical specification set for this is that the base must be able to support the turbine at 70 mph winds because this is the maximum wind speed reported for Troy, NY. To cope with this force, two concepts were discussed: counterweights and a mounting system. Because counterweights can be heavy, will take up unnecessary space within the base, and can cost more than the other option, a mounting system was chosen. This concept proved to be the most sensible option once the team decided the turbine would be placed on top of the customer's roof in order to have the greatest wind exposure.

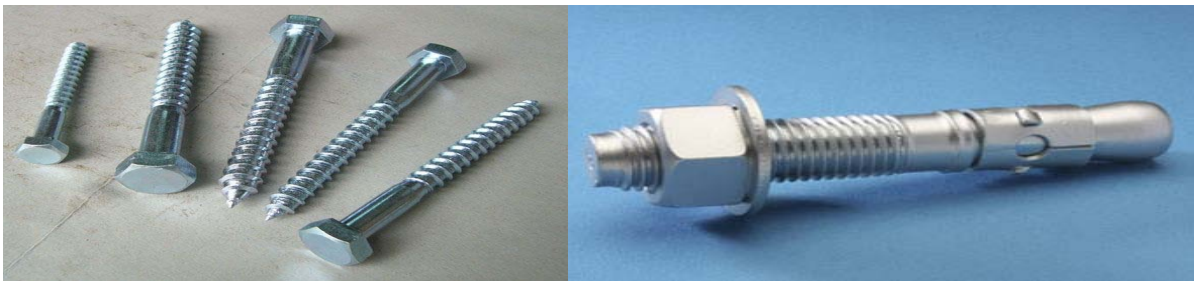

Figure 6.48: *Low-Carbon Hex Lag Bolt (left, (Concrete Fastening Systems, 2012)) and Zinc-plated Steel Wedge Anchor Bolt (right, (Hangzhou TianTian Hardware, Ltd, 2012))*

After consulting with the owner and head contractor of White Construction (based in California), Christopher White recommended this type of mounting system: either lag bolts (Figure 6.48) for usual wood-type or wood-similar roofing or wedge anchor bolts for concrete roofing. The standard bolt issued with the turbine in the future will be a low carbon steel hex lag bolt since the homeowners and small business owners comprising the targeted customer base will more likely have standard roofing as opposed to industrial concrete roofing, but both bolt options will be available. Either of the bolt types would be mounted through drilled holes in the bottom four corners of the base frame in the final product.

During testing, the team did not face winds great enough to knock the prototype over, so bolts were not ordered or attached to it. This was also the case because to mount the current prototype's base with these bolts would require an extra mounting piece (one for each bolt) that can be ordered from *80/20 Inc*. so as not to damage the 80/20 kit by drilling holes into the t-slotted bars. Because of these reasons, physical testing was not able to be done to determine the effectiveness of this mounting system. Instead, mathematical research was done. Equation 6.22 was used to calculate the force that would be imparted on the turbine by the wind:

$$D = \frac{1}{2}\rho v_{\infty}^{2} * S * C_D$$

Equation 6.22*: Drag Force Equation*

D is the drag force imparted on the turbine by the wind, ρ is the density of the air, v_{∞} is the wind's velocity, S is the area of the surface the wind acts on, and C_D is the coefficient of drag of the surface acted on by the wind (which was assumed to be 2, worst case scenario, for the turbine blades mentioned earlier). Two surfaces need to be considered in this scenario, the turbine blades' exposed surfaces and the side panel of the base that will experience a similar pushing force imparted by the wind. The force the team is concerned with is where the wind speed is at its maximum of 70 mph due to customer technical specifications, so that was used as v_{∞}. Doing so yielded 667.25 Newtons or approximately 150.0 lbs. of force. Assuming the same drag coefficient of the base's largest side panel and same density (density at sea level, .0225$kg/$

m^3), the force calculated is 80.7 N (approximately 18.1 lbs.). Combined, the total force imparted on the full turbine system is 748.0 N—168.1 lbs. There will be four bolts to hold the base down, so each one will only need to be able to cope with 42.0 lbs. of shearing force in order for the turbine to remain upright.

After researching both wedge anchor bolts and hex lag bolts, the following table was created with the dimensions of the bolts, the force load each bolt can withstand, and the cost per bolt listed.

***Table 6.11**: Mounting Bolts and their Force Resistance Abilities (Kinetics, 2003)*

Screw/Bolt Type	Diameter (inches)	Length (inches)	Shear (lbs.)	Tension (lbs.)	Cost per Unit
Wedge Anchor Bolt (Zinc-Plated Steel)	5/8	3-3/4	8264	4999	.86
Hex Lag Bolt (Low Carbon Steel)	3/8	3	432	893	.48

As can be seen, both methods are viable for mounting the turbine. This mounting method will keep the team within the required weight range (where counterweights could have made the system exceed the 100 lbs.) and is quite easy to apply. One hole can be drilled into the steel bars at the bottom corners, and the bolts will be run through the bars and driven into the roof. The length of the bolts chosen allow for the bolt to travel all the way through the bar and still have most of the length still embedded into the roof being mounted on.

6.7.4 Expenses

The parts used to manufacture the base prototype were the 80/20 T-Slotted Aluminum kit and the plastic sheeting for the sides. The PVC sheeting used was available to the team for free. Furthermore, because the 80/20 kit was acquired through a deposit, which will be given back once returned, the team did not include this amount into the expense report, making the total amount spent on the base come out to $0.00. This fell well within the $50.00 budget allotted to each team member. However, a theoretical cost analysis was drafted for the base including materials that would have been used in actual production.

***Table 6.12**: Base Component Expenses*

Item	*Unit Price*	*Quantity*	*Item Total*	*Paid For It?*	*Actual Cost to Team*
20' Square Bar Steel	$14.80	2	$29.60	No	$0.00

PVC Sheeting/Square Foot	$1.25	24.4	$30.50	No	$0.00
Hex Lag Screw (3/8" X 4")	$0.48	4	$1.92	No	$0.00
80/20 T-Slotted 1010 Series Kit (Deposit)	($100.00)	2	($200.00)	No	$0.00
Total			$62.02		**$0.00**

The theoretical budget, as can be seen in Table 6.12 above, exceeds the $50.00 team budget; however, in actual production, the team budget would be allowed to be greater, and bulk products would be available at cheaper values per unit. The 80/20 used in this prototype was not counted towards the Item Total because the base would not use it in bulk production, just the 20 foot Square Bar Steel.

6.7.5 Overall Base Analysis

The materials used to construct the base allowed it to meet the design requirements outlined in the technical specifications of this project. The 80/20 kit proved not only a sufficient support system but also an adaptable one that could be altered when revisions were made to the other internal subsystems. Furthermore, the materials were able to be gathered with no expense to the team, and replacement products for actual production were discovered that could meet the remaining requirements not met by the prototype; for example, the mounting system ensures that the turbine does not fall over, even though the team did not have a chance to test this, since there was no place to properly mount the turbine on campus. Testing and mathematical analysis were carried out to prove that the base is a working, viable subsystem.

7 Final Assembly

Upon completion of the individual subsystems, assembly of the wind powered air compressor was performed by the team. Assembly began with attaching the turbine blades to the drive shaft through the use of shaft collars. In parallel, the drive shaft bearing and flange were centered and secured to the base frame. Next, as the drive shaft was inserted into the shaft bearing, the primary gearing pulley and brake disk were secured to the drive shaft. At this stage, the monitoring system, brake, and the secondary gearing component were installed. Lastly, the compressor and base covers were installed to yield the complete assembly. Figure 7.1 and Figure 7.2 below shows the complete wind powered air compressor. The final assembly measures 4 x 3 x 2 feet and weighs 89 lbs.

Figure 7.1: *Wind Powered Air Compressor (side panels removed)*

Figure 7.2: Wind Powered Air Compressor (internal compartments)

8 Results and Discussion

Since the team successfully created a working product, a variety of testing was able to be performed to measure its performance and assess whether it met the technical specifications. This testing revealed that some subsystems met or exceeded their individual goals, while some require further improvement. A lack of proper testing facilities was a hindrance to the testing process. A large quantity of the data would ideally have been gathered at a constant, controllable wind speed. However, the use of a large wind tunnel was not an option for the team and testing was instead performed in natural wind conditions. All wind velocities are appropriate averages for the interval in which a test was conducted.

8.1 Turbine Power Testing

During the feasibility research for this product, turbine power curves were generated for a variety of conditions and assumptions. It was important to test the validity of this theoretical data through controlled experiments. Ideally this would be accomplished by placing the turbine and drive shaft into a dynamometer, a device which measures the rotational output of a drive shaft. The data is then traditionally reported as a graph of torque vs. angular velocity and power vs. angular velocity. The dynamometer would also have to be located inside a suitably sized wind tunnel for Air-to-Air's testing purposes. Unfortunately, neither a wind tunnel nor a dynamometer are tools available to the team. Instead, the team created the torque and power curves for the turbine by measuring two points, the torque output at zero angular velocity and the maximum angular velocity corresponding to zero torque output. A linear torque curve was assumed to connect these two points. The power curve was created by simply multiplying the torque curve by angular velocity at every point along its range. This was repeated for a variety of average wind speeds. The results of turbine power testing can be found in Appendix J.

Some of the highlights from this data include the maximum power output at 12.5 mph of 0.01 hp. This corresponds to a stall torque of 1.55 ft-lb and a maximum angular velocity of 144 RPM. However, there is a very important non-dimensional metric which can represent all of the data. Coefficient of power (Cp) is a measure of the aerodynamic efficiency of a wind turbine. A Cp of 1 represents a turbine which harnesses 100% of the energy of the incoming flow. It should be noted that this is impossible. If all energy is captured, the flow velocity will be zero at the exit of the turbine and further flow will not be possible. Betz law states that the maximum coefficient of power a turbine can obtain is 0.593. The derivation of this value will not be discussed here.

$$P = C_p \frac{1}{2} \rho A V^3$$

***Equation 8.1**: Wind Power Equation*

In practice, the coefficient of power is calculated by measuring the power experimentally and solving the wind power equation for C_p. During preliminary analysis, a C_p of 0.2 - 0.25 was expected based on background research. The average coefficient of power for the team's wind

turbine was calculated to be 0.135. This means the turbine puts out a little over half what was initially expected during the design process. However, this experimentally measured C_p may be of limited accuracy. The largest source of error is the measured wind speed, which was obtained from a hand held anemometer. Because the torque and RPM were measured over the course of approximately a minute in variable wind speeds, the average wind speed is not perfectly representative of the testing conditions. This introduces a large source of error since the C_p is cubically related to wind speed in the wind power equation. Constant, accurate wind speed data is necessary to calculate a meaningful C_p for the turbine.

Another explanation of the lower than expected C_p is the quasi-functionality of the flaps. Videos of testing clearly show the flaps opening 1 - 2 inches. However, for the flaps to truly be effective, they need to open much farther. Ideally they would form an angle of approximately 45 degrees with the blade surface. Thus, a possible improvement in the next turbine produced would be to use a thinner flap of the same material or use more flexible material.

8.2 Payoff Period

Using the aforementioned C_p calculations, the payoff period could then be calculated for a variety of locations. Since there are not convenient metrics for measuring the cost of compressing air, the turbine was isolated from the compressor and the payoff period calculated based on the assumption that the turbine would be replacing an electric motor with a belt drive connection to a separate air compressor. The retail price of the turbine was assumed to be $500 and the cost of the electric motor it would theoretically be replacing was set at $40. The efficiency of the electric motor was assumed to be 80% and the average wind speed was used to calculate an assumed constant power output from the turbine. Finally, the average wind speeds and electricity costs for each location are determined from research. Using these assumptions and data, the payoff period was calculated using the spreadsheet in Appendix K. For example, in New York, the local market for this turbine, with an average wind speed of 5.5 m/s and an electricity cost of $0.1765 per kWh yield a payoff period of 28 years. However, since power output is cubically related to wind speed, in a location such as Nebraska with an average wind speed of 9 m/s and an electricity cost of $0.09 per kWh, the payoff period is only 12.5 years. If the assumption is made that the turbine's C_p is inaccurate and could be as high as 0.25, the payoff period for Nebraska drops to 6.8 years. This is still above the technical specification of meeting a payoff period of 5 years (Administration, 2007) (Wind Resource Estimates, 2007).

The team would like to comment that the target payoff period may have been overly ambitious. It is difficult to currently justify wind power even at a large scale, being twice the cost of coal or nuclear per kWh. Additionally, wind power can only supplement other energy sources due to its unreliability. However, in defense of the team's product and wind energy in general, the preceding analysis did not take into account the increasing costs of fossil fuel-based energy sources, nor the tax subsidies available to encourage the shift over to renewable energy sources

such as wind. These two facts could have a huge effect in reducing the payoff period of the Air-to-Air product line.

8.3 Flow Rate Testing

Using the 5 gallon pressure vessel available to IED students, the team tested the flow rate of the compressor in average wind speeds of 11 mph. Over the course of an hour, the team collected three data points. At 20 minutes the tank was at a pressure of 6 psi, at 40 minutes it had reached 12 psi, and by 60 minutes it had reached 17 psi. Assuming the process was isothermal, which is accurate for slow processes such as this one, the flow rate can be calculated using the ideal gas law. Doing so yields a flow rate of 0.0129 Cubic Feet per Minute at 9 psi. This means that while the pressure in the tank is in the vicinity of 9 psi, in wind speeds of 11 mph, the compressor can pump 0.0129 cubic feet of air at atmospheric pressure into the tank in one minute. As the pressure in the tank increases, the resistance to pumping will increase as well, reducing the flow rate at a given wind speed. Given the proper time and facilities, the team could have performed further flow rate testing at higher pressure levels to confirm this. Unfortunately, wind speeds were becoming increasingly variable that day and another opportunity to test did not present itself. This is just another example of how the team was at the mercy of Mother Nature with regard to testing the product yet collected the best data possible with the tools available.

8.4 Brake Testing

The requirement of the braking system is to stop the turbine at speeds up to 70 mph. This corresponds to a torque of 21.8 ft-lb. Thus, the braking torque was measured to assess whether it was capable of applying a torque of this magnitude. This was done by using a 10 lb. rated spring scale hooked to a 3 foot moment arm clamped to the drive shaft. One group member applied the brake using the brake lever while another pulled on the end of the spring scale to apply a torque. The torque values for static and kinetic states were measured and recorded.

***Table 8.1**: Braking Torque*

Static Braking Torque	8.3 ft-lb
Kinetic Braking torque	9.7 ft-lb

The data shows an unexpected result. Typically, the static friction for two materials is greater than the kinetic friction for the same two materials. In this case, the opposite effect is apparent. The team believes that this is the result of heating of the brake pads during the kinetic test. This is reasonable since the kinetic energy of the driveshaft will be dissipated as heat in the brake disc and brake pads during testing. Rubber is known to become “stickier,” that is, to move to a higher friction coefficient when heated. This is a common effect which is critical to the performance of motorcycle tires for example.

8.5 Weight

The customer requirements dictated a maximum weight of 100 lbs. Preliminary estimates based off the CAD assembly suggested a total weight of 77.74 lbs. However, this does not include some of the fasteners, the monitoring system circuitry, or the brake pads. Therefore, it is not surprising that actual weight of the turbine is 89 lbs. This meets the team's technical specifications.

8.6 Compressor Testing

Using a C-clamp to seal the air hose, the team was able to generate a pressure of 60 psi at wind speeds of 10 mph. The torque required to rotate the turbine did not significantly increase with increasing pressures. At 60 psi, the maximum torque required to rotate the turbine was only .45 ft-lb whereas the turbine creates a torque of 1.55 ft-lb at 12.5 mph. Thus, the turbine is capable of outputting the power necessary to achieve higher pressures. Unfortunately, the compressor was inexpensive and imperfect. There are small compression leaks associated with all piston and cylinder arrangements since even the best machining cannot completely seal the gap between the piston rings and cylinder wall. These compression leaks became significant enough to limit the team from creating more than 60 psi. If the compressor was operating at a higher RPM the time available for gases to leak past the piston would decrease and a higher pressure would be possible. A more expensive, higher quality compressor would likely be able to exceed 60 psi at the lower RPM created by the turbine.

8.7 Gearing Testing

The gearing system ideally would reach an angular velocity of 411 RPM at the compressor. The system exceeded this during testing, reaching 432 RPM. This was tested indirectly by analyzing a video of the compressor in operation under wind speeds of 19 mph. By stepping through the video frame by frame, counting rotations of the compressor, and dividing this value by the time interval, a maximum angular velocity of 432 RPM was calculated.

8.8 Driveshaft Testing

Using a 10 lb. spring scale and a 3 foot lever arm clamped to the drive shaft, a torque of 30 ft-lb was applied to the drive shaft. It did not fail structurally nor deform under this loading even though it exceeds the theoretical maximum torque value of 21.8 ft-lb at 70 mph.

9 Conclusion

The goal of the Air-to-Air wind turbine air compressor is to convert wind energy into air pressure using only mechanical energy utilizing a more efficient process than existing wind turbines by foregoing the typical electrical energy conversion. In this process, the wind moves a turbine whose rotational energy is translated through the gearing subsystem to an air compressor. The compressor then takes this mechanical energy and uses it to produce the compressed air required by our customers.

This product has addressed the needs of its targeted customers, primarily industrial sites and small business owners who frequently use hand held pneumatic tools. Secondary customers include homeowners doing home improvement that require pneumatic power tools. By utilizing the energy of the wind, a product that is not only a sustainable source of energy but also has minimal environmental impact has been created.

To create this product, a design process that included competitive benchmarking, mind-mapping, concept combinations, and selection matrices was employed. The solution consists of a vertical axis Savonius wind turbine made of steel and attached to the drive shaft. A belt and pulley system will be used for torque conversion, bearings for drive shaft mounting, and a reciprocating air compressor for the conversion of rotational energy from the drive shaft to compressed air for storage. A micro-controller monitors and reports performance details of the system, and a braking system is used to manage the systems operation, while the base holds all the subsystems together.

When selecting the materials for the subsystems, machinability, weight, strength, resistance to weather, and cost were all taken into account. While team members were working on their individual subsystems, many engineering challenges were faced, such as machining tolerances and damaged parts, which required help from other team members or the opinions of experts to solve. In addition to this, the team had neither an ideal testing environment nor the ideal measurement instruments to acquire the highest quality data.

The final prototype is functional and features five fully functional subsystems and two that are partially functional ones. Although the compressor and the braking system's performance did not meet the specifications that were set, the drive shaft and the compressor were able to exceed theirs. However, the system in its current state is not a feasible substitute for existing air compression systems due to its inability to compress air to the required 100 psi and its slow compression rate of .0129 cubic feet per minute. Also, the payoff period calculated of 28 years in New York (12.5 in Nebraska) was five times longer (two and a half times in Nebraska) than the customer's required period of 5 years. This fact lead the team to conclude that the prototype in its current state would not be a practical product.

Various improvements must be made to this prototype before it is ready for production. The partially functional subsystems will need to be redesigned in order for their set specifications to be met. Also, various inefficiencies, including those associated with the compressor will need be removed or decreased in order to decrease the time required to compress the air. After these improvements have been made, the team can look into patenting the project. After a patent is obtained, the product can be streamlined for manufacturing, reducing the cost of production and the cost to the user.

The group has completed this project through a process defined by the group, mini-groups, and individual work; governed by deadlines and responsibilities dictated by the Gantt

chart and Team Contract. By synergizing the strengths and weaknesses of the team members as well as utilizing outside resources, the team was able to accomplish its goals. Through communication between members and the sharing of information, the team was able to achieve shared success.

10 References

(2006). Retrieved from Mine Lab: http://www.minelab.com/__files/i/5895/SquareWave.gif

Administration, E. I. (2007). *Residential Retail Prices.* Retrieved from Energy Band Gap: http://www.energybandgap.com/wp-content/uploads/2011/02/electricity-by-state.jpg

ATMega DIP Chip. (n.d.). Retrieved from Roboics.org: http://robotics.org.za/image/cache/data/pdip-27-500x500.jpg

Atmel. (2009). *ATMega328P-PU Datasheet.* Retrieved April 2012, from Atmel.com: http://atmel.com/images/8161s.pdf

Bayman, H. L. (2002). Retrieved March 2012, from Science Direct: http://www.sciencedirect.com/science/article/pii/

Brandt, J. (2005, October). *Brakes from Skid Pads to V-brakes.* Retrieved May 5, 2012, from http://sheldonbrown.com/brandt/brakes.html

BroadStar Wind Corporation. (2011). *The AeroCam (TM) Type III Wind Turbine System Highlights*. Retrieved March 4, 2012, from www.broadstarwindsystems.com: http://www.broadstarwindsystems.com/files/Aerocam%20description%20and%20technology%20highlights.pdf

BroadStar Wind Corporation. (2011). *The BroadStar AeroCam Type III*. Retrieved March 4, 2012, from www.broadstarwindsystems.com: http://www.broadstarwindsystems.com/assets/AeroCam3.pdf

BroadStar Wind Systems. (2008, June 2). *Press Release.* Retrieved March 4, 2012, from www.broadstarwindsystems.com: http://www.broadstarwindsystems.com/news/pr_2008_06_02.pdf

Brown, S. (2007). *Brown's Bicycle Glossary.* Retrieved from http://sheldonbrown.com/glossary.html

Concrete Fastening Systems. (2012). Retrieved April 2012, from Confast: http://www.confast.com/products/thunderstud-anchor.aspx

CorrectEnergySolutions. (2005, October). *XDOBS Wind Turbine*. Retrieved March 4, 2012, from correctenergysolutions.com: http://correctenergysolutions.com/wind/

DIXIE Closed-Head Plastic Drums - Blue. (n.d.). Retrieved March 4, 2012, from Amazon.com: http://www.amazon.com/DIXIE-Closed-Head-Plastic-Drums-Blue/dp/B002SVZAHM/ref=pd_sbs_indust_5

Engineering Tool Box. (n.d.). *Types of Air Compressors*. Retrieved March 4, 2012, from engineeringtoolbox.com: http://www.engineeringtoolbox.com/air-compressor-types-d_441.html

Evan'sCycles. (2012). Retrieved 2012, from http://www.evanscycles.com/products/diamond-back/bmx-sidepull-caliper-brake-ec026394

Hangzhou TianTian Hardware, Ltd. (2012). Retrieved April 2012, from http://www.china-tiantian.com/index.php/product/Lag+Screws.html

Harbor Freight Tools. (2012). *60 Gallon Air Compressor*. Retrieved March 4, 2012, from harborfreight.com: http://www.harborfreight.com/5-hp-60-gallon-165-psi-two-stage-air-compressor-93274.html

Johnson, C. (2000). *Practical Wind Generated Electricity*. Retrieved March 4, 2012, from enery.saving.nu: http://energy.saving.nu/wind/winddesignprimer.shtml

Kinetics. (2003). *Kinetics Noise Control*. Retrieved April 2012, from Kinetics Noise: http://www.kineticsnoise.com/SeismicBook/pdfs/a7/a7.3%20-%20seismic%20design%20data%20for%20lag%20screws.pdf

LivingSteel. (2010). *Steel Corrosion*. Retrieved 2012, from Living Steel: http://livingsteel.org/corrosion-5

Menet. (2009, November). Retrieved from Wind Energy Conference: http://www.2004ewec.info/files/23_1400_jeanlucmenet_01.pdf

Morgan, J. (2010, April 2). *Comparing Energy Costs of Nuclear, Coal, Gas, Wind, and Solar*. Retrieved from Nuclear Fissionary: http://nuclearfissionary.com/2010/04/02/comparing-energy-costs-of-nuclear-coal-gas-wind-and-solar/

Ohya, Y., & Karasudani, T. (2010). A Shrouded Wind Turbine Generating High Output Power with Wind Lens Technology. *Energies* .

PWEagle. (1999). Retrieved April 2012, from PWPipe: http://www.google.com/url?sa=t&rct=j&q=&esrc=s&source=web&cd=1&ved=0CIABEBYwAA&url=http%3A%2F%2Fwww.pwpipe.com%2Fliterature%2Fw%2FWaterInstallGuide.pdf&ei=UOOnT9KsBOWC6AHO8rDUBA&usg=AFQjCNGZtD2bbhyNvEy0etGtGoD1zUcHFQ&sig2=xnuGqa86qAZMkGtUas4wJA

Synchronous Motor. (2012). *AC Synchronous Motor.* Retrieved May 2012, from http://www.ac-synchronous-motor.com/china-12v_constant_7_00a_stall_current_carbon_bursh_motor_for_office_automation_equipment-229530.html

Toolcraft Plastic. (n.d.). Retrieved April 2012, from Tool Craft: http://www.toolcraft.co.uk/vacuum_forming_material_specs_ABS_HIPS_HDPE_PETG_PP_PVC.htm

U.S. Dept. Energy: Energy Efficiency & Renewable Energy. (2012, February 7). *Wind Powering America: New York 80-meter Wind Map and Wind Resource Potential*. Retrieved March 4, 2012, from windpoweringamerica.gov: http://www.windpoweringamerica.gov/wind_resource_maps.asp?stateab=ny

Wind Resource Estimates. (2007). Retrieved March 27, 2012, from National Renewable Energy Laboratory: http://www.windnavigator.com

Wind Turbine Power Calculations. (n.d.). Retrieved March 4, 2012, from http://www.raeng.org.uk/education/diploma/maths/pdf/exemplars_advanced/23_Wind_Turbine.pdf

Zingman, A. (2007, May 11). Retrieved from MIT: http://dspace.mit.edu/bitstream/handle/1721.1/40927/212409044.pdf

Appendix A: Selection of Team Project

At the onset of this project, each team member had chosen to work on a project in the category of sustainable energy. To further specify the type of project the team would develop, the team used the mind mapping and concept selection tools. The team examined current sustainable energy problems being faced by people of the world and generated a mind map outlining these problems. The mind map generated can be seen below in Figure A.1.

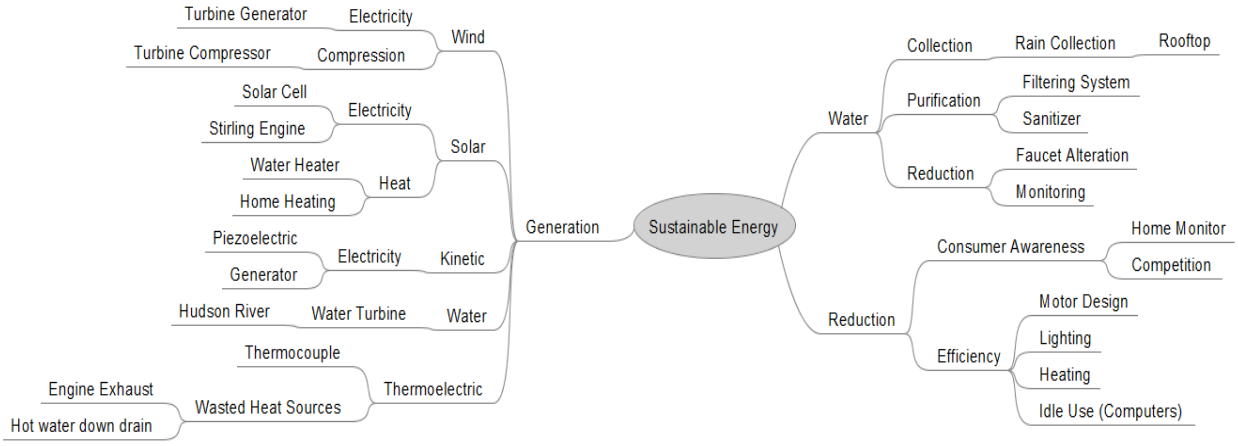

Figure A.1: *Project Selection Mind Map*

After generation of the project mind map, each team member voted for the topic they were most interested in. This ensured that the project the team developed would be something members were interested in rather than a potentially disinteresting one. Members voted for a thermoelectric generator, a Fresnel lens solar water heater, or a wind turbine compressor. To determine which of the three projects the group would develop, a concept selection matrix was created and each possible project scored against a set of criteria. After totaling the weighted scores of each proposed project, the project of developing a wind turbine compressor was selected. The concept selection matrix is seen below in Table A.1.

***Table A.1**: Concept Selection Matrix*

	Segment	A Thermo-electric generator		B Fresnel Lens Solar Water Heater		C Windturbine Compressor	
Selection Criteria	Weight	Rating	Wtd	Rating	Wtd	Rating	Wtd
Cost	60%	-1	0.36	1	0.22	0	0.13
Feasability	100%	-1	1.00	1	1.00	1	1.00
Creativity	20%	1	0.04	1	0.01	0	0.00
Practicality	80%	0	0.64	0	0.51	1	0.41
Reliability	90%	0	0.81	-1	0.73	0	0.66
Performance	70%	0	0.49	0	0.34	1	0.24
Efficiency	20%	0	0.04	-1	0.01	0	0.00
Durability	100%	0	1.00	1	1.00	0	1.00
Documentation	100%	0	1.00	0	1.00	1	1.00
	Total Score	-1.4		1.7		4.44	
	Rank	5		2		1	
	Continue?	NO		NO		YES	

Appendix B: Customer Requirements/Technical Specifications

Customer Requirement	Importance	Technical Specification	Target Value / Range of Values
Return on Investment	5	Payoff period	5 years
Stability-It shouldn't fall over.	5	Wind speed required for tip condition	70 mph
Sustainable energy	5	Wind energy	-
Safe to the surrounding environment	5	Gives off no toxins or harmful substances	-
Pressure needed	5	Minimum air pressure	100 psi
Safe	5	Factor of Safety of Pressure Vessel	3
Reliability	4	Limit mechanical failures	< 0.1% mechanical downtown
Maintenance Free	4	Maintenance Cost	$0
Size-fit through the door	4	Maximum height x width	80 inch x 30 inch
Monitoring system	4	Monitor angular velocity	-
Cost	3	Maximum cost	$350
No animal interference	3	Enclosed base	-
Maintain continuous operation without overheating	3	Downtime due to overheating (%)	0%
Weight	2	Maximum weight	100 lbs.
Can be used traditional with automotive tools	2	Compatible with impact wrenches, air ratchets, chisels, drills, cutoff wheels, die grinders, car lifts.	-

Appendix C: Gantt Chart

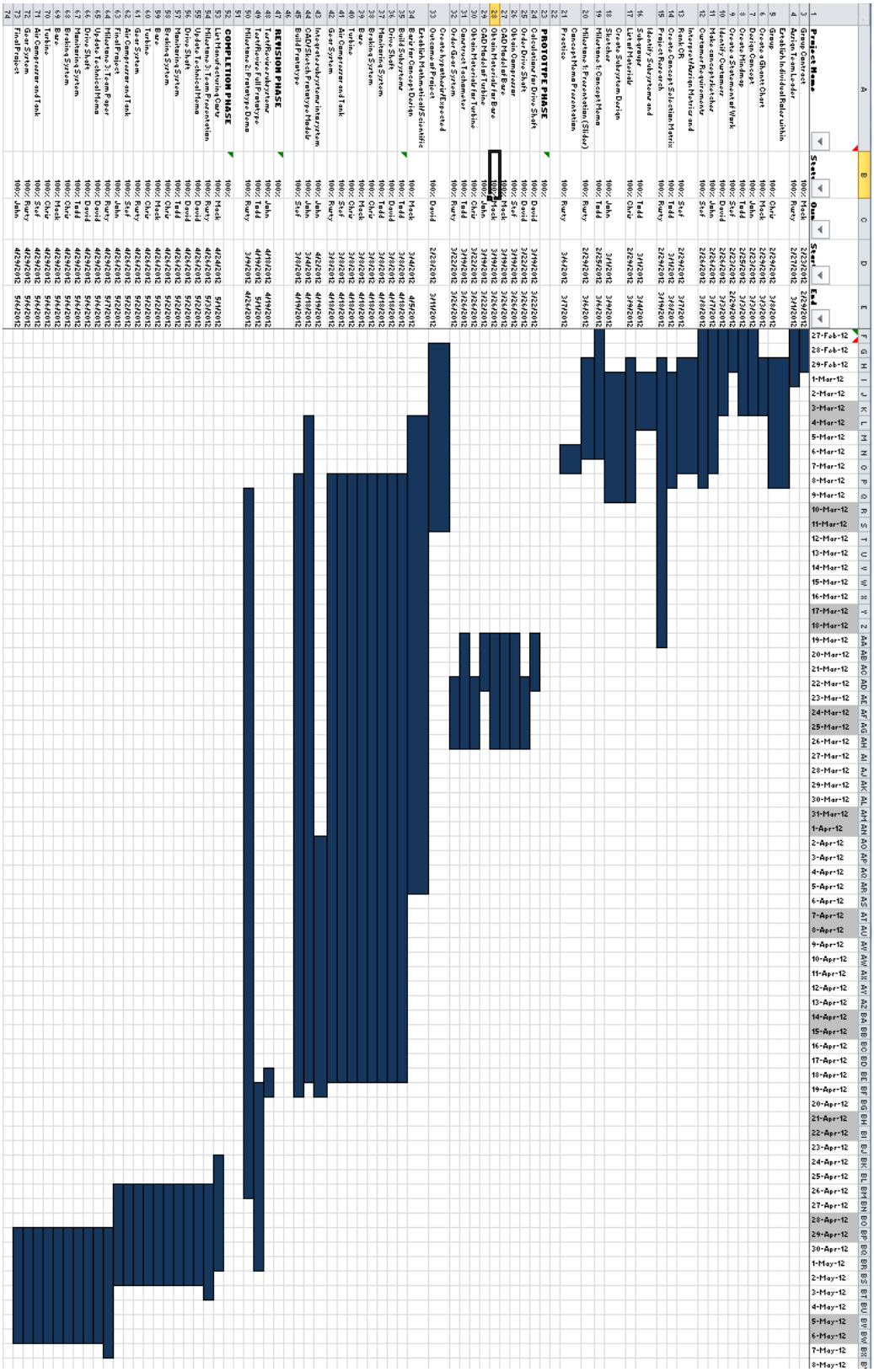

The team's process of work was to meet in large groups at least once a week to update each other on individual progress of subsystem production and idea generation, meet in mini groups during testing and when working on major deliverables (i.e. technical memos), and as individuals during subsystem manufacturing and benchmarking research. In order for the team to maintain cohesion within the group and meet deadlines, a Gantt chart was developed to set and maintain smaller project deadlines for the group. This provided reference for the group, allowing enough time for the subsystems to be integrated with substantial room for revision and testing. However, much like the group contract, the group did not need to regularly consult the Gantt chart to remain on task. The chart was updated every week by team leader Russell Teller, who would remind the group of certain deadlines—for example, subsystem development and fabrication was set to be completed on April 18th—and keep all members on task. In this way, the Gantt chart allowed the team to meet deliverable deadlines despite having at least one notable procrastinator within the group.

Appendix D: Expense Report

Subsystem	Item	Unit Price	Quantity	Item Total	Actual Cost to Team	Theoretical Subtotal	Actual Subtotal
Compressor							
	Air compressor	$8.99	1	$8.99	$8.99	$18.96	$18.96
	Schreder valves	$3.99	2	$7.98	$7.98		
	Teflon tape	$1.99	1	$1.99	$1.99		
Drive shaft							
	Low-Carbon Steel 6' long 1" OD tube	$20.26	1	$20.26	$20.26	$120.72	$82.36
	1" ID Shielded Thrust Bearing	$20.26	1	$20.26	$20.26		
	Black Oxide steel 1" ID Shaft Collar	$3.27	2	$6.54	$6.54		
	Aluminum Sliding Holder Pieces	$10.82	1	$10.82	$0.00		
	Steel Plate (McMaster Price)	$27.54	1	$27.54	$0.00		
	Steel Plate (Scrap Price)	$6.00	1	$6.00	$6.00		
	Assorted Fasteners (Whole Project)	$20.00	1	$20.00	$20.00		
Braking							
	Flange Bearing	$9.30	1	$9.30	$9.30		
	Brake Disc Steel	$17.81	1	$17.81	$0.00	$42.92	$17.92
	Pad	$0.79	1	$0.79	$0.79		
	Lever	$1.69	1	$1.69	$1.69		
	Fixture	$2.19	1	$2.19	$2.19		
	Cable	$0.49	1	$0.49	$0.49		
	Lever Mounting Bar	$7.19	1	$7.19	$0.00		
	Shaft Collar	$7.98	1	$7.98	$7.98		
	Shipping	$4.78	1	$4.78	$4.78		
Monitoring							
	120v to 13v Transformer	$2.90	2	$5.80	$0.00	$21.67	$2.87
	5V Regulator	$0.19	2	$0.38	$0.00		
	Atmel ATMega328	$2.29	2	$4.58	$0.00		
	Capacitor	$0.02	4	$0.08	$0.00		
	Crystal Oscillator	$0.39	2	$0.78	$0.78		

	Header Pins	$0.05	1	$0.05	$0.00		
	Hinge Set	$1.19	1	$1.19	$1.19		
	Insulated Copper Wire (price / foot)	$0.03	10	$0.30	$0.00		
	LCD Display	$5.90	1	$5.90	$0.00		
	LEDs	$0.04	2	$0.08	$0.00		
	Perf Prototyping Board	$0.20	2	$0.40	$0.40		
	Plastic Housing	$0.99	1	$0.99	$0.00		
	Potentiometer	$0.19	1	$0.19	$0.00		
	Resistor	$0.01	5	$0.05	$0.00		
	Ribbon Cable	$0.19	1	$0.19	$0.00		
	Solder (price / gram)	$0.05	10	$0.50	$0.50		
	Wire Connector	$0.04	3	$0.12	$0.00		
	Wooden Mount	$0.09	1	$0.09	$0.00		
Gearing							
	Flange Bearing	$22.23	1	$22.23	$22.23	$46.10	$46.10
	1.5" Pulley	$3.79	1	$3.79	$3.79		
	5" Pulley	$10.52	1	$10.52	$10.52		
	Shipping	$4.78	2	$9.56	$9.56		
Turbine							
	32 sq ft of 22 Gauge Steel	$45.00	1	$45.00	$45.00	$138.30	$138.30
	Threaded Shaft Collar	$7.98	3	$23.94	$23.94		
	3 sq ft of PVC Rubber	$15.90	1	$15.90	$15.90		
	Water Jet Cutting	$24.00	1	$24.00	$24.00		
	Shipping	$19.48	1	$19.48	$19.48		
	Paint	$4.99	2	$9.98	$9.98		
Base							
	20' Square Bar Steel	$14.80	2	$29.60	$0.00	$62.02	$0.00
	PVC Sheeting/Square Foot	$1.25	24.4	$30.50	$0.00		
	Hex Lag Screw (3/8" X 4")	$0.48	4	$1.92	$0.00		
	80/20 T-Slotted 1010 Series Kit*	Deposit-$100	2	$0.00	$0.00		
Totals						Theoretical Total	**Actual Total**
						$450.69	**$306.51**

Based on the time and cost that was required to build this product a cost of production of $500 was estimated. This number comes from the additional money that the team would use to improve the project, specifically automating the braking system and acquiring a more efficient compressor. Since improving these systems would put the theoretical total above $500 without including the cost of labor additional saving would be created through the standardization of bolts and the selection of standard gears. Also the turbine blades would be molded and cast minimizing the amount of time required for fabrication. The entire product would be assembled on an assembly line which could either be operated by robotic machinery or people. Additional savings could be generated through economy of scale. The cost associated with the components utilized is listed in the expense report table above.

Appendix E: Team Members and Their Contributions

E.1 Student 1 (editor's note - all team member names were removed)

Student 1was responsible for developing the monitoring subsystem and worked closely with Christopher O'Neal's development of the braking subsystem. For the Milestone I memo, he was responsible for the Concept Selection and Competitive Benchmarking section as well as the Proposed Solution section. For the Milestone II demonstration, he demonstrated the monitoring subsystem. In the Milestone III report, he wrote the Concept Selection, Monitoring Subsystem, Final Assembly, and Project Selection sections.

E.2 Student 2

Student 2 was responsible for the selection, design, and construction of the turbine subsystem. He performed initial research into Savonius type wind turbines and the governing characteristics of their power output. He created a CAD model of the conceptual design. During spring break, he prototyped and tested three different turbine designs resulting in the selection of the final design. Working with another team member, he selected the material for the turbine construction. He worked with another team member to optimize the drive shaft dimensions to minimize cost while meeting structural requirements. This was done by performing multiple instances of Finite Element Analysis on a variety of turbine and driveshaft combinations. In order to fabricate the parts for the turbine, he consulted various faculty including John Szczesniak, Joe Baca, and Mark Anderson. He created and assembled the CAD parts for all subsystems except for the gearing and compressor system. All welding and assembly was performed by Student 2 with the assistance of another team member. Student 2 was present for all final testing of the turbine.

For Milestone I, he was responsible for the Customer Needs, Technical Specifications, and the Proposal sections. During Milestone II, he successfully demonstrated his subsystem. For the Milestone III presentation and final report, he was responsible for the turbine subsystem, Statement of Work, and Testing and Analysis sections.

E.3 Student 3

Student 3 was responsible for the compressor subsystem. She did benchmarking and research on the correct type of compressor to purchase as well as how to adapt the compressor hose to the air tank. In order to integrate the compressor with the gearing system, she helped another student create a base for both subsystems. She also helped a different student fabricate parts for the gearing subsystem.

For Milestone I, she was responsible for the Problem Statement and Mission Statement. For Milestone II, she demonstrated the compressor subsystem. For the Milestone III report, she wrote the Executive Summary, Introduction, Project Objectives and Scope, and the compressor subsystem.

E.4 Student 4

Student 4 was responsible for the drive shaft subsystem. He worked with a team member to do initial calculations for the system to determine the basics of size and material choice. He wrote the Materials Section of the Milestone I Technical Memo and helped create the basis for the Milestone I presentation slideshow.

Student 4 machined and assembled the entire drive shaft subsystem. He also demonstrated the drive shaft subsystem for Milestone II in addition to again creating the basis for the slideshow presentation. For the Milestone III presentation, he made several slides. In the final Technical Report, he was responsible for the Professional and Societal Considerations, Drive Shaft, and Customer and Technical Specifications sections.

E.5 Student 5

Student 5 was responsible for the base subsystem, which she demonstrated during Milestone II. She put down a deposit for two 80/20 kits from the school and acquired an anemometer for later testing on campus. For Milestone I, she was responsible for the Project Plan and Gantt Chart. For Milestone III, she was responsible for the Gantt Chart, Base subsystem, and User Manual sections in the Technical Report; the Executed Plan, Base, and Full Prototype slides for the presentation.

E.6 Student 6

Student 6 worked with a team member on the turbine subsystem and another student on the braking subsystem. He assisted the assembly of each of these subsystems and performed theoretical calculations on the turbine as well as CAD models of an alternative turbine design. He created the materials table for the Technical Memo and contributed slides to the Milestone I presentation. Student 6 also demonstrated the braking subsystem for Milestone II. He later created slides for the Milestone III presentation and wrote the Conclusion, Expense Report, and Braking Subsystem sections of the Technical Report.

E.7 Student 7

Student 7 was responsible for the torque conversion subsystem. He conducted preliminary analysis and CAD models of the proposed solution, parts procurement and fabrication, assembly of the gearing system, and integration of the subsystem into the overall project.

Student 7 was also awarded the responsibility of team leader. He organized team meetings, set deadlines, and checked progress on the subsystems. When papers or presentations were necessary, he supervised the division of labor as well as group cohesiveness to obtain a final product.

For the Milestone I Technical Memo, Student 7 was in charge of the conclusion section and was part of the editing team. For the corresponding presentation, he presented the proposed solution and was in charge of editing the presentation. With regards to the Milestone III presentation, Student 7 presented his own subsystem (torque conversion), as well as the future developments, team effort, and lessons learned slides. For the Milestone III paper, Student 7 wrote the Assessment of Relevant Existing Technologies, Torque Conversion Subsystem, Lessons Learned portions, and his individual contribution section. He also was in charge of formatting the paper.

Appendix F: Statement of Work

Team

Seven Student Names Here

Semester Objectives

1. Design a wind powered air compressor in order to convert kinetic wind energy into stored pressure energy.
2. The designed wind powered air compressor must fully meet customer requirements in terms of produced power and pressure
3. Design the wind powered air compressor to be both scalable and modular.
4. Create a design which augments or offsets unsustainable air compression methods used by companies.
5. Overcome the expense and difficulty associated with acquiring materials and the lack of fabrication skills of team members.
6. To improve on the weaknesses of existing designs
7. Obtain an 'A' grade on the final project.
8. Have the final selected design reflect the entirety of the engineering design process.
9. Utilize the individual strengths of the members of the group to create a product reflecting the sum of those strengths
10. To improve the weaknesses of team members.

Approach

Utilize effective benchmarking to analyze competing, or already existing, systems to find the best possible wind turbine design. From that design, analyze available materials to optimize both weight and durability while still creating enough power output to meet the customer specifications. From this initial investigation, use the engineering design process to develop an optimum final concept and design for prototyping and fabrication. Synergize the group members' available talents to finalize and create the selected design.

Deliverables and Dates

1. Milestone One: System Concept Review (3/8)
2. Prototype Design (3/19)
3. Prototype Fabrication and Review (4/5)
4. Modifications and Testing (4/12)
5. Milestone Two: Project Demonstration (4/26)
6. Milestone Three: Team Presentation (5/3)
7. Milestone Three: Final Report (5/7)

Appendix G: Lessons Learned

G.1 Ideas that Worked

Overall, the wind turbine powered air compressor is a fully functional project; many aspects of this group's approach worked, including division of labor, group cohesiveness, and the procurement of the parts. The subsystem approach functioned admirably. Group members were assigned a subsystem based on their technical skills; for example, the Electrical Engineer worked on the monitoring system, and the Mechanical Engineer worked on the gearing system. Every subsystem was functional, and only two of the seven didn't fully meet their ideal technical specifications. Even though the project was divided into subsystems, the group still convened and worked together. Individual work was often the method, but sometimes mini-groups were assembled to tackle more challenging problems. For instance, two students put a team effort into constructing the wind turbine blades, and two students paired up to perfect the braking system. With the amount of parts involved in constructing the wind turbine powered air compressor, there had to be a mix of fabrication and procurement of parts. Project-specific parts, such as the wind turbine and the monitoring system, were built by the team. However, pieces like the air compressor and the bearings were purchased because of the complexity involved in fabrication. If the wind turbine powered air compressor was to be built again, the subsystem approach; individual, mini group, and group work; and mix of ordered and fabricated parts tactics would be kept and used again.

G.2 Problems and Solutions to Try

Although the wind turbine powered air compressor was functional, it did have its setbacks: not enough analysis was done beforehand, tolerances became an issue during construction, and testing conditions were not ideal upon the completion of the assembly. Although the turbine functioned well, additional analysis in the preliminary stages could have improved the subsystem and project as a whole. Analysis of the power output from the turbine was completed but not the resistance it might receive from the loading of the compressor and the corresponding torque conversion. This led to a loss in efficiency, and though the compressor gear reached its goal of 411 RPM, it required a much higher wind speed than anticipated. In the future, a more thorough inquiry into each subsystem would streamline the project. Another issue that arose was tolerances. The bottom bearing rod that supports the second gear in the torque conversion system had two set screw holes that needed to be centered and separated precisely. After initial fabrication of the part, this was not the case. The set screw holes were misaligned and the screws would not go all the way through the top bearing rod, second gear, and bottom bearing rod. So, the part was machined again and functioned the second time. In the future, more precise machining would save lost time and increase the robustness of the wind turbine powered air compressor. Once the product was completed, testing was performed. From this, the group obtained adequate power output, wind speed, and resulting pressure data. However, there were significant sources of error, namely the wind speed. This team did not have access to a wind

tunnel so the wind speeds used were variable according to Mother Nature and difficult to measure accurately. In the future, much more precise data could be obtained with access to a steady, adjustable, and measurable wind speed in a wind tunnel. In response to the shortcomings of the wind turbine powered air compressor, this group would conduct more analysis, precise machining, and more accurate testing in the future.

Appendix H: User Manual

AIR-to-AIR: Wind Turbine Air Compressor Model 1

User Manual

Turbine comes fully assembled, and *Air-to-Air* will provide installation of device included in the cost of purchase. For extra assistance in future installation of the system (usually in the case of a move), *Air-to-Air* will provide additional assistance for a service fee. The number to call is: 917-xxx-xxx

Air-to-Air does not advise customers to install their *Air-to-Air* product on their own and will not be held responsible if injuries or damages result, should a user choose to do so.

Use:

The *Air-to-Air* wind turbine should only be used as described, to compress air and store it in appropriate air storage tanks. *Air-to-Air* will not be responsible for any injuries and damages caused by improper use of this machine.

No human interaction is required for this product to operate. Once mounted on the customer's roof, the customer should not need to be in direct contact with the machine except for the external electronic monitoring. Should the turbine need a repair within the 5 year guaranteed warranty period, customers are advised to call *Air-to-Air* for professional assistance. If the customer is unsure whether their turbine needs maintenance, one is able to inspect the turbine by first using the braking system to slow the blades, if they are in motion, then remove one of the side panels once the brake is properly locked in place (following the braking system protocols detailed in this manual), and remove one of the grey side panels for inspection. If the customer finds that the system requires maintenance or is unable to determine and needs assistance, the number to call is xxx-xxx-xxxx (support phone number).

Braking System:

In the event of an upcoming storm (where winds are expected to exceed the turbine's withstanding limit of 70 mph), the user must first use the hand brake to slow and then stop the blades from turning, then lock the brake into place. [This lock-in feature is not present in the prototype due to time constraints; however, ideally the weather brake would be an automatic system in the final product so the user would not need to interact personally with the turbine in this case.]

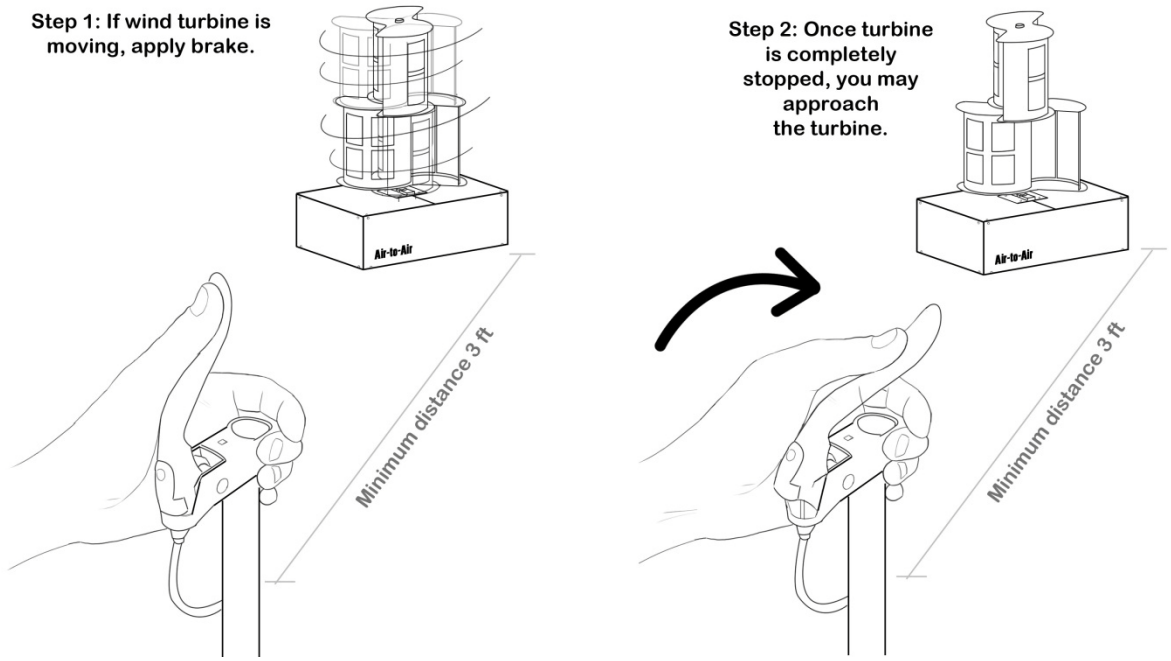

WARNING

User(s) should **NOT** do any of the following:

-Come within three feet of the turbine while blades are in motion. The user must follow proper braking protocol. First stop the blade with the handbrake, then the user may approach the turbine.

-Try to adjust the internal system without capable knowledge of function. *Air-to-Air* will not be responsible for any detrimental effects caused by alterations made by users on the system/turbine.

-Under outside temperatures with risk of burning or freezing upon contact (less than 32 degrees and above 90 degrees Fahrenheit), directly touch any metal features of the turbine.

THIS PRODUCT IS INTENDED FOR USE UPON A RAISED STRUCTURE SUCH AS A ROOF. *Air-to-Air* is NOT responsible for any and all injuries and damages resulting from inappropriate placement of the turbine on ground level.

Appendix I: Arduino C Code

```
#include <SoftwareSerial.h>

#define sensorPin A0

unsigned int timeSet = 0, temp = 0, rpm = 0, elapsed = 0;
SoftwareSerial mySerial(9, 10);
unsigned char state = 0;

void setup(){
  mySerial.begin(9600);
}

void loop(){
  if (state == 0 && getSensorState() == 1){
    state = !state;
    temp = millis();
    elapsed = temp - timeSet;
    timeSet = temp;
    rpm = 60000 / (elapsed * 4);
    sendIntPacket(rpm);
  } else if (state == 1 && getSensorState() == 0){
    state = !state;
  }
  delayMicroseconds(50);
}

void sendIntPacket(unsigned int a){
  mySerial.write(a >> 8);
  mySerial.write(a);
}

byte getSensorState(){
  if (analogRead(sensorPin) > 10){
    return 1;
  }
  return 0;
}

#include <LiquidCrystal.h>
#include <SoftwareSerial.h>

LiquidCrystal lcd (2,3,8,7,6,5);
SoftwareSerial mySerial(9, 10);
#define PB 4
unsigned int temp = 0, timeSet = 0, rpm = 0;

void setup(){
  mySerial.begin(9600);
  lcd.begin(16,2);
}
```

```
void loop(){
  lcd.clear();
  //lcd.setCursor(0,1);
  //temp = timeSet =  millis();
  //lcd.print("ACTIVE");
    //while (temp - timeSet < 20000){
      lcd.setCursor(0,0);
      lcd.print("RPM");
      lcd.setCursor(0,1);
      lcd.print("        ");
      lcd.setCursor(0,1);
      lcd.print(rpm);
      //temp = millis();
      mySerial.flush();
      while(!mySerial.available());
      delay(1);
      getIntPacket(&rpm);
  delay(100);
}

void getIntPacket(unsigned int* a){
  *a = (mySerial.read() << 8);
  *a += mySerial.read();
}
```

Appendix J: Turbine Power Curves

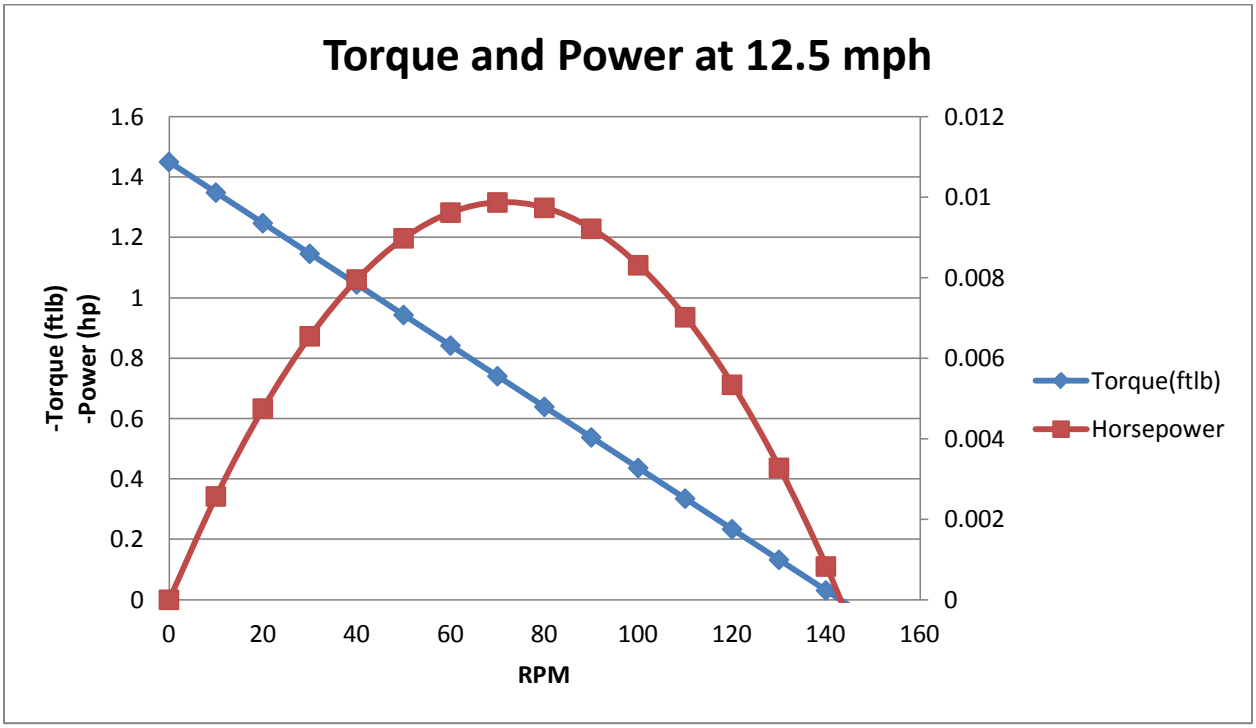

No-Load RPM	Wind speed (mph)	Torque (ftlb)	Brake	Pmax	Cp
86	8.3	1	Y	0.004094	0.161567356
48	5.5	0.5	Y	0.001142	0.154957506
46	5.8	0.45	Y	0.000985	0.113966132
56	6.2	0.575	Y	0.001533	0.145134362
136	12	1.325	Y	0.008578	0.11202127
142	12.4	1.35	Y	0.009125	0.108005657
62	7.1	0.75	Y	0.002213	0.139562053
132	12.1	1.5	Y	0.009425	0.120060051
98	9.7	1.275	Y	0.005948	0.147065398
74	7.9	1.05	Y	0.003699	0.169289175
128	10.9	1.25	Y	0.007616	0.132718032
144	12.5	1.55	Y	0.010625	0.122759072
				AVG Cp	0.135592172

Appendix K: Payoff Period Data

Location	Cp	Wind Speed (m/s)	$/kWh	Payoff Period (yrs)
New York	0.1356	5.5	0.1765	27.99
Nebraska	0.1356	9	0.09	12.53
California	0.1356	4	0.147	87.36
Florida	0.1356	5	0.112	58.71
Maine	0.1356	6	0.148	25.71
New York	0.25	5.5	0.1765	15.18
Nebraska	0.25	9	0.09	6.79
California	0.25	4	0.147	47.39
Florida	0.25	5	0.112	31.84
Maine	0.25	6	0.148	13.95

Appendix L: Finite Element Analysis of Turbine/Drive Shaft

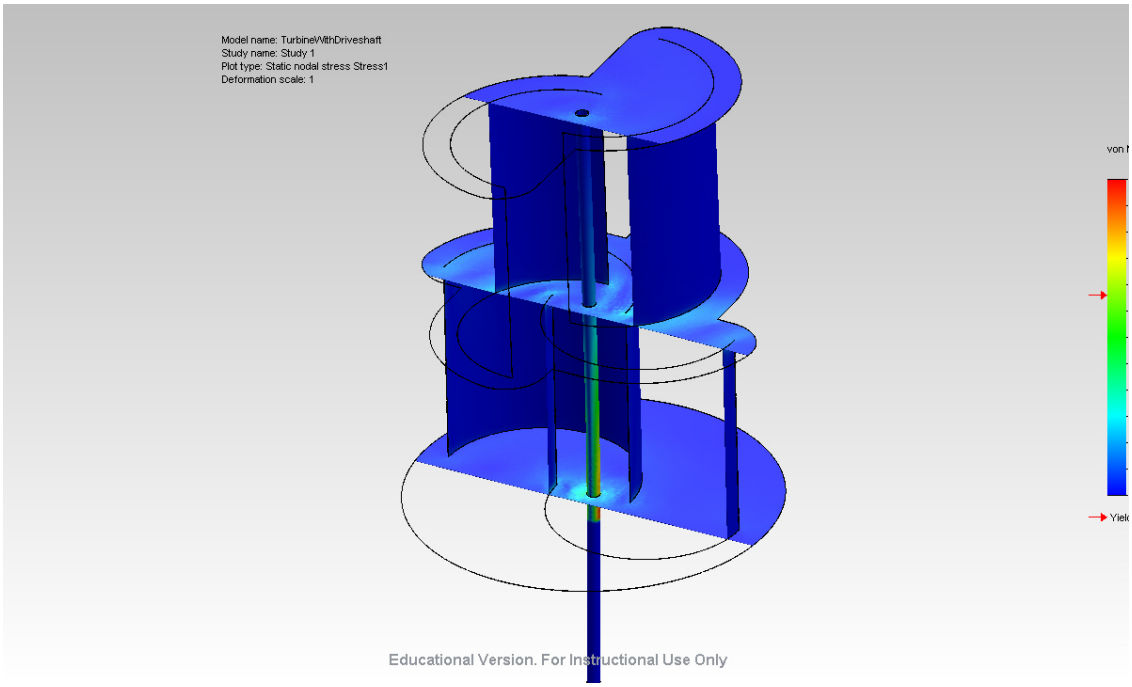

Figure L.1 : Stress Analysis

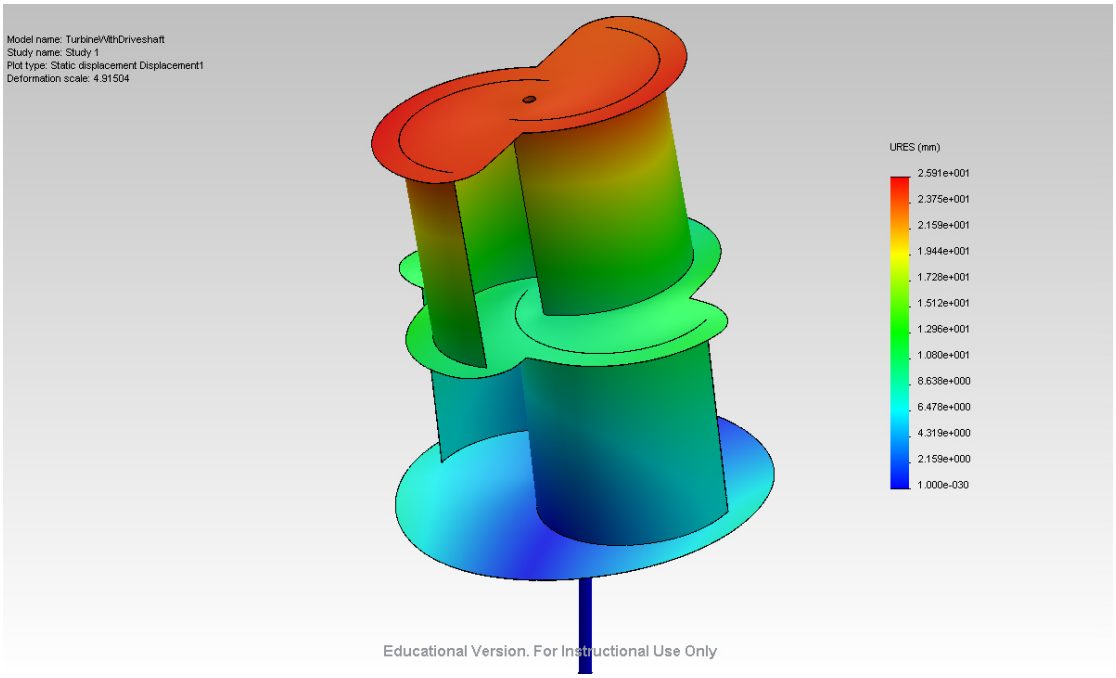

Figure L.2 : Displacement Analysis

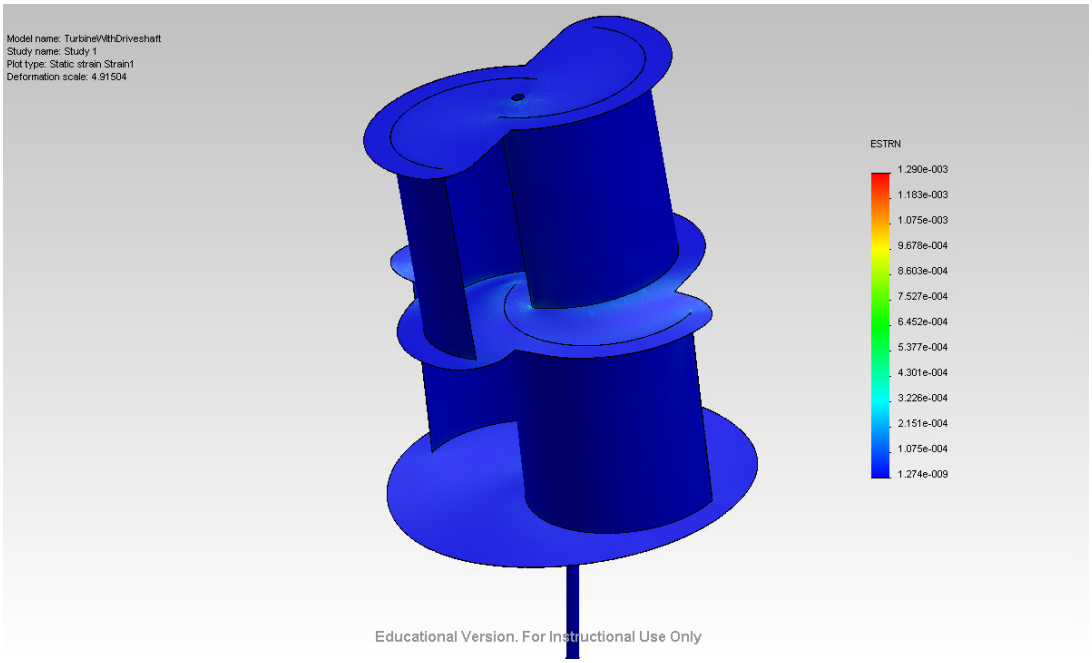

Figure L.3 : Strain Analysis

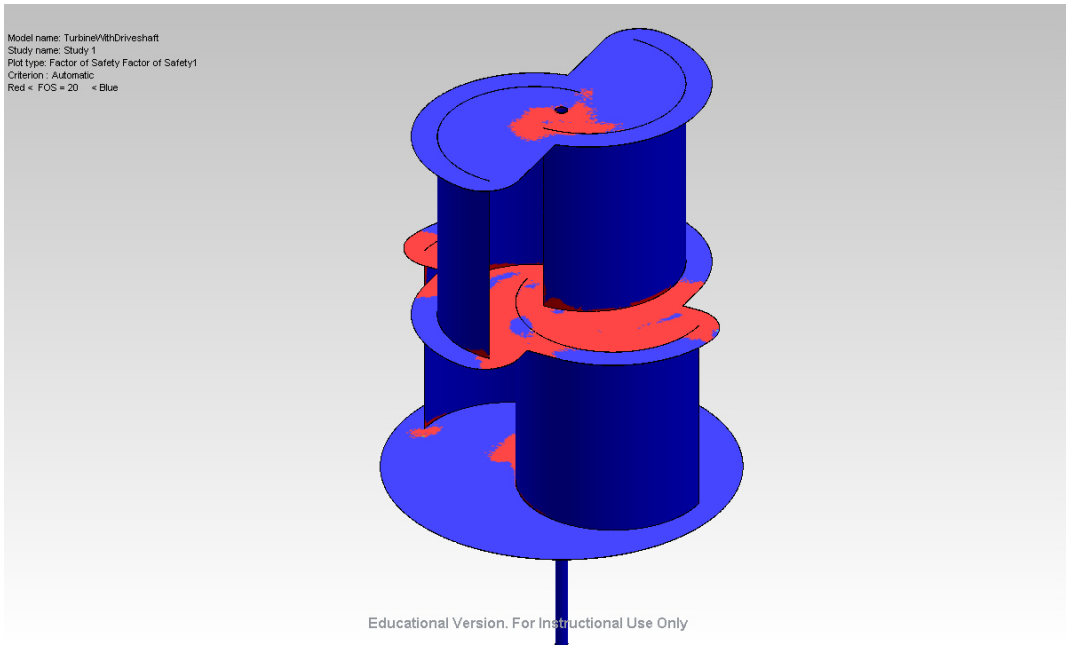

Figure L.4 : Factor of Safety Analysis

Appendix M: Technical Drawings

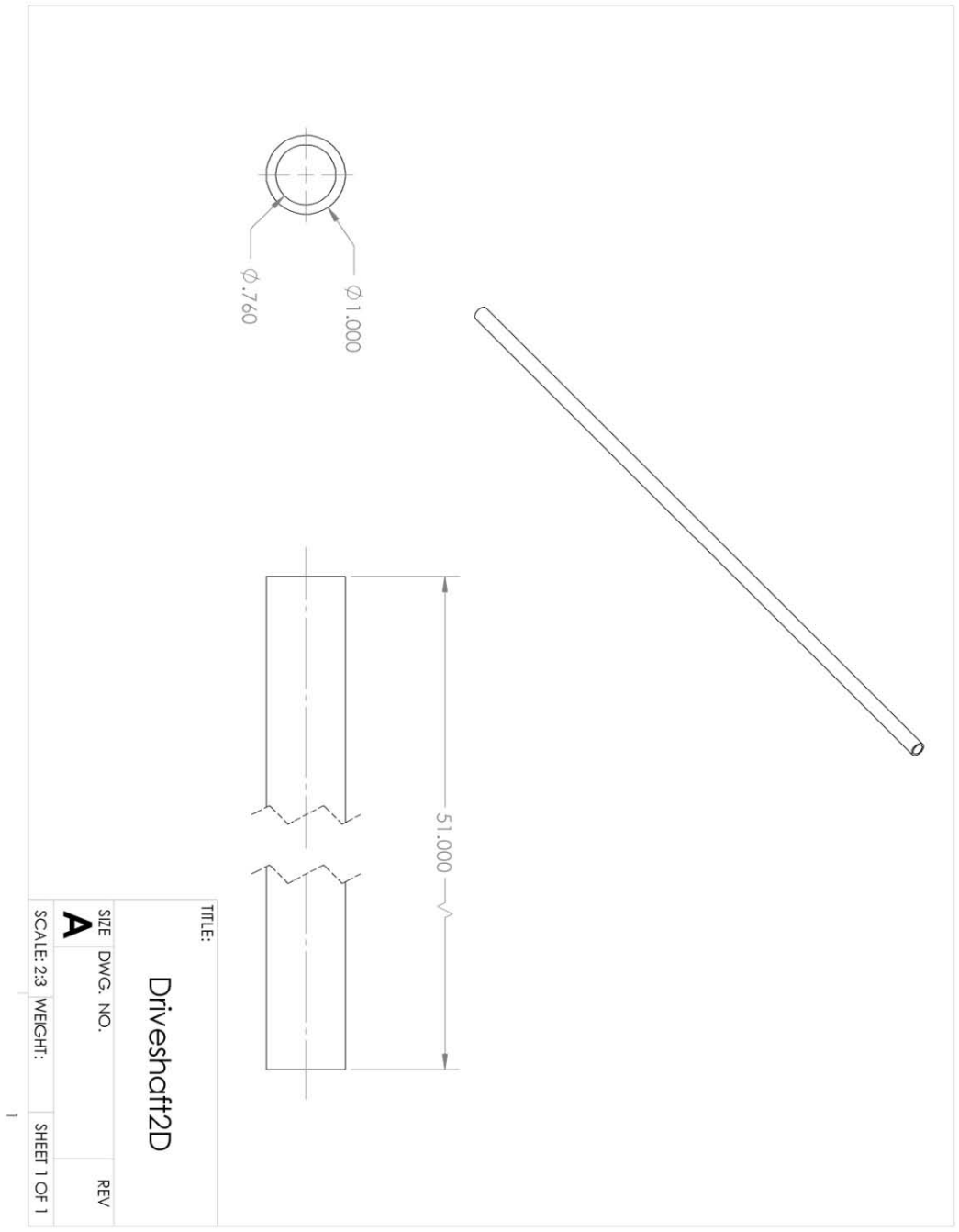

Figure M.1 : Drive Shaft

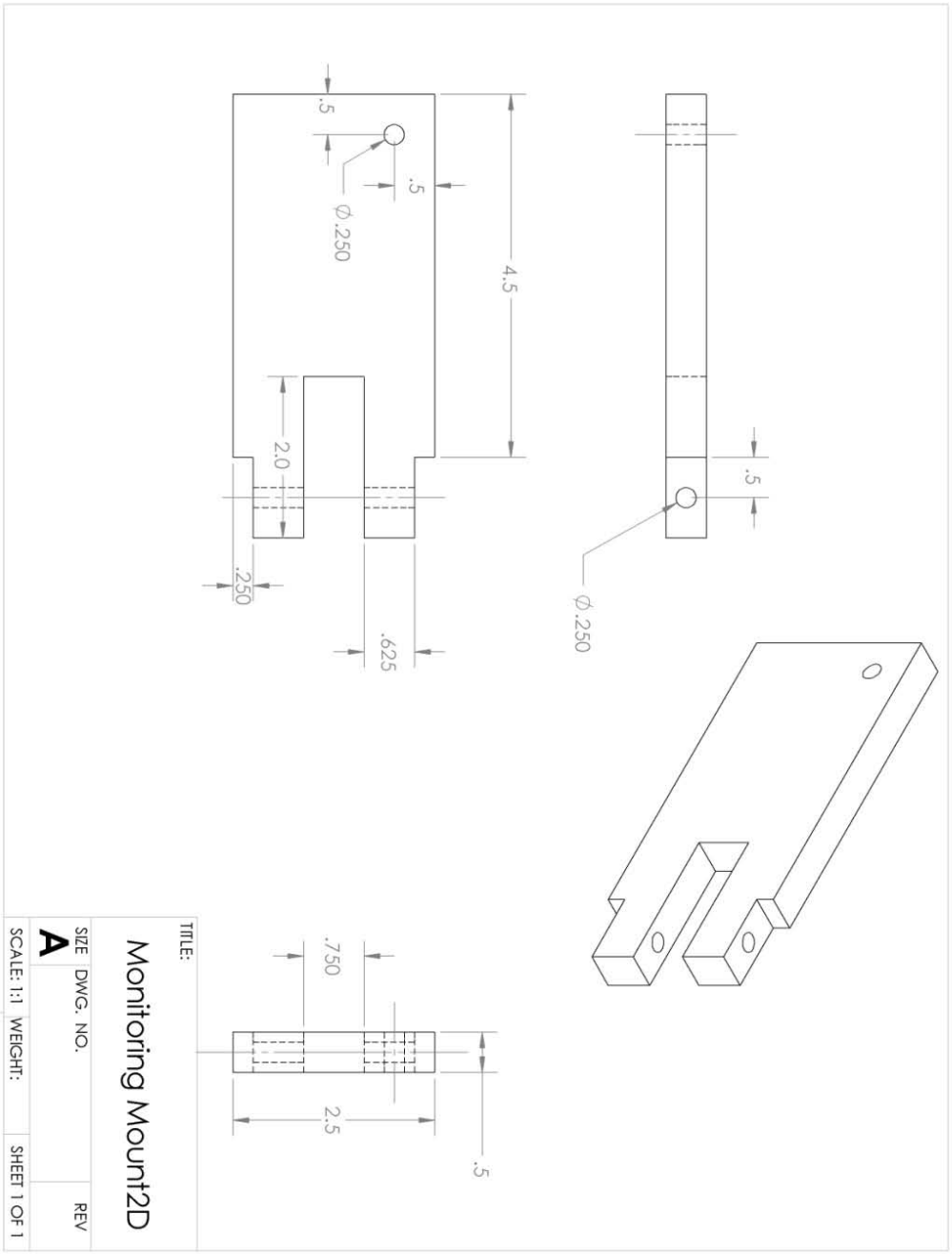

Figure M.2 : Monitoring Mount

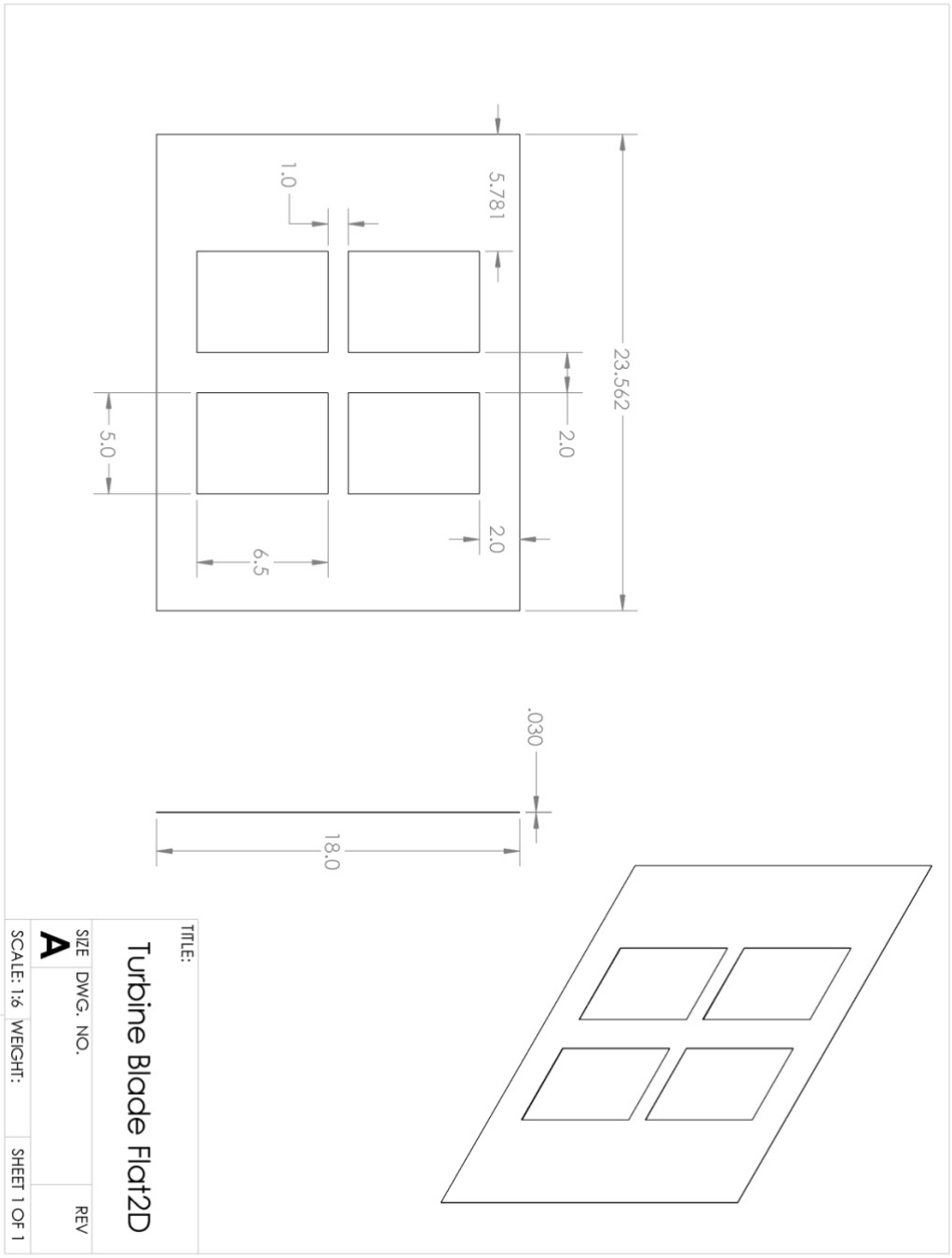

Figure M.3 : Turbine Blade

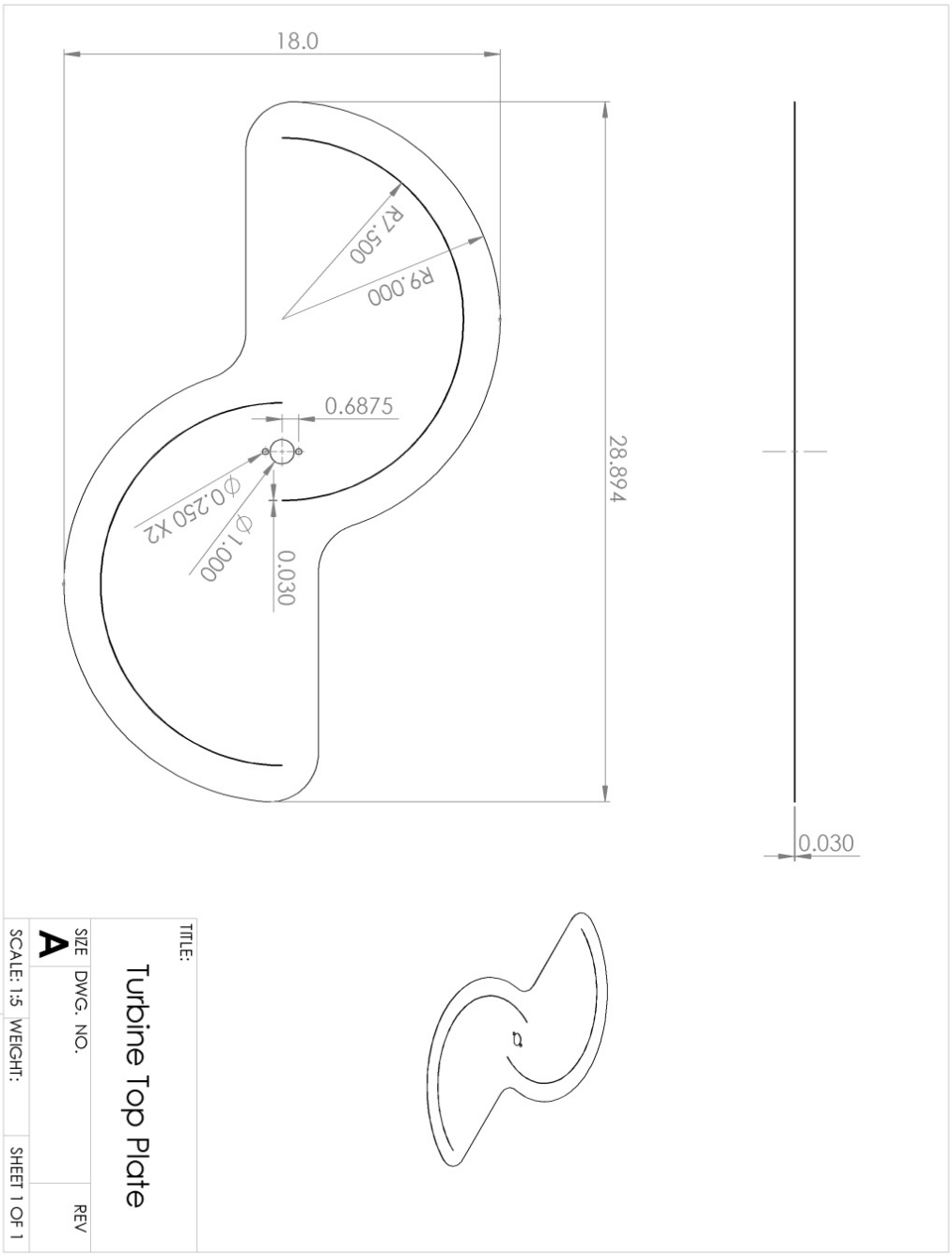

Figure M.4 : Turbine Top Plate

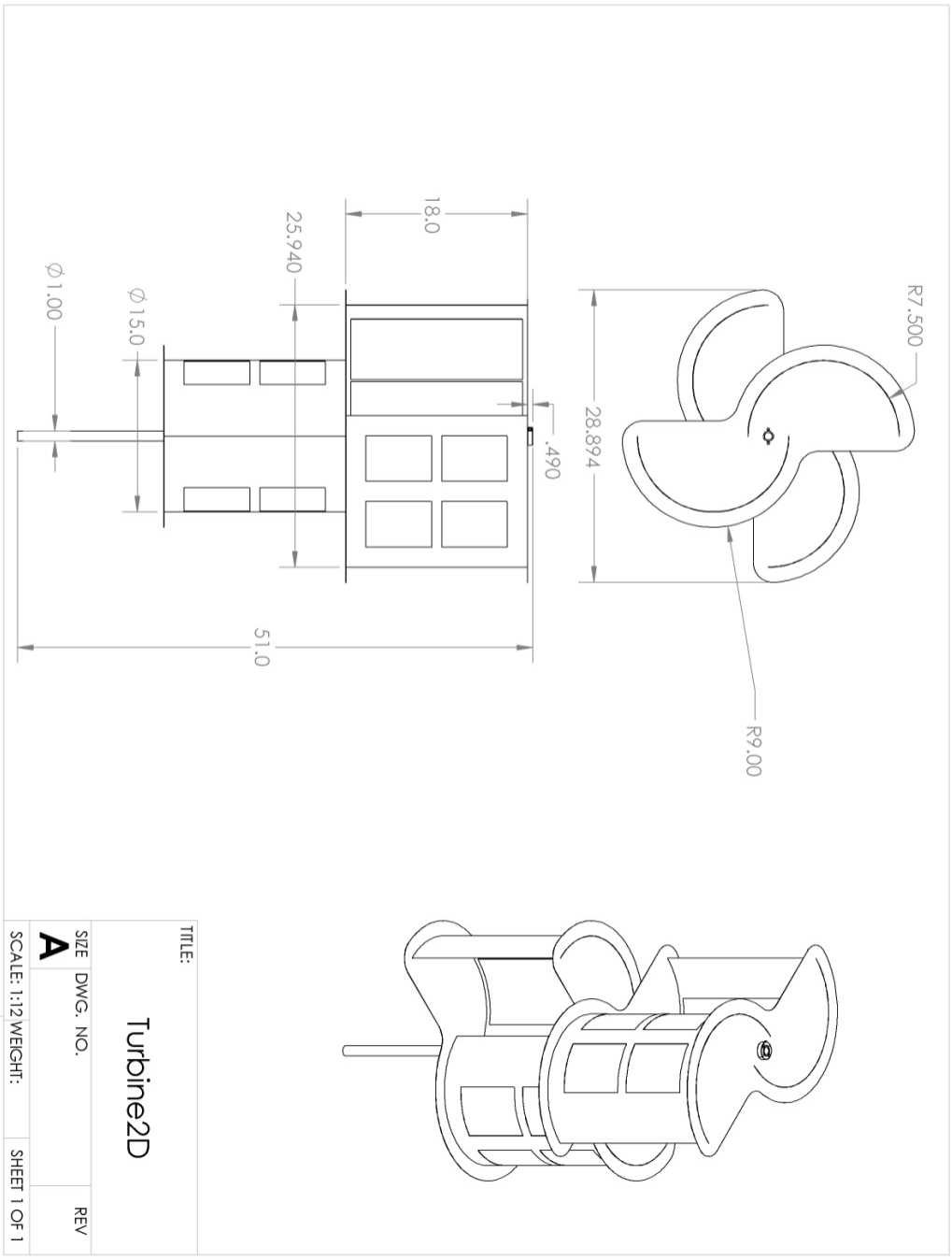

Figure M.5 : Turbine

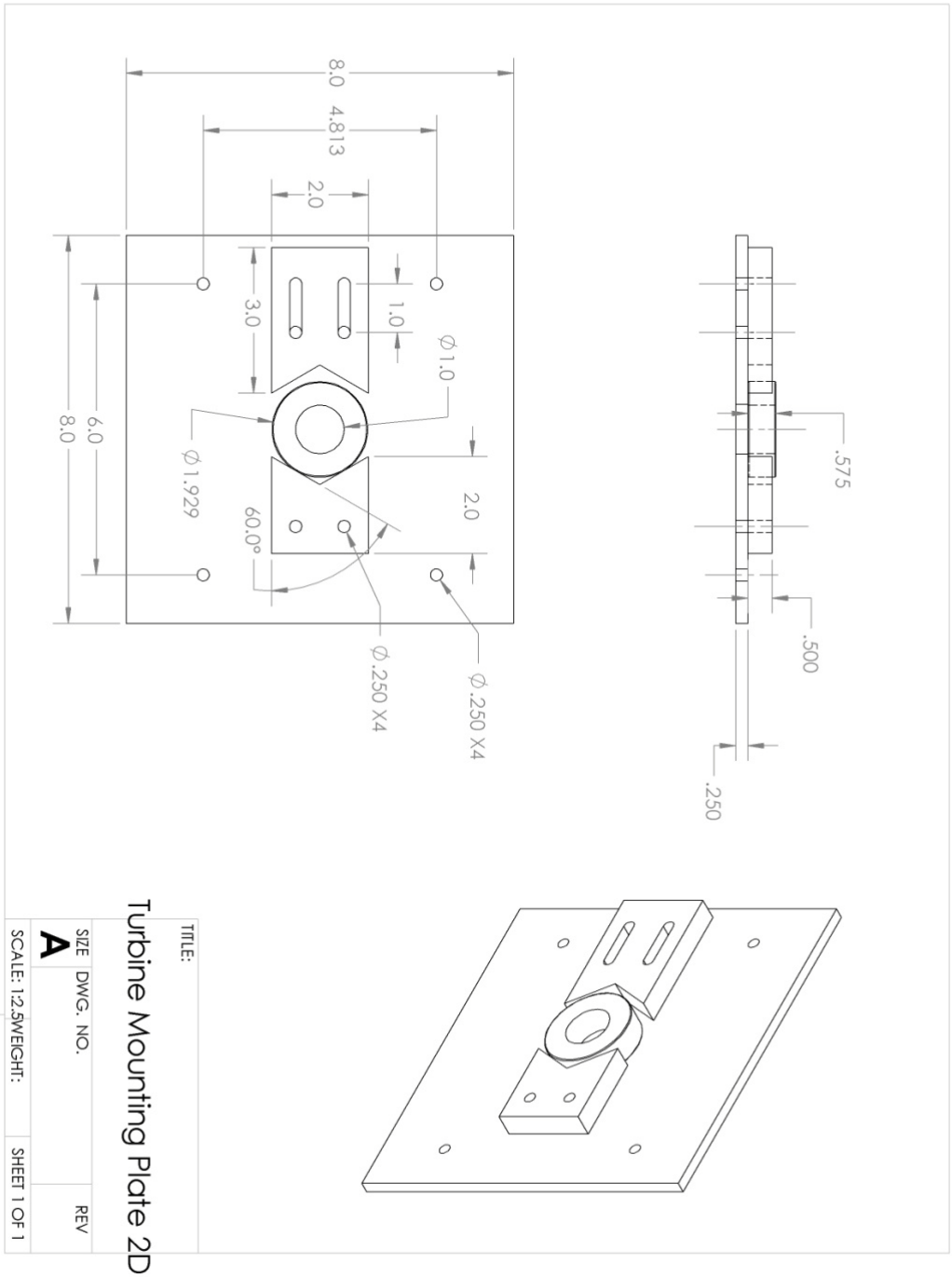

Figure M.6 : Turbine Mounting Plate

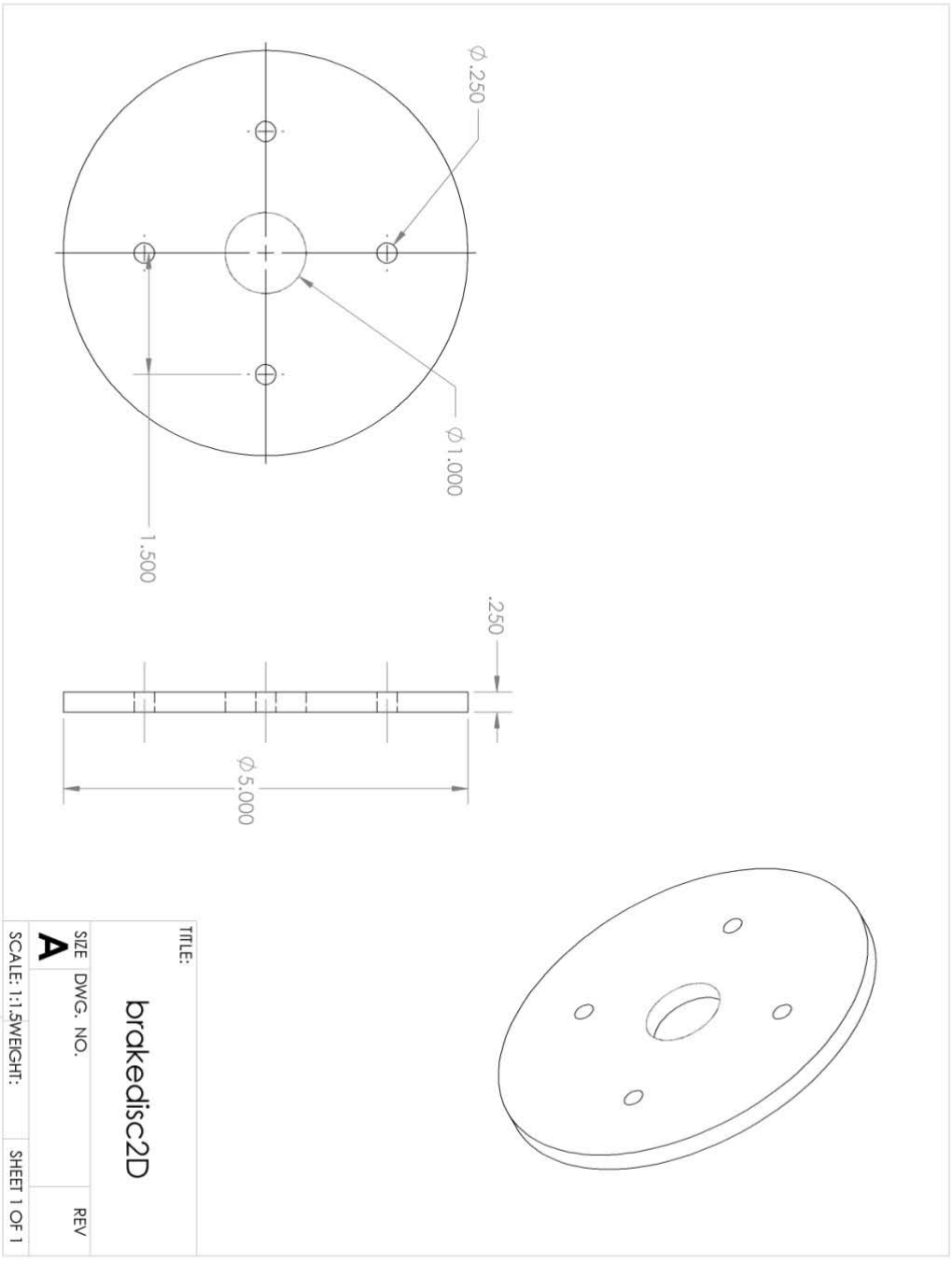

Figure M.7 : Brake Disk

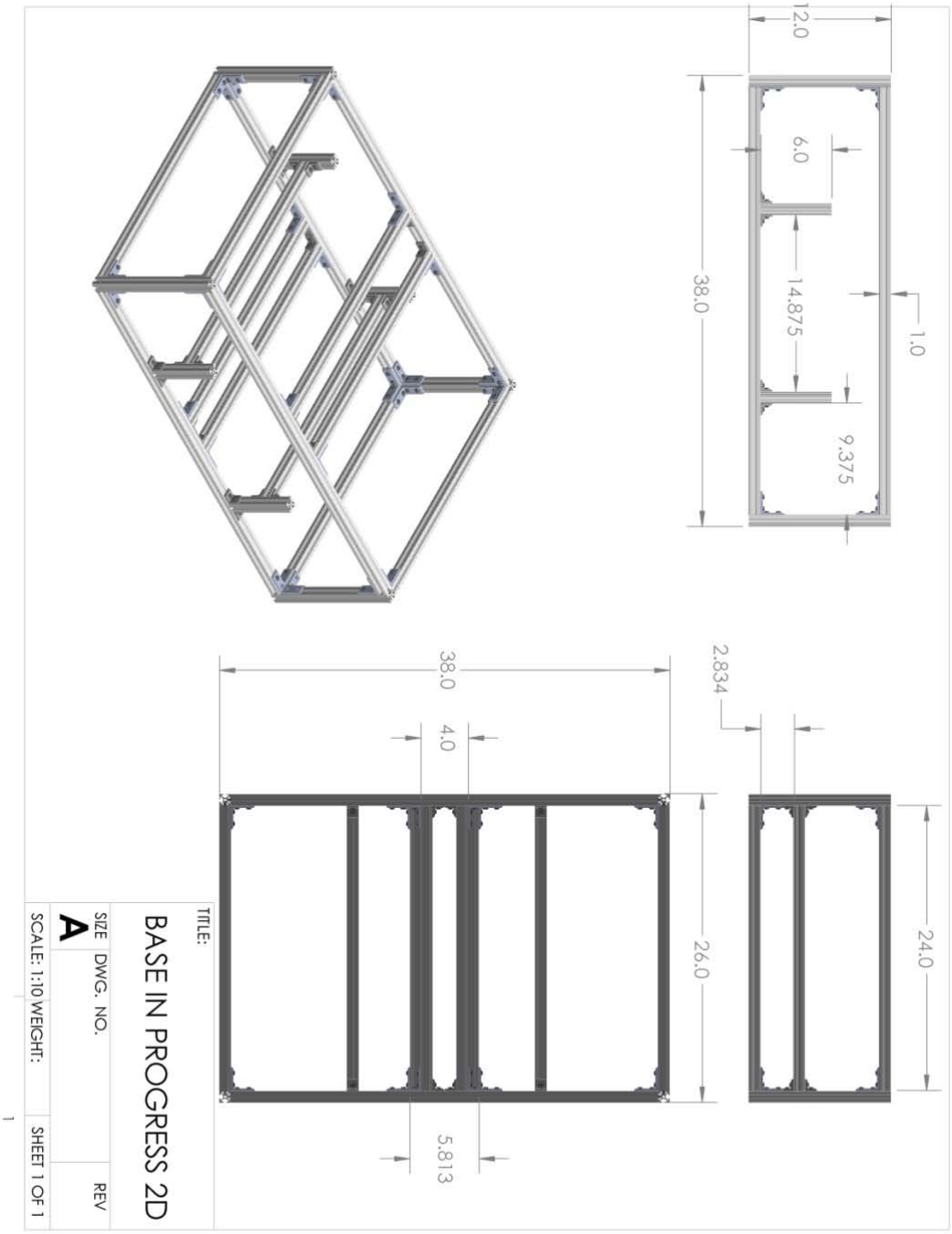

Figure M.8 : Base

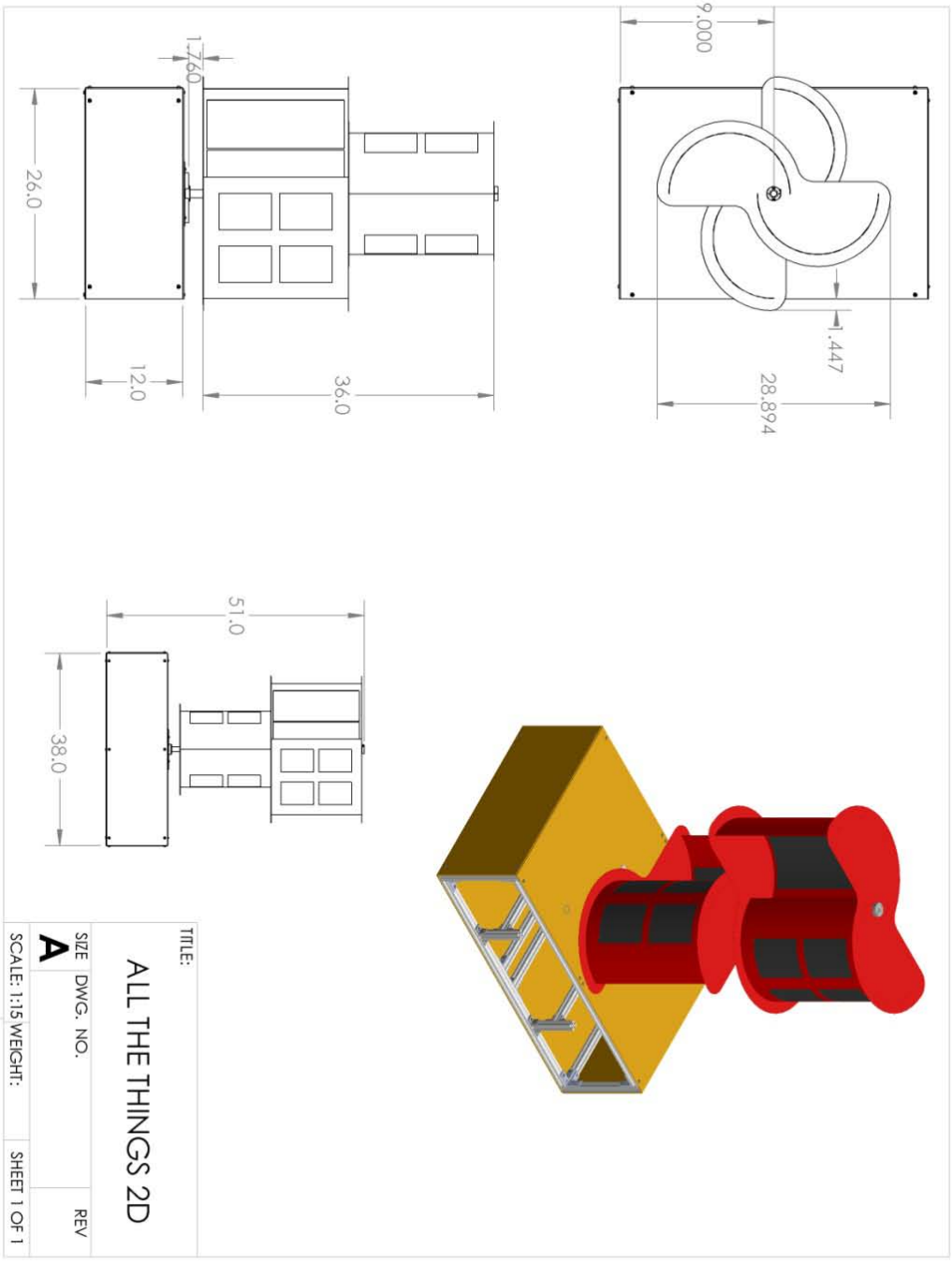

Figure M.9 : Assembled Turbine